International Geology Review

Vol. 1, No. 11 November 1959

published by the
AMERICAN GEOLOGICAL INSTITUTE

The American Geological Institute operates under the National Academy of Sciences. It is governed by an Executive Committee and a Board of Directors composed of two directors from each of the fourteen Member Societies.

International Geology Review is published monthly by the American Geological Institute with the assistance of an initiating grant from the National Science Foundation. The journal will report, in English, significant contributions to pure and applied research in the earth sciences which appear in foreign-language journals, especially those published in the U.S.S.R.

The editors of International Geology Review will give consideration to full English translations, condensations, and reviews submitted voluntarily for publication. Translators will be appropriately credited.

Readers are invited to direct to the editors their comments and discussions of articles published in the International Geology Review. Readers are encouraged also to submit suggestions as to published foreign literature considered worthy of translation and publication. Such suggestions should relate to materials of broad, general interest, rather than materials of limited reader interest.

Address editorial and subscription inquiries to

AGI TRANSLATIONS OFFICE
AMERICAN GEOLOGICAL INSTITUTE
2101 Constitution Avenue, N.W., Washington 25, D. C.

The basic subscription rate for International Geology Review is $55 per year, 12 issues. A special subscription rate of $15 per year is available to members of AGI Member Societies who are on the GEOTIMES mailing list and who will pledge to restrict the journal to their personal use. The $15 per year subscription rate is also available to educational institutions and personnel. Foreign postage: No additional charge to Canada and Mexico; to Pan American Union countries add $0.50 per year; to all other foreign countries add $1.00 per year. Single copy price $5.00 ($1.50 to subscribers qualifying for special rates) Second class postage paid at Washington, D. C.

International Geology Review

published monthly by the
AMERICAN GEOLOGICAL INSTITUTE

Vol. 1, No. 11 November 1959

CONTENTS

IGR TRANSLITERATION OF RUSSIAN

The AGI Translation Center has adopted the essential features of Cyrillic Transliteration recommended by the U. S. Department of the Interior, Board of Geographical Names, Washington, D. C.

Alphabet		transliteration
А	а	a
Б	б	b
В	в	v
Г	г	g
Д	д	d
Е	е	e, ye(1)
Ё	ё	ë, yë
Ж	ж	zh
З	з	z
И	и	i(2)
Й	й	y
К	к	k
Л	л	l
М	м	m
Н	н	n
О	о	o
П	п	p
Р	р	r
С	с	s
Т	т	t
У	у	u
Ф	ф	f
Х	х	kh
Ц	ц	ts
Ч	ч	ch
Ш	ш	sh
Щ	щ	shch
Ъ	ъ	''(3)
Ы	ы	y
Ь	ь	'(3)
Э	э	e
Ю	ю	yu
Я	я	ya

However, the AGI Translation Center recommends the following modifications:

1. Ye initially, after vowels, and after ъ, ь. Customary usage calls for "ie" in many names, e.g., SOVIET KIEV, DNIEPER, etc.; or "ye", e.g., BYELORUSSIA, where "e" follows consonants. "e" with dieresis in Russian should be given as "yo".

2. Omitted if preceding a y, e.g., Arkhangelsky (not iy; not ii).

3. Generally omitted.

NOTE: The well-known place and personnel names that have wide acceptance in international literature will be here adopted. However, German-type transliteration e.g., J for Y will not be used.

CONTRIBUTIONS TO RESEARCH ON QUARTZ-FORMING SYSTEMS[1]

by

Ye. I. Vulchin

• *translated by V. P. Sokoloff* •

ABSTRACT

Investigation of quartz inclusions has yielded data on concentrations, temperatures, and pressures of mineral-forming systems; important in application to problems of mineral genesis and prospecting criteria. An integrated method involving preliminary microscopic examination of inclusions, analyses of aqueous extracts, and spectrographic analyses of powdered material, both derived from inclusions. Solutions available only in small quantity or of high dilution were subjected to optical-spectrographic and microturbidimetric, qualitative and quantitative analyses. Chemically, the solutions showed alkaline reaction; Na, K, Ca and Cl were prominent. In secondary inclusions cations Na^+, K^+, Ca^{2+}, Mg^{2+}, Al^{3+}, Fe, and Mn with anions Cl^-, SO_4^{2-} and BO_3^{3-} were present in dissolved state. The presence of boron was noted for the first time in analysis, although it is known to be characteristic in quartz forming solutions. The concentration calculated for dissolved salts ranged from 30 to 35 percent. Transfer of Si appears to occur through metasilicate anions, SiO^{3-} and Si_2O_5; OH^- is present along with SiO_2 resulting evidently from hydrolysis of SiO_3^{2-}.

PT diagrams of binary systems are used to gage the extent of mineral-formation possibilities. Three-component fields indicate: phase composition of saturated solutions, saturated solutions with gaseous phase, and saturated gaseous solutions. Recurrent metastability phenomena are discussed with respect to their modification of theoretical phase systems. Use of VT diagrams implements calculation of homogenization temperature for included phases, by examination of volume-ratio curves for liquid and gaseous phases during heat application. Multicomponent-system PT diagrams are derived from those describing simpler systems they are a resultant of the phase interrelationships under consideration. - - D. D. Fisher.

Thorough understanding of phenomena which determined the very process of mineral formation is one of the major prerequisites to establishment of prospecting criteria for exploration of mineral deposits. Up to the present, problems of mineral genesis have received very little attention. Comprehensive and detailed studies of these problems were begun only recently; the principal contributions to their solution have been made by Soviet scientists.

Research on mineral origins means, first of all, investigation of mineral-forming systems; studies of mineral associations constitute the premises of this research. Logically, one can derive the characteristics of mineral-forming systems from the theory of physical chemistry. Such working procedures involve many difficulties and misconceptions.

Gases and liquid inclusions, a very interesting area of mineralogy has attracted considerable interest recently; as samples of mineral-forming systems captured by the crystallizing substance. Until it became a subject of particular interest for a wide circle of mineralogists and geologists, this topic was studied almost entirely by crystallographers-morphologists. The importance of these most interesting phenomena may be illustrated by words of Alexander Petrovich Karpinsky, Member of the Academy:

"Among many kinds of inclusions in minerals and rocks, the liquid inclusions are especially interesting; as they are believed to be, not without reason, parts of the medium wherein the crystallization of the minerals has taken place. Moreover, properties of the included liquids by themselves may provide indications as to the kind of environments formerly operative" [22].

Studies of the inclusions are conducted along three fundamental lines: 1) investigation of gas-liquid phase ratio in inclusions, as well as of homogenization temperatures, for use in thermometric purposes and in definition of the aggregate state of mineral-forming system; 2) observation on inclusions applicable to determination of pressures during mineral-forming process; and 3) chemical composition of liquid and gaseous inclusions.

Our commitment to the study of quartz-forming systems led, without entering some other aspects of our problem, to investigation of certain physicochemical aspects of the quartz formation theory in hydrothermal systems and

---

[1]Translated from Materialy k izucheniyu kvartobrazuyushchikh sistem: Naukovi Zapiski, Lvovsky Derzhavny Universitet im. Ivana Franka, Seriya Geologichna, v. 23, no. 6, p. 136-139, 1953.

of the thermometric methods for homogenization of gaseous-liquid inclusions.

Our studies were directed by Professor E. K. Lazarenko, to whom the author is obliged to offer his sincere thanks; moreover, the author is deeply indebted to Professor V. S. Sobolev and to Dozent V. K. Zolotukhin for consultation during his work.

INVESTIGATION OF CHEMICAL COMPOSITION OF QUARTZ-FORMING SOLUTIONS IN INCLUSIONS

Chemical Analyses of Inclusion Solutions as the Means of Understanding Mineral-Forming Systems

Development of thermometric methods had led to the necessity for theoretical studies of such fundamental problems as the temperature interval between sealing of an inclusion (blocking-off of a part of the crystal) and appearance, or disappearance, of a gaseous bubble. It is understood that interpretation of this problem may be undertaken only through phase-equilibria diagrams of well-defined, concrete systems; an understanding of these systems is contingent upon chemical analysis of included solutions.

Effects of solid, liquid, and gaseous micro-inclusions are highly important on chemical analysis of minerals; their neglect leads to major errors, chiefly in spectrographic analysis. In the case of opaque minerals, where homogeneity of the test materials is not easily ascertained, this is particularly dangerous. Ya. Samoylov, a Russian mineralogist, had called attention long ago to such difficulties: "These inclusions, gaseous, liquid, and solid, while making the mineral substance "impure", for the purpose of the chemical analysis, constitute at the same time priceless material for major conclusions in reference to the mineral origins [45].

Secondary inclusions in quartz (early secondary, pseudo secondary) were the subject of our study.

Quartz is an important and convenient material for our work. For these reasons, inclusions in quartz are the principal materials for thermometric measurements that now stand in a need of interpretation. The suitability of quartz for the purpose is determined by its transparency, important in ascertaining purity of test material. Quartz is practically insoluble; this is important in the extractions. Quartz is one of the most widely distributed minerals in major economic mineral deposits. Studies of of quartz-forming systems, taking this into consideration, acquire particular interest in the development of techniques for artificial growth of quartz.

The fundamentals of our work procedure were as follows:

Recognition of test material preparation for analysis as a highly responsible operation; we devoted considerable care to this problem, in breaking it down to four stages:

1. Selection of test materials from a definite geologic district, either as single crystals or as fragments of crystals, which would be pertinent to our studies and would contain a sufficiently large number of inclusions for analysis.

2. Preparation of test material containing inclusions of one particular type, or of closely similar types, considered to be characteristic, with sufficient degree of reliability, of some definite type of mineral-forming system. Decisions made in this respect involved determination as to whether the inclusions were of syngenetic or the epigenetic character.

3. Measurements to determine the volume of inclusions in the sample.

4. Examination of the test materials with respect to purity and to solid inclusions and admixtures.

The second stage consisted of fragmentation and leaching with water (extraction) of materials from the inclusions.

The third stage involved chemical analysis of the extracts and pulverized materials; both chemical and physical methods were employed.

The fourth stage consisted of calculation, on the basis of the analytical data, to determine the original concentration of included solutions; analyses of the pulverized materials were taken into account, as was a critical review of the results.

Thus our work procedure involved, essentially, selection of the purest possible minerals logic materials, containing the same type of inclusion, characteristic of some definite type of mineral-forming system; measurements to determine the volume of inclusion cavities; analysis of solutions using their extracts along with spectrographic analysis of the host mineral and, final calculation of concentrations.

Analytical Techniques

The following procedure was employed:

A. Preparation of test material for analysis and fragmentation.
   1) Microscopic examination:
      a) studies of zones (areas) containing syngenetic inclusions
      b) isolation of pure areas.

2) The first fragmentation; mechanical isolation of previously studied areas for analysis.
3) The second fragmentation; breaking into piece suitable for microscopic studies.
4) Microscopic studies:
   a) investigation of material purity;
   b) investigation of syngenetic (monotype) inclusions and of inclusions in general (morphology, thermometry);
   c) measurement of cavity volumes (percent).
5) The third fragmentation and mass determination of the sample:
   - milling of the mineral to a powder suitable for the extraction and spectrographic analysis.

B. Aqueous extraction (leaching):
1) Aqueous extraction (5 hours);
2) Collection of solution with a pipette, and washing the residue by decantation;
3) Evaporation of extract (and washings VPS) to 10-15 cm^3.

C. Chemical studies of the extract:
1) Qualitative and semiquantitative spectrographic analysis;
2) Qualitative and semiquantitative microchemical analysis;
3) Quantitative microchemical analysis; in addition spectrographic analysis of the powdered mineral.

D. Calculation of the "Lower Limit" of the concentration.

The solution-inclusions in quartz were studied in materials collected as four [Tr.: 25-32 are not identified. VPS] geologic sources. A total of 15 specimens were examined: These included 11 quartz specimens from the Aldan quartz veins and quartzites (samples 1-19); [Tr.: "11-19" in the original. Should be "1-19" as it is clear from the context. VPS]; 1 specimen of quartz from sulfide veins at Berezovsk, Ural (samples 20-25); and 1 specimen of quartz from the Ukrainian crystalline shield pegmatites of Volyn'. [Tr.: "Massiv", in the Russian usage, is freely used non-specific term for a) an intrusive body of rock whose shape and the geologic history are not well known; b) any small part of the crystalline base of a platform; c) a weakly dissected, uplifted body of rock isolated from mountain chains; in this case it is used in the sense of "shield". VPS]

(Samples 32-38a). The space available does not permit us, unfortunately, to attempt a detailed description of the individual quartz specimens or to present their thermometric and facies characteristics. We limit ourselves, therefore, to a brief description of test materials and extracts examined in the analysis (table 1).

As is evident from table 1, our extracts were characteristically low in concentrations (hundredths of 1 percent, and lower); thus, it became necessary to employ highly sensitive analytical procedures, (in the broad sense of the term): Optical spectrographic analysis were carried out first, and secondly, highly sensitive microchemical determinations. We chose to use the microturbidimetric method as the most quantitatively reliable and recognized procedure.

The aqueous extraction permits us to leach soluble constituents out of the inclusions after fragmentation, to have these constituents concentrated in the dry residue from the evaporated extract, or simply to have them transferred from inclusions to a solution suitable for chemical analysis. Washing by water serves to minimize analytical errors caused, to some extent, by the presence of solid inclusions, in powdered quartz analysis. There is an easy chance that contamination during washing, however, may have an appreciable effect on the results. In order to eliminate effects of occasional contamination on analytical results and in order to detect certain poorly leachable constituents, analysis of aqueous extracts must be confirmed by spectrographic analysis of pulverized samples. In addition, final results must be stabilized by the use of the two independent methods. Replicate analyses of a sample taken from one specimen are essential, as the means of generalization and averaging of the results, to eliminate occasional errors. The results obtained by qualitative spectrographic analysis of our samples are reported in table 2.

Dry residues of aqueous extracts were studied by spectrographic analysis (using copper electrodes); [Tr.: "Electrons" in the original; a misprint. VPS] these results are shown in table 3.

Semiquantitative spectrographic and microchemical investigations [21, 23, 25, 31] were carried out on the extracts after the qualitative spectrographic analyses [7, 20, 44]. These results are shown in table 4 (pp. 142-143) [Tr.: Of the original publication. VPS].

Now let us consider briefly the quantitative microturbidimetric determination of chloride.

All of our quantitative measurements were performed with the aid of a special microturbidimeter; i. e. a glass plate with flat-bottomed cavities. The assembly is shown in figure 1. Intensity of the transmitted light was measured by photo-electric nonregistering microphotometer MF-2.

The microturbidimetric analysis [49] was conducted as follows: 0. 3 milliliters of test solution were transferred, with a micropipette, into the cavity of the glass slide. Then the cavity was covered by a cover glass whose

TABLE 1. Characteristics of the analyzed samples of quartz

Specimen number	Sample number	Mass of sample		Inclusions, by volume %	Volume of inclusion cavity in sample, mm^3	Gaseous phase in inclusions %	Volume of liquid phase mm^3	Volume of extract ml	Dilution r*
		grams	cm^3						
1 - 11	1	33.41	12.80	0.09	11.45	20	9.15	6.4	700
	2	24.85	9.38	0.09	8.4	20	6.7	1.4	210
	3	23.56	8.90	0.09	8.0	20	6.4	4.8	750
	4	7.40	2.80	0.34	9.4	20	7.2	1.6	226
	5	6.16	2.32	1.9	25.4	20	20.6	20.4	925
	6	18.28	7.05	0.154	10.85	20	8.7	3.5	405
	7	19.32	7.28	0.15	11.25	20	9.0	8.1	900
	8	19.99	7.52	0.04	2.78	25	2.08	2.7	1,300
	9	13.86	5.26	0.04	2.10	25	1.57	1.6	1,000
	10	11 42	4.32	0.18	4.7	25	3.52	7.2	2,060
	11	13.75	5.18	0.18	9.7	20	7.75	17.9	2,310
	12	18.32	6.9	0.18	12.2	20	9.78	24.5	2,500
	13	11.72	4.4	0.47	20.6	20	16.5	17.8	1,080
	14	9.54	3.6	0.5	18.0	20	14.4	15.8	1,100
	15	7.96	3.0	0.17	5.1	20	4.08	3.6	880
	16	15.97	6.02	0.19	11.2	20	8.95	7.5	835
	17	10.34	3.9	0.20	7.8	20	6.25	5.3	850
	18	12.97	4.9	0.17	8.3	20	6.65	9.1	1,380
	19	14.55	5.48	0.17	9.8	20	7.85	11.4	1,450
12	20	11.32	4.25	0.15	2.76	40	1.66	0.65	392
	21	14.18	5.3	0.15	3.15	40	1.89	0.75	400
	22	10.27	3.9	0.15	5.85	40	3.51	2.52	720
	23	12.45	4.7	0.15	7.20	40	4.3	2.37	567
	24	9.53	3.6	0.16	5.77	40	3.43	2.05	600
	25	11.84	4.1	0.15	6.15	40	3.7	1.60	431
13	26	15.02	5.7	0.47	26.5	50	13.25	10.6	800
	27	14.53	5.5	0.47	25.5	50	12.75	11.6	910
	28	12.18	4.58	0.48	22.0	50	11.0	11.0	1,000
	29	13.82	5.2	0.48	25.0	50	12.5	8.1	650
	30	15.85	6.0	0.47	28.2	50	14.1	13.5	960
	31	14.18	5.3	0.47	25.5	50	12.75	9.9	763
14 - 15	32	19.12	7.25	0.30	21.8	90	2.18	8.2	3,760
	33	17.45	6.6	0.30	19.8	90	1.92	8.4	4,250
	34	18.18	6.88	0.30	20.6	90	2.06	5.9	2,853
	35	11.56	4.34	0.05	2.16	90	0.22	11.2	51,000
	36	14.23	5.39	0.05	2.70	90	0.27	12.9	48,000
	37	10.20	3.85	0.05	1.92	90	0.19	10.4	55,000
	38	11.18	4.46	0.05	2.23	90	0.22	10.9	49,560

* The dilution factor (r) was calculated by us as follows:

$$r = \frac{\text{(volume of solution)} - \text{(volume of extract), } mm^3}{\text{(volume of solutions in inclusions), } mm^3}$$

(Note: "mm^2" in the original; this misprint is here corrected. VPS)

TABLE 2. Qualitative spectrographic analysis of pulverized samples of quartz (carbon electrodes and copper plates)

Spectrograph ISP-22. Source of light: voltaic arc from Sventitskii generator.

Sample number	Elements present in all samples	Analytical lines present (A)	Elements characteristic of individual samples	Analytical lines present
1 2 3	Na	Na 3, 302. 99 3, 302. 32 d	-	-
4 5	K	K 4, 044. 14 4, 047. 20 d	-	-
6 7 8 9 10	Ca Mg	Ca 2, 994. 96 3, 000. 86 3, 006. 86 3, 933. 67 3, 968. 47	-	-
11 12 13 14 15	Al	Mg 2, 795. 5 2, 802. 7 2, 852. 1	-	Ti 3, 078. 64 3, 088. 02 d
16 17 18 19 20	Si	Al 3, 082. 16 3, 092. 71 3, 961. 53 3, 944. 03	Ti	-
21 22 23 24 25	Fe B	Si Many lines in abundance	-	Ag 3, 280. 6 3, 382. 8 Cu 3, 247. 54 3, 273. 90
26 27 28 29 30	-	Fe 2, 598. 37 2, 599. 40 3, 020. 64 B 2, 496. 7 2, 497. 7	Cu, Ag, Be	Be 3, 130. 4 3, 131. 1 d
31	-	-	Cu, Ag, Be	-
32 33 34 35 36 37 38	-	-	Cu, Ti	-

Note: The results are reported on the basis of three (replicate) analyses for every sample. K was not determined in the carbon electrodes. Copper was determined only in the carbon electrodes. Boron was determined only in the copper electrodes because it was present in all of the carbons. Titanium, like boron, was determined only in the copper electrodes.

TABLE 3. Qualitative spectrographic analysis of dry residue from 1 ml of aqueous extract; copper electrodes

Sample number	Elements present in all samples	Analytical lines present (A)	Elements present in individual samples	Analytical lines present (A)
1				
2	Na	Na 3, 302. 99; 3, 302. 32 d		
3			Mn	Mn 2, 794. 8; 2, 798. 2; 2, 801. 0
4				
5	K			
6		K 4, 044. 1; 4, 047. 2 d; 3, 446. 7; 3, 447. 7 d		
7			-	-
8				
9	Ca			
10	Mg			
11		Ca 2, 994. 96; 3, 000. 86; 3, 006. 86; 3, 158. 87	Mn	-
12				
13	Al			
14		Ca 3, 179. 33; 3, 181. 27; 3, 933. 67; 3, 968. 47	Mn	-
15				
16				
17	Si			
18				
19	Fe	Mg 2, 795. 5; 2, 802. 7; 2, 852. 1		
20				
21	B			
22		Al 3, 082. 16; 3, 092. 71; 3, 961. 53; 3, 944. 03		
23				
24			Mn	-
25				
26		Si Numerous lines abundant		
27				
28				
29				
30		Fe 2, 598. 37; 2, 599. 40; 3, 020. 64		
31				
32				
33		B 2, 496. 7; 2, 497. 7	-	-
34				
35				
36				
37				
38				

Results are based on three (replicate) analyses of every sample.

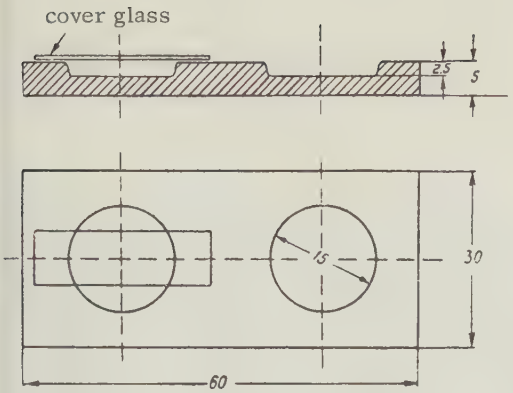

FIGURE 1. Plan of apparatus for turbidimetric measurements

diameter was somewhat smaller than that of the cavity; in order to eliminate the gas bubbles and to facilitate addition to the reagent, this difference was essential. The underside of the cover glass was marked with a diamond needle, so that the objective might be more easily brought into focus. Transfer of solution onto the slide was done under the microturbidimeter objective. The logarithmic scale of the photometric element was set at zero. Then, 0.1 milliliters (ml) of the reagent was added, using a micropipette, to the test solution on the slide; this brought the total volume to 0.4 ml. The microturbidimeter could not be disturbed after its scale was set on zero, otherwise the results would be erroneous. Because of the convenience afforded by the logarithmic graph [Tr. : nomogram? VPS] the logarithmic scale of the microturbidimeter was used in relating the amount of absorbed light to that of precipitate.

Measurements of log I were made from 5 to 10 minutes after addition of the reagent, so that sufficient time be allowed for the reaction to come to completion. Readings had to be taken several times (for every test). There should be no excessive delays in measurements because in time, homogeneity of turbidity might be disturbed and, concentration of the solution affected by evaporation. The usually insignificant changes in the microturbidimeter scale might be due to mechanical agitations of the instrument, micro-currents in the test solution, irregularities of electric current in the photometric element and the lamp.

We studied the curve log I = f(log C), with reference to standard samples. Data used in construction of this curve core [Ed. : as translated.] (presented in table 5) and the curve itself, log I = f (log C), for AgCl, is shown in figure 2.

The corresponding curve for AgCL was derived from data in table 5; coordinates for the graph were log I and log C. By examination it is apparent that this curve may be divided

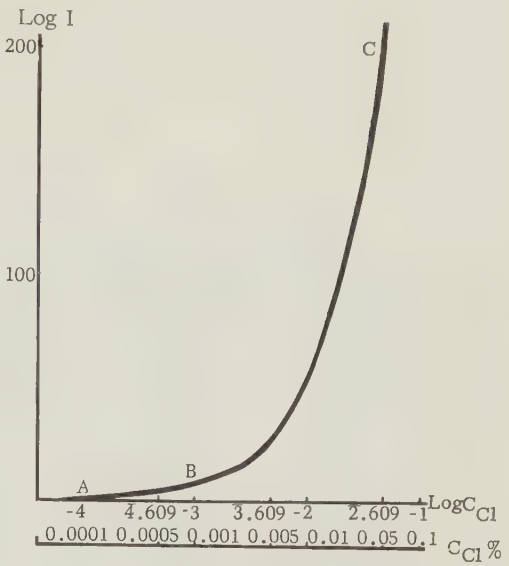

FIGURE 2. Log I = f (log C) Curve used in turbidimetric method

TABLE 5. Data for construction of the log I (log C) curve for AgCl

Item number	Concentration of Cl ion, %	Log (concentration Cl^-)	Log I	Conditions
1	0.0001	-4	ca. 0	Microphotometer MF-2
2	0.0005	$\bar{4}$.6990	5	
3	0.001	-3	8	Amount of solution: 0.4 cm^3
4	0.005	$\bar{3}$.6990	27	
5	0.01	-2	54	Thickness of solution layer: 2.5 mm
6	0.05	$\bar{2}$.6990	200	
7	0.1	-1	∞	

into four areas: the area below "A", the areas "AB", "BC". [Tr.: The letters in the original diagram are "A", "AG", "GB", and "B" respectively; they could be transliterated as "A", "AB", "BV", and "B". VPS] The working part of the curve log I = f (log C) is "AG": That portion of the curve preceding "A" represents extremely dilute solutions (below 1 x 10^{-4}%); $AgNO_3$ reaction is insufficiently sensitive below this range. We should remember that caution is indicated in the case of solutions whose concentrations fall within the "AB" range; even the smallest error in the intensity measurement might cause significant distortion of analytical results. Best suited for our work is the range "BC". In the range beyond "C", the function log I = f (log C) vanishes and the curve becomes a straight line parallel to the ordinate. Empirically, it is very easy to avoid this difficulty by diluting test solutions to make them fit the "BC" range. The part "AC" of the curve embraces the 1 x 10^{-4} to 5 x 10^{-5}% range of concentrations; all of our solutions fall within this range.

TABLE 4. Semiquantitative microchemical and

Sample number	Cl^- (Microchem.)	SO_4^{2-} (Microchem.)	BO_3^{3-} (Microchem.)	BO_3^{3-} (Spectr.)	Na^+ (Spectr.)	K^+ (Microchem.)
1	0.0090	0.0035	0.0050-55	0.0050-55	0.0080	0.0040
2	0.0280	0.0150	0.0185	0.0185	0.0280	0.0130
3	0.0080	0.0035	0.0050	0.0050	0.0075	0.0040
4	0.0200	0.0190	0.0190	0.0190	0.0210	0.0130
5	0.0010	0.0035	0.0020-30	0.0020-30	0.0045	0.0015-20
6	0.0200	0.0065	0.0075	0.0075	0.0150	0.0040
7	0.0100	-	0.0055	0.0055	0.0070	0.0030
8	0.0035	0.0015-20	0.0015-20	0.0015-20	0.0010	0.0035-40
9	0.0045-50	0.0020	0.0025	0.0025	0.0015	0.0050
10	0.0020	0.0010	0.0001-5	0.0001-5	0.0020	0.0015
11	0.0020	0.0015	0.0020-25	0.0020-25	0.0015-20	0.0015
12	0.0015-20	0.0010	0.0020-25	0.0020-25	0.0015	0.0010-15
13	0.0040	0.0010	0.0025	0.0025	0.0035	0.0025-30
14	0.0040-50	0.0015	0.0020-25	0.0020-25	0.0035	0.0025-30
15	0.0100	0.0015	0.0045	0.0045	0.0030	0.0100
16	0.0045-50	0.0030-35	0.0030-35	0.0030-35	0.0050-55	0.0030-35
17	0.0045-50	0.0030-35	0.0030-35	0.0030-35	0.0050	0.0030-35
18	0.0030	0.0020	0.0010	0.0010	0.0025	0.0020-25
19	0.0030-35	0.0020-25	0.0010	0.0010	0.0020-25	0.0020-25
20	0.0145	0.0025-30	0.0085-90	0.0090	0.0200	0.0100
21	0.0145	0.0025-30	0.0085-90	0.0090	0.0110	0.0035
22	0.0080	0.0010-15	0.0045	0.0045	0.0110	0.0035
23	0.0100	0.0015-20	0.0060	0.0060	0.0055-60	0.0020
24	0.0095-100	0.0010-15	0.0055-60	0.0055-60	0.0070-75	0.0040
25	0.0130	0.0025	0.0080	0.0080	0.0070	0.0020-25
26	0.0050	0.0065	0.0055	0.0055	0.0035-40	0.0050
27	0.0045	0.0055-60	0.0045-50	0.0045-50	0.0030-35	0.0040-45
28	0.0040	0.0050-55	0.0040-45	0.0040-45	0.0045-50	0.0040-45
29	0.0060	0.0080	0.0065	0.0065	0.0050-55	0.0055-60
30	0.0040	0.0055	0.0045	0.0045	0.0050-55	0.0045
31	0.0050	0.0070	0.0055	0.0055	0.0070	0.0055-60
32	0.0010	-	0.0045	0.0045	0.0005	0.0005
33	0.0010	-	0.0040	0.0040	0.0001-5	0.0001-5
34	0.0010	-	0.0030	0.0030	0.0001-5	0.0001-5
35	0.0010	-	0.0010	0.0010	0.0001-5	0.0001-5
36	0.0010	-	0.0010	0.0010	<0.0001	<0.0001
37	0.0010	-	0.0010	0.0010	<0.0001	<0.0001
38	0.0010	-	0.0010	0.0010	<0.0001	<0.0001

spectrographic analysis of aqueous extracts (%)

K^+ (Spectra)	Mg^{++} (Spectr.)	Ca^{++} (Microchem.)	Ca^{++} (Spectr.)	Al	Fe	Mn
				(Microchem. & Spectr.)		
0.0040	0.0005	0.0020-25	0.0020-25			
0.0130	0.0015	0.0070	0.0070			
0.0040	0.0001-5	0.0020	0.0020			0.0010-0.0001
0.0130	0.0010	0.0010	0.0010			
0.0015-30	0.0001-5	0.0010	0.0010			
0.0040	0.0001-5	0.0010	0.0010			
0.0030	0.0010-05	0.0020	0.0020			
0.0035-40	0.0005	0.0020	0.0020			
0.0050	0.0010	0.0030	0.0030			
0.0015	0.0001	0.0010	0.0010			
0.0015	0.0001	0.0020	0.0020			0.0010-0.0001
0.0010-15	0.0001	0.0001-5	0.001 -5 *			
0.0025-30	0.0010-05	0.0010	0.0010			
0.0025-30	0.0010-05	0.0010	0.0010			
0.0100	0.0005	0.0020	0.0020			0.0010-0.0001
0.0030-35	0.0001-5	0.0020	0.0020			
0.0030-35	0.0001-5	0.0020	0.0020			
0.0020-25	0.0001-5	0.0005	0.0005			
0.0020-25	0.0001-5	0.0010-5	0.0010-05			
0.0100	0.0005	0.0050	0.0050	0.0010 to 0.0001	0.0010 to 0.0001	
0.0035	0.0001-5	0.0055	0.0055			
0.0035	0.0001-5	0.0055	0.0055			
0.0020	0.0001-5	0.0030	0.0030			
0.0040	0.0001-5	0.0040	0.0040			0.0010-0.0001
0.0020-25	0.0001-5	0.0035	0.0035			
0.0050	0.0005	0.0010	0.0010			
0.0040-45	0.0001-5	0.0010-05	0.0010-05			
0.0040-45	0.0001-5	0.0010-05	0.0010-05			
0.0055-60	0.0010-05	0.0010-05	0.0010-05			
0.0045	0.0001-5	0.0010-05	0.0010-05			
0.0055-60	0.0005	0.0010	0.0010			
0.0005	<0.0001	<0.0001	<0.0001			
0.0001-5	<0.0001	<0.0001	<0.0001			
0.0001-5	<0.0001	<0.0001	<0.0001			
0.0001-5	<0.0001	<0.0001	<0.0001			
<0.0001	<0.0001	<0.0001	<0.0001			
<0.0001	<0.0001	<0.0001	<0.0001			
<0.0001	<0.0001	<0.0001	<0.0001			

* Possibly a misprint for 0.0001-5 -- VPS

In reactions from K and Na, $K_2NaCo(NO_2)_6$ and $NaUO_2(CH_3COO)_2$ respectively, the "A" portion of the curve represents solutions more concentrated than ours. Consequently, these reactions cannot be utilized in microturbidimetric procedure.

After our studies of the log I = f (log C) function for AgCl and construction of the appropriate diagram, we proceeded to analyze all of the solutions. Photometric measurements of absorbed light gave us the required points on the ordinate log I, making it easy to obtain the corresponding concentrations; these results are presented in table 6.

TABLE 6. Quantitative analysis of solutions-extracts for chloride ion by the microturbidimetric method

Sample number	log I	log C	C %
1	49	$\bar{3}.95$	0.0089-91
2	132	$\bar{2}.45$	0.027-29
3	43	$\bar{3}.90$	0.0079-81
4	102	$\bar{2}.31$	0.0200
5	8	$\bar{3}.00$	0.0010
6	102	$\bar{2}.31$	0.0200
7	54	$\bar{2}.00$	0.0100
8	20	$\bar{3}.55$	0.0034-36
9	26	$\bar{3}.68$	0.0047-49
10	13	$\bar{3}.30$	0.0019-21
11	13	$\bar{3}.30$	0.0019-21
12	11	$\bar{3}.23$	0.0016-18
13	22	$\bar{3}.60$	0.0039-41
14	25	$\bar{3}.66$	0.0045-47
15	54	$\bar{2}.00$	0.010
16	24	$\bar{3}.65$	0.0044-46
17	24	$\bar{3}.65$	0.0044-46
18	18	$\bar{3}.47$	0.0029-31
19	19	$\bar{3}.50$	0.0031-33
20	76	$\bar{2}.16$	0.013-15
21	79	$\bar{2}.18$	0.014-16
22	43	$\bar{3}.90$	0.0079-81
23	54	$\bar{2}.00$	0.010
24	52	$\bar{3}.99$	0.0097-99
25	69	$\bar{2}.11$	0.012-14
26	27	$\bar{3}.70$*	0.0050
27	24	$\bar{3}.65$	0.0044-46
28	22	$\bar{3}.60$	0.0039-41
29	32	$\bar{3}.77$	0.0059-61
30	22	$\bar{3}.60$	0.0039-41
31	27	$\bar{3}.70$*	0.0050

* ($\bar{3}.6990$)

Practice with the graph (fig. 2) indicated that estimates of log C (logarithm of the concentration), might be reliable only to the second significant figure. In addition, the reliability of log C estimates was found to diminish with increase in concentrations, due to certain peculiarities of the curve log I = f (log C). Within the log C area from 3.00 to 2.00, it was possible to estimate the concentration (C) to the fourth significant figure (± 0.0001); and within the log C area >2.00, only to the third significant figure (± 0.001).

Calculation of Solution Concentrations

Concentrations of our solutions were calculated from the equation:

$C\% = r \frac{c'}{d}$, where C' represents concentration of the constituent in the extract; d, specific gravity of the solution; and r, the dilution factor. Specific gravity of the solution was taken as 1.15, by analogy with the specific gravity of NaCl and KCl solutions having the same concentration.

A preliminary (rough) estimate of concentration was made using a complex equation, where d = f (C). The results are shown in table 7.

Analytical Results

Now let us examine the results of our analyses. We should state, first of all, that our results are chiefly semiquantitative (based on comparison with standards), with the exception of quantitative chloride determinations by the turbidimetric method. At first glance, our results give the impression of contradiction; and, of unwarranted calculations leading to seemingly exact magnitudes based on relatively inexact semiquantitative determinations of many constituents (with the exception of chloride), as well as on volume measurements that are not particularly quantitative. Our results are sufficiently well founded, nevertheless, to permit discussion of basic chemistry principles applicable to included solutions. In making this claim, we realize that certain concrete magnitudes must be at our disposal in any evaluation of the data; particularly in any interpretation of the results. Moreover, analytical error (on the average) is reduced somewhat, in our statistical approach to the replicate analyses thus clarifying general relationships involved.

Analyses (microchemical and spectrographic) of qualitative composition of the included solutions indicate Na^+, K^+, Ca^{2+}, Mg^{2+}, Al^{3+}, Fe, and, occasionally, Mn to be the principal solutes, along with Cl^-, SO_4^{2-}, and BO_3^{3-}.

Quantitative analyses give the following relationships: Na>K>Ca (rarely K>Na) and Ca>Mg. The sum of Al, Mn, and Fe may be as high as 2 percent. Calculations also show that total salt content may be as high as 30 to 35 percent. Presence of only two phases (liquid plus gas), is an additional indication of such magnitudes.

Hydrochloric acid extracts (more thorough and more concentrated than aqueous extracts; r = 500) and their analyses demonstrated heavy metals, Cu, Pb, Zn, Ag, to be present in low concentrations.

Qualitative and quantitative analyses (spectrographic and microchemical) established the presence in all samples of boron (probably as BO_3^{3-}) in relatively high concentrations; a fact not previously reported in the literature. The higher boron content is especially characteristic for quartz inclusions from Ukrainian Crystalline Shield pegmatites. Undoubtedly, this presence of boron is reflected in chemical properties of quartz-forming and quartz-healing systems.

Calculations of molecular and atomic quantities for individual constituents showed a significant excess of cations. Probably this excess is compensated by metasilicates, SiO_3^{2-} and $Si_2O_5^{2-}$ and by hydroxide OH^-, derived from metasilicates by hydrolysis, as well as by CO_3^{2-} with formation of SiO_2 + ROH. Calculation of dissolved Si, as SiO_3^{2-}, indicates that its concentration may be as high as 6 to 12 percent (if we assume its quantitative preponderance in the solution). Concentration of hydroxide and carbonate ions must be relatively low in every case where precipitation of Ca, Mg, Fe, Al, Mn hydroxides and carbonates is an impossibility; attested further by transparency of our solutions. In addition, one should note that solubility of carbonates and hydroxides is probably higher in solutions of this type. Analogous findings by Ravich [43], who observed an increase in solubility of sparingly soluble sulfates in aqueous solutions of alkali chlorides, would support our interpretation.

CONCEPTS OF SOME QUARTZ-FORMING HYDROTHERMAL SYSTEMS

Our concepts of quartz-forming hydrothermal systems are to be based on analyses of solutions from inclusions and on the experimental studies involving physicochemical aspects of silicate systems.

Analyses of included quartz-forming (or quartz-healing) solutions allow us to understand the main chemical properties of these hydrothermal mineral-forming systems. The analyses indicate, as follows:

1. Quantitatively, Na and K are markedly preponderant over other cations in included solutions; next is Ca; then, Mg, Fe, Al, Mn, and others follow.

2. Among the anions Cl^- is quantitatively, markedly preponderant and BO_3^{3-} are subordinate.

3. Heavy-metal cations (of which ore minerals are composed) are present in relatively small amounts.

4. In our case (considering 2-phase inclusions), the lower concentration limit for quartz-forming solutions, with respect to Na, K, and Cl, is from 5 to 6 percent; concentrations of Ca, Mg, Fe, Al, Mn, SO_4^{2-}, BO_3^{3-} are 1 percent and lower.

We refer now, for comparison, to analytical data obtained by other investigators:

Davy, [62], Brewster [61], and Nicol [69] established presence of $CaCl_2$ and $MgCl_2$ in the solutions. Sorby [73], after his prolonged studies of the solutions, concluded that inclusions contain not less than 15 percent K, Na, and Ca chlorides and sulfates. Zirkel [76] demonstrated presence of Na, by the spectrographic analysis of powdered quartz; and, by chemical analysis presence of Cl in aqueous extracts. Pfaff [70] also proved chlorides of Na to be present in inclusions. Prinz [71] described immiscible liquids (apparently the H_2O-CO_2 system) from inclusion. Khruschev [58], made spectrographic observations on Na and Li in the inclusions. Lasaulx [65], while analyzing included solutions, established presence of NaCl, Na_2SO_4, $CaCl_2$, K, Ba, and Sr. Sjorgan [72], during his investigation of inclusions in Sicilian gypsum, determined the dissolved salt as follows: NaCl, 66 percent; Na_2SO_4, 11.4 percent; $CaSO_4$, 9.7 percent; $MgCl_2$, 9 percent, and K_2SO_4, 3.7 percent; Lindgren and Steigl [66] proved large quantities of Ca and SO_3^{2-} to be present in California quartz, in association with smaller quantities of (K, Na)$_2$, O, Cl, Mg, Al_2O_3, and Fe_2O_3. Konigsberger and Muller [64] who studied inclusions in Alpine quartz, made the following list of dissolved constituents: first of all, Na, then Cl^-, CO_3^{2-}, SO_4^{2-}, K, Li, and Ca; according to these authors, Na is vastly preponderant over K in the solutions. Lindgren and Whitehead [67] described inclusions containing up to 37 percent NaCl by volume (using the immersion method); by recalculation, this corresponds to 57 percent by weight. Bowen [60] pointed out that KCl crystals are present in the liquid phase of inclusions. In his investigation of sphalerite inclusions, Newhouse [68] proved that NaCl and $CaCl_2$ are found in included solutions and that the NaCl concentration to be 4.5 mols per liter (L) (approximately 25 percent); as well, he demonstrated presence of Ca and Mg sulfates. M. N. Ivantishin [19] established the following composition for galena inclusions: 9.33 percent Na_2O+K_2O, and 8.66 percent Cl (in dry residue of the filtrate); he also found CaO, MgO, and SO_3^{2-} in aqueous extracts and in the galena itself.

We should pause here to consider the very interesting studies by A. I. Zakharchenko [17] on quartz from Pamir. The inclusions contained crystals of halite, sylvinite, calcite, and hematite; he reported 54.8 milligrams (mg), total content of salts per 100 grams (g) of quartz 38.1 mg Cl^-; 0.7 mg SO_4^{2-}; 6.1 mg HCO_3^-; 14.3 mg Na). By spectrographic analysis of solution obtained upon opening a single inclusion, Zakharchenko proved this solution to contain Na, Ca, Mg, Fe, Al with Na>Ca>Mg. Quantitative analysis

TABLE 7. Chemical composition of solutions of secondary inclusions in quartz

Specimen number	Sample number	% or Mols	Cl^-	SO_4^{2-}	BO_3^{3-}	Na^+	K^-	Mg^{2+}	Ca^{2+}	Al+Fe+Mn[1]	Excess of cations, Mols	SiO_3^{2-}(+CO_3^{2-}+OH^-)[2] %	Sum of salts, %	Water[3] %
1	1	%	5.45	2.10	3.10	4.80	2.40	0.28	1.40	2.00				
	2	%	5.20	2.60	3.40	4.80	2.35	0.22	1.30	2.00				
	3	%	5.30	2.26	3.25	4.80	2.62	0.24	1.25	2.00				
	av.	%	5.12*	2.35*	3.20*	4.80	2.45	0.24	1.33*	2.00				
		Mols	0.146	0.028	0.054	0.206	0.063	0.010	0.033	0.050	0.134	10.02	31.49	68.51
2	4	%	3.86	3.80	3.75	4.10	2.56	0.79	0.26	2.00				
		Mols	0.110	0.044	0.064	0.178	0.066	0.033	0.006	0.050	0.115	8.75	20.87	79.13
3	5	%	0.84	2.78	1.85	2.78	0.93	0.16	0.84	0.5				
		Mols	0.024	0.032	0.031	0.120	0.023	0.007	0.021	0.012	0.096	7.30	17.98	82.02
4	6	%	7.10	2.35	2.75	6.07	1.62	0.16	1.05	2.00				
		Mols	0.200	0.027	0.046	0.264	0.042	0.007	0.026	0.050	0.116	8.85	31.95	68.05
4	7	%	7.80	-	4.30	5.80	2.60	0.60	0.53	2.00				
		Mols	0.222	-	0.073	0.250	0.067	0.025	0.013	0.050	0.110	8.38	32.01	67.99
5	8	%	4.00	2.00	1.90	1.10	4.15	0.70	2.40	2.00				
	9	%	4.20	1.86	2.10	1.15	4.20	0.84	2.52	2.00				
	av.	%	4.10	1.94*	2.00	1.12	4.18	0.77	2.46	2.00				
		Mols	0.117	0.022	0.034	0.055	0.107	0.032	0.061	0.050	0.128	9.70	28.52	71.48
6	10	%	3.57	1.75	0.36	4.20	2.20	0.18	0.20	2.00				
		Mols	0.102	0.020	0.061	0.180	0.056	0.007	0.005	0.050	0.115	8.75	23.25	76.75
7	11	%	3.94	2.30	4.52	3.50	3.10	0.20	0.39	2.00				
		%	4.00	2.10	4.30	3.40	3.20	0.20	0.40	2.00				
		%	3.98	2.20	4.41	3.45	3.15	0.20	0.40	2.00				
		Mols	0.109	0.025	0.075	0.148	0.082	0.008	0.010	0.050	0.089	6.75	26.54	73.46

8	13	%	3.80	1.15	2.5	3.20	2.60	0.50	0.80	2.00				
	14	%	3.80	1.10	2.20	3.20	2.55	0.50	0.80	2.00				
	av.	%	3.80	1.12	2.25*	3.20	2.55*	0.50	0.80	2.00				
		Mols	0.110	0.013	0.040	0.140	0.064	0.023	0.020	0.050	0.134	10.02	26.38	73.62
9	15	%	7.65	0.88	3.78	3.09	7.65	0.38	1.50	2.00				
		Mols	0.318	0.012	0.064	0.134	0.196	0.016	0.037	0.050	0.139	10.06	36.99	63.01
10	16	%	3.50	2.50	2.30	3.85	2.40	0.20	1.40	2.00				
	17	%	3.50	2.30	2.30	3.75	2.50	0.20	1.40	2.00				
	av.	%	3.50	2.40	2.30	3.80	2.45	0.20	1.40	2.00				
		Mols	0.100	0.028	0.039	0.165	0.063	0.008	0.035	0.050	0.154	11.70	27.75	72.25
11	18	%	3.80	2.40	1.20	3.10	2.80	0.40	0.60	2.00				
	19	%	4.20	2.60	1.20	2.90	2.80	0.40	1.00	2.00				
	av.	%	4.00	2.50	1.20	3.00	2.80	0.40	0.80	2.00				
		Mols	0.114	0.029	0.020	0.130	0.072	0.016	0.020	0.050	0.125	9.50	26.20	73.80
12	20	%	4.93	0.79	2.84	3.72	1.20	0.08	1.85	2.00				
	21	%	4.92	0.91	2.85	3.70	1.21	0.07	1.90	2.00				
	22	%	4.95	0.80	2.86	3.68	1.10	0.08	1.91	2.00				
	23	%	4.91	0.78	2.90	3.60	1.19	0.09	1.89	2.00				
	24	%	4.96	0.90	2.89	3.62	1.20	0.08	1.85	2.00				
	25	%	4.97	0.89	2.88	3.64	1.20	0.08	1.80	2.00				
	av.	%	4.94	0.85	2.87	3.66	1.20*	0.008	1.85*	2.00				
		Mols	0.140	0.009	0.048	0.160	0.031	0.003	0.046	0.050	0.093	7.08	24.53	75.47
13	26	%	3.46	4.55	3.79	2.60	3.50	0.34	0.70	2.00				
	27	%	3.48	4.58	3.78	3.00	3.40	0.35	0.70	2.00				
	28	%	3.50	4.61	3.77	4.20	3.70	0.35	0.70	2.00				
	29	%	3.40	4.67	3.75	3.40	3.30	0.36	0.70	2.00				
	30	%	3.42	4.70	3.73	4.40	3.80	0.34	0.70	2.00				
	31	%	3.44	4.73	3.74	4.80	3.90	0.34	0.70	2.00				
	av.	%	3.44*	4.64	3.76	3.80*	3.60	0.34	0.70	2.00				
		Mols	0.098	0.054	0.064	0.165	0.092	0.014	0.017	0.050	0.122	9.30	29.58	70.42

* Averages appear to be incorrect. 1/ All percent values approximate. 2/ "By Difference": to balance the excess of cations. --VPS.
3/ "By difference": 100 minus total salts. --VPS

showed Na and Ca content amounting to tens of percent, and Mg, of a few percent. Determination of hydrogen ion levels (pH) indicated definitely alkaline reaction. One must remark that this is the only determination on record of pH that has any value, in our understanding of the chemistry applicable to quartz-forming solutions. A. I. Zakharchenko described a noteworthy phenomenon, observed on opening inclusions: i.e., browning of the cracks, indicative of iron dissolved in high concentration.

N. P. Yermakov [10] made some objections to the possibility that any appreciable amount of substance could be deposited from mineral-forming solutions, as a coating [Tr.: in the inclusion cavity. VPS], after sealing of the inclusion. Yermakov, however, did describe some inclusions whose margins were lined substantially with a precipitated substance; he attributed the origin of these inclusions to some special mechanism of the precipitation. In addition, he noted presence of the cognate substance precipitated on inclusion-cavity walls as a thin "band" to be a phenomenon relatively common to high-temperature inclusions. This circumstance amounts to substantial proof of the rather appreciable solubility of Si in quartz-forming solutions. Yermakov pointed out that V. A. Kaliuzhnyi, of the Laboratory of Thermometric Analysis, University of L'vov, had succeeded in isolating halite and sylvinite crystals from multi-phase inclusions, and in their identification by halite immersion method. Multi-phase inclusions in Pamir quartz, containing halite up to 40 percent by volume, were investigated by Yermakov. Multi-phase inclusions of this type may be homogenized completely by a careful application of heat; an indication to the effect that the solid substance was precipitated after inclusions were sealed.

G. G. Lemmleyn [29] described an interesting example of inclusion morphology in quartz and topaz where cavity walls of a primary inclusion had been lined by a precipitated substance. According to his calculations, there had been a 25 percent and a 20 percent volume decrease in quartz and topaz, respectively, after the deposition of the precipitated substance.

G. G. Lemmleyn and M. O. Kliya [30] performed some interesting measurements on thickness of precipitated topaz, owing to blocking effects of the gaseous bubble in certain parts of the inclusion in depressions and on inclusion-cavity walls. Their measurements revealed not less than 2 volume-percent of substance, in reference to total volume of inclusion cavity, to have been occupied by precipitated topaz, in the case of a multi-phase inclusion. Let us undertake here a simple calculation: 2 volume-percent per 100 cm^3 total volume in 2 cm^3 2 x 3.5 (specific gravity of topaz) = 7 g. Topaz contains from 39 to 28 percent SiO_2; hence, we have 2.08 g SiO_2 per 7 g of topaz. The result is 2.08 percent of solution mass. This simple calculation, based on the interesting data of G. G. Lemmlein and M. O. Kliya, indicates appreciable solubility of Si in topaz-forming solutions.

We pass, at this time, to experimental studies of certain silicate mineral-forming systems and, of their analogues. O. F. Tuttle and I. I. Freedman [52] investigated the H_2O-Na_2O-SiO_2 system. A part of this system was studied previously from the melting point of $Na_2Si_2O_5$ (874°C.) to 735°C, by Morey and Ingerson [32]. These studies indicated that solutions containing as high as 45 percent SiO_2 at 250°C (one liquidus) as high as 50 percent SiO_2 at 300°C and as high as 60 percent SiO_2 at 350°C (two liquidi) may exist in systems of the type here discussed. Liquation was observed in the system [Tr.: i.e., H_2O-Na_2O-SiO_2. VPS]. According to Tuttle and Freedman, the lower critical point of the two liquidi ranges from 200 to 250°C approximately; liquation disappears at lower temperatures. We may observe certain analogies in the chemistry of included solutions and, of the system H_2O-Na_2O-SiO_2. From our point of view, accordingly, ideas regarding principal characteristics of quartz-forming systems must be based on this particular type of system.

Morey and Fenner studied the ternary system H_2O-K_2O-SiO_2 [2]. Morey showed that the K_2SiO_3 system contains no immiscible liquids in the saturated solution field comprising the gaseous phase. The 3-phase equilibrium curve is not interrupted by any critical phenomena and carries only indications of incongruent melting points.

Smit [46], in studying a multi-component system which he assumed to be the prototype of magmatic systems, proved the SiO_2 concentration could reach 7 percent, in the liquidus (the system is rich in alkali metals). He indicated, as well, the technical possibility of quartz production from alkaline solutions (Devile, Mashke, Fridel [6]; Sarazen, and others).

A. Uoker and E. Biuler [38] used alkaline solutions containing carbonate and hydroxide of Na, in technological quartz-crystal production; crystallization temperature was fluctuating in the vicinity of 400°C and pressure ranged from as much as 850 to 1,000 atmospheres. G. Van Praag [37] employed aqueous solutions of Na_2CO_3, $NaHCO_3$, $NaBO_2$, CH_3COONa, NaCl, Na_2HPO_4, and NH_4F in his laboratory studies of artificial quartz production. Spechiya [37, 38] produced quartz crystals from sodium metasilicate and sodium chloride solutions, by adding quartz fragments to the solutions. L. Tomas and N. and V. Vuster [37] employed the same type of system for quartz production in the laboratory.

Vyart [38] crystallized quartz from alkaline solutions. Easy solubility of quartz in alkaline solutions was noted by R. Barrer [37].

Research by Soviet scientists, first of all, D. S. Belyankin [1] and N. I. Khitarov and coworkers [53-57] is of major importance to our understanding of silica transfers, critical phenomena in solutions, and high-temperature characteristics of aqueous solutions.

With reference to ternary systems, we must call attention to the very interesting study of Ravich [43]: On the basis of his experimental studies of eutonic solutions H_2O-NaCl-KCl, H_2O-KCl-K_2SO_4, H_2O-NaCl-Na_2SO_4, and $H_2O + (2KCl + Na_2SO_4 \rightleftharpoons 2NaCl + K_2SO_4)$, the author concluded that behavior of the salt mixture (in reference to behavior of component salts as single entities) is not intermediate in its characteristics. Therefore, it is not possible to surmise behavior of salt mixtures, even approximately, from vapour-pressure curves for saturated solutions of corresponding salts in binary systems [43, p. 135]. The [B] + L + G curve for the eutonic H_2O-NaCl-KCl. mixture shows pressures appreciably too low by comparison with individual 3-phase curves for the binary systems H_2O-NaCl and H_2O-KCl. Ravich cited the example of the sulfate system. It was demonstrated experimentally that K and Na sulfates, moderately soluble in water, are very soluble in alkali chloride solutions, and, that their solubility increases with temperature.

The foregoing review of experimental findings should be, on one hand, a warning to us not to treat complex systems by means of generalization (summation) of simpler systems. Consequently, one must be very careful when using premises of binary systems, in the construction of generalized diagrams for systems containing three or more components. On the other hand, a wide range of possibilities is evident in natural multicomponent systems, with regard to solubility and transfer of their less mobile components. Metasilicates and hydroxides, because of their higher solubility in chloride solutions, should exhibit behavior analogous to that of moderately soluble sulfates.

The principal quartz-forming systems, taking taking into account all of the foregoing consideration may be represented as follows:

1. Major constituents of the systems will be:

H_2O (solvent), Na^+, K^+, Ca^{2+}, Mg^{2+}, Fe^{2+}, Al^{3+}, Mn, Cl^-, SO_4^{2-}, SiO^{2-}, $(Si_2O_5^{2-})$, BO_3^{3-}, and OH^- ions. Quartz-forming systems, of our investigation, were found to contain relatively high concentrations, (from 30 to 35 percent total salts, approximately): chlorides, sulfates, and borates of Na, K, Ca, Mg, Al, Fe, Mn and alkali metasilicates such as $Na\,SiO_3$, $K_2\,SiO_3$, $Na_2\,Si_2O_5$, and $K_2\,Si_2O_5$. Alkalinity of these solutions should be ascribed to hydrolysis of alkali metasilicates, accompanied by SiO_2 precipitation and by hydroxide ion formation, according to the equations:

$$R_2SiO_3 \longrightarrow SiO_2 + R_2O;$$
$$R_2O + H_2O \longrightarrow 2ROH \longrightarrow 2R^+ + 2OH^-;$$
$$R_2Si_2O_5 \longrightarrow 2SiO_2 + R_2O;$$
$$R_2O + H_2O \longrightarrow 2ROH \longrightarrow 2R^+ + 2OH^-.$$

2. Commonly observed contamination of quartz by Fe, Al, and Mn hydroxides is one convincing proof to the effect that pH >7 for quartz-forming solutions; their co-precipitation never should be expected in acid environments. Presence of solid iron hydroxides and of carbonates in solid phase of many inclusions is another indication of original alkalinity of the quartz-forming solutions.

3. We should bear in mind, on appearance of hydrogen ion (H^+) in these solutions and consequent neutralization of the hydroxide, alkali-meta-silicate hydrolysis increases and the reaction $R_2SiO_3 + H_2O \rightleftharpoons SiO_2$ shifts rapidly to the right. Hydroxide ion neutralization is brought about by hydrogen ion easily formed by SO_2, SO_3, CO_2, B_2O_3, Cl_2 ($+H_2$) interaction, and that of other bases with water, as, for example: $SO_3 + H_2O \longrightarrow 2H^+ + SO_4^{2-}$. In such solutions, as shown by the analyses, SO_4^{2-}, BO_3^{2-}, Cl^- are present in appreciable quantities. This means that alkalinity decrease is responsible for increased SiO_2 precipitation from its solutions.

4. On consideration of the hydrolysis $R_2\,SiO_3 + H_2O \rightleftharpoons 2ROH + SiO_2$, it is possible to state, in the instance of confined systems (e. g., included solutions), this reaction to be inhibited entirely when hydroxide concentrations are increased to a certain level (by metasilicate hydrolysis). Thus, the equilibrium of a solution sealed within an inclusion shall be markedly different from that of the identical solution in a relatively open system (i. e., in solutions not captured by the crystal, nor those in which crystal is immersed); where hydroxide ions have a chance to react with the host rock, with other available minerals, or, to neutralize gases (should any SO_2, SO_3, B_2O_3, CO_2, etc., be present) at the given temperature. In a confined system, hydrolysis will be inhibited but will proceed to its end in an open system. Moreover, at a given temperature, metasilicate concentration will be immeasurably greater in the included solution (hydrolysis inhibition) than in the solution outside the crystal.

a) Acidity (pH) of quartz-forming solutions cannot be expressed as any particular magnitude; pH of the system changes with temperature, concentration, and crystallization with environment (open systems). Solution alkalinity increases in confined systems following SiO_2 precipitation. In open systems, on the other

hand, with their low pH and Si concentration gradients, slow quartz deposition, with insignificant pressure and temperature fluctuations, should be conducive to the growth of good single-crystals.

b) Equilibrium conditions and, consequently, solution equilibrium itself are markedly different in the inclusions (confined systems) from open-system equilibrium conditions (solutions outside the crystal). After having been sealed within inclusions, quantities of precipitated quartz are markedly different also from quantities of quartz precipitated by the solution outside the crystal, on its exterior surfaces (from comparable volumes of other solutions).

Consequently, exterior quartz-crystal boundaries formed after the inclusion was sealed, are characteristic only of some lower concentration limit for solutions (with respect to soluble silica salts). Concentration of these salts is undoubtedly higher in quartz-forming solutions than one would suppose it to be, judging by the margins of deposited substance.

It must be emphasized that our views, as here stated, refer to principal quartz-forming hydrothermal systems, basic mechanisms of Si transfers in hydrothermal environments. Undoubtedly, there do exist in nature quartz-forming systems of other types; for example, systems where pH <7, containing large amounts of acid anhydrides, CO_2, SO_3, and others. Si transfers are retarded significantly in acid environments. Quartz-forming systems at pH <7 are apparently younger than the alkaline systems.

It should be noted, by analogy with the systems of H_2O-Na_2O-SiO_2 and H_2O-K_2O-SiO_2, there is no reason to expect any critical phenomena in saturated solutions of relatively concentrated, quartz-forming hydrothermal systems.

MULTICOMPONENT PT DIAGRAMS OF HYDROTHERMAL QUARTZ-FORMING SYSTEMS; THEIR USE IN INTERPRETATION OF QUARTZ FORMATION AND THERMOMETRIC MEASUREMENTS IN QUARTZ

Principal Features of Systems Containing Volatile and Non-Volatile Components

Systems containing volatile and sparingly volatile components are among the most complicated in physical chemistry; all aqueous solution (water-salt) are of this type. Marked differences in the volatility of their components are characteristic of these systems; while certain of these may be present in the gaseous phase above the critical point, others exist concurrently, only in the solid phase.

Theoretical premises for diagrams of these systems (essentially binary) were developed by A. N. Zavaritskiy [15, 16], G. Tamman [50], G. B. Roozeboom [78], P. Niggli [33], and others.

VTX and PTX diagrams must be employed in interpretations of mineral formation in systems where water is the principal component.

VTX diagrams are especially useful for systems of constant specific volume; we are dealing with systems of this type in homogenization thermometry of inclusions. The appropriate diagrams were discussed by I. A. Ostrovsky [40, 42] and cited in our earlier publications [4, 5].

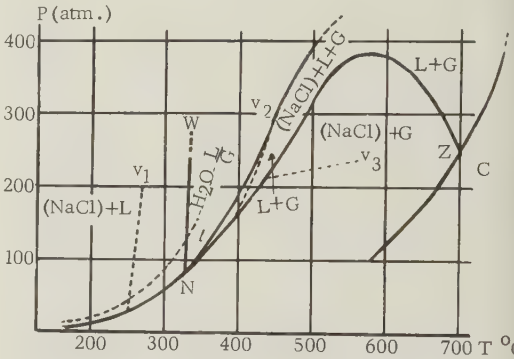

FIGURE 3. Pressure-temperature diagram for Na_2O-NaCl (X = 40 percent Cl)

Utilization of VT diagrams enabled us to consider theoretically the volume-ratio curves for the liquid and gaseous phases, V_{liquid}: V_{vapor}, during application of heat, and to calculate homogenization temperatures. The results may be used, in turn, as a means to study the chemistry of these systems. In this particular case, use of analogous interpretations enabled us to prove the aqueous nature of solutions [5]. In addition, we employed PT profiles of binary-system PTX diagrams at x = constant [4, 75]. Figure 3 shows the PT diagram of the system H_2O-NaCl, x = 40 percent NaCl, constructed from data in the literature [2]. Curves divide this entire PT diagram into discrete stability fields of the phases.

The saturated-solution curve with the gaseous phase, [B]+L+G, has a maximum. The L+G field borders on the upper part of this curve; the saturated-solution field, [B]+L, borders on its lower part. The saturated-gaseous-solution field develops at lower pressures. The solubility curve NW, which may be drawn almost parallel to the pressure axis, emerges from point N (N represents intersection of the concentration curve with the liquidus branch for saturated solutions in the TX projection).

Thus, we have three areas where crystal-

lization of the B component is possible:
a) The saturated-aqueous-solution field [B]+L;
b) The saturated-gaseous-solution field [B]+G;
and c) the saturated-solution field [B]+L+G.

On the application of heat, inclusions developed during crystallization of any one phase are homogenized differently; they have their own characteristics [Tr. : i. e. depending on the phase in which crystallization occurred. VPS], and ranges of error in measurement.

Magnitudes of error in temperature measurement by homogenization method depend on position of the given isochore in the given field (for example: V_1, V_2, or V_3, in figure 3); specifically, by isochore slope with respect to the T axis ($\Delta t = \Delta pt \times \cot\alpha$, where α is the angle between the isochore and the T axis). [Tr. : A complete physicochemical interpretation of homogenization method is omitted here; inasmuch as this subject was discussed in our earlier publications in greater detail [4, 5].

Let us consider, in brief, metastable-state phenomena not previously discussed, which undoubtedly distort the anticipated theoretical pattern in a number of instances.

The phase state of included substances is a function of thermodynamic factors (p, t, x). Individual isochores (V = constant; p = f (t) of the PT diagram for a given system (x = constant), serve to characterize phase composition for the system. We may employ these diagrams to interpret the state of the system as a verification of experimental results. One must remember, however, that the metastable-state phenomena may be imposed on theoretically rational patterns; particularly in the low temperature field, where it distorts these patterns significantly.

Let us refer now to several empirical facts: 1) N. P. Yermakov describes [10, p. 138] his interesting observations on heterogenization of an homogenized system: "The bubbles of gas that had disappeared from inclusions on heating of their host crystal to a given temperature, became reestablished upon cooling to temperature several degrees or tens of degrees below homogenization temperature."

Analogous phenomena are reported by S. A. Chaykovsky [59], who points out a 10°C drop in temperature (185-175°C) of gaseous-bubble reappearance.

These same facts were established by L. I. Koltun at the Thermometric Laboratory, L'vov University (oral communication). While measuring homogenization temperatures of quartz inclusions from Aldan quartz veins, he noted a 5 to 50°C delay, as opposed to homogenization temperature, in reappearance on cooling gas bubbles. L. I. Koltun emphasizes that this phenomenon is very common; it depends significantly on the shape of the inclusion cavity.

It should be noted that heterogenization delays, with reference to homogenization, are characteristic to a very large extent for temperatures up to 100°C. N. P. Yermakov believes (10, p. 139), on occasional inclusion homogenization below temperatures from 70 to 80°C: "gas bubbles do not reappear on cooling, even though inclusion systems were not disturbed by heating." Crystal-growth experiments described by N. P. Yermakov showed "discrete gas bubbles in inclusions to develop generally, from 65 to 70°C."

At the same time, based on entirely theoretical premises, we know through consideration of PT diagrams for water that single-phase inclusions should be expected to develop only at low temperatures and high pressures (within the field, to the left, and above the 1.00018 isochore; for example, judging by the water diagram, for 40°, 50°, 200°C corresponding pressures must exceed 180, 300, 3000 bars, respectively, if inclusions are to form); or, when the temperature of observation exceeds temperature of inclusion formation from a homogeneous system.

Thus, metastability phenomena become superimposed on the theoretical pattern of phases, and, in consequence, modify this pattern to a substantial degree.

In his book, Investigation of Mineral-Forming Solutions [10, p. 140], N. P. Yermakov describes appearance of a gaseous phase as taking place not at once but only after a certain time, in crystal inclusions of halite and alum grown artificially at low temperatures. He explains this phenomenon to result from a "leakage" of substance out of the inclusion through the crystal lattice. It is not our intention to argue against this view, that requires detailed experimental proofs. We believe the common state of metastability also to be effective in the case here discussed; and, that the system attains its regular stable heterogeneous state only after a period of time and under the influence of different external and internal factors: temperature changes, mechanical agitations, and inclusion-cavity transformation.

It follows, therefore, from metastability effects here considered in brief, that one must be very careful in formulating conclusions about single-phase inclusions, inasmuch as we are never sure whether the system is present in its stable or metastable state.

Single-phase inclusions may be indicative in general of relatively low formation temperatures (up to 100°C); although, not commonly, they may represent temperatures higher than those of low-temperature two-phase inclusions.

PT Diagrams of Ternary Systems

Principal features and practical applications of binary system diagrams to be taken into account in dealing with multicomponent systems were already discussed in brief. Let us consider 3-component systems that illustrate modifications caused by additional components.

First of all, one may be reminded of an early remark by N. Niggli [33, p. 289] to the effect that marked distinctions in fugacity [Tr.: i. e., escaping tendency. VPS] of components (the primary feature of the system) already are graphically conspicuous in binary system diagrams and, in this connection, multicomponent systems present no new fundamental problems. The phenomena remain the same; our only need is to have them projected in a higher-dimensional space.

Our discussion of ternary system diagrams is to be conducted for mixed-type 3-component systems, with Nikolaev's "special component C", which he takes to be the prototype of magmatic systems. A diagram of this kind is composed of one easily volatile component, one sparingly volatile component of the rock-forming silicate type, and one sparingly volatile component of the chloride or alkali-metasilicate type (the "special component C"). PT profiles of such diagram indicate clearly that increases in component-C concentration cause alterations in phase-equilibria of the system.

Let us consider briefly PT profiles of 3-component systems represented in figures 4 and 5, so that we may become acquainted with principal features of these diagrams. The profiles were made at a definite composition (x = constant).

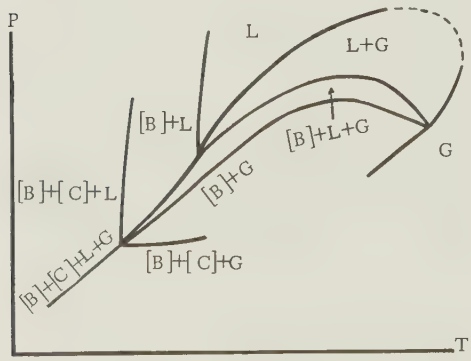

FIGURE 4. Pressure-temperature diagram of a three-component system (x = constant) (there are no critical phenomena in the field of saturated solutions)

Figure 4 represents a 3-component system, Type I, with continuous phase equilibrium, [B]+L+G. The 3-phase equilibrium (fig. 5) is interrupted by critical phenomena which cause

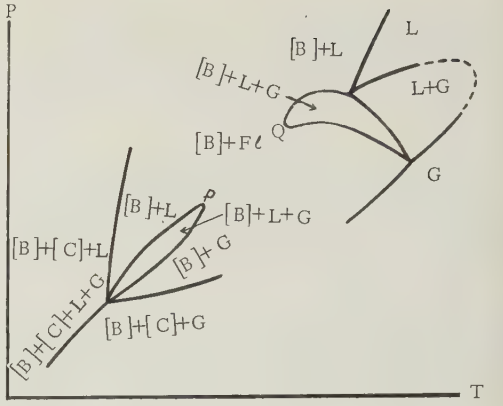

FIGURE 5. Pressure-temperature diagram of a three-component system (the PQ type)

the appearance of two critical points, P and Q. This diagram shows what particular elements are subjected to changes resulting from an increased number of components. As a result of an increased number of components, the monovariant 3-phase equilibrium [B]+L+G of 2-component systems is transformed into a bivariant equilibrium and the [B]+L+G line becomes a band.

Figure 4, with an increased number of phases in the saturation field with respect to the second non-volatile component C ([B]+[C]+L+G), the bivariant equilibrium [C]+L+G becomes monovariant; [B]+[C]+L+G. There develop, moreover, 3-phase equilibria fields with solid phases [B] and [C]: [B]+[C]+L and [B]+[C]+G.

Let us examine a more complex diagram representing liquation without critical phenomena in the field of saturated solutions with gaseous phase.

An analogous diagram for binary systems involving liquation was considered by V. A. Nikolayev [36] and I. A. Ostrovsky [41; Pattern "a", fig. 1]. A PTX diagram for binary systems involving liquation was also by Ostrovsky [40]. The PT diagram for a 2-component system (x = constant) involving liquation is represented in figure 6. The 3-phase-equilibrium curve is

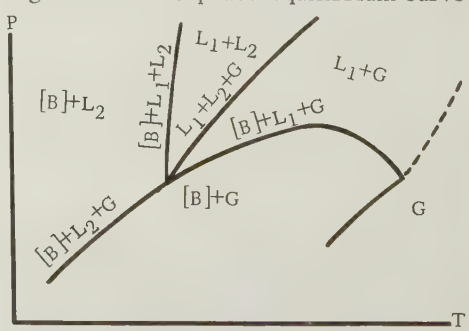

FIGURE 6. Pressure-temperature diagram of a two-component system with liquation phenomena (without critical phenomena)

divided into two parts, L_1 and L_2, by the non-variant point. The 3-phase equilibrium curve, L_1+L_2+G, has its origin also in the 4-phase equilibrium non-variant point, $[B]+L_1+L_2+G$. The 2-phase equilibrium fields occupy their appropriate positions between the two: $[B]+L_2$, L_1+L_2, L_1+G, $[B]+G$. Upon introduction of the C component, this system becomes a 3-component system; and, in agreement with phase rule, all monovariant equilibrium curves will pass to bivariant-equilibria fields (fig. 7). For example, the 3-phase bivariant equilibrium field in the lower part will fall within the saturation area, with respect to C components, but will pass into the monovariant equilibrium (line) after introduction of the 4th phase.

The 3-phase equilibrium fields, $[B]+[C]+L_2$ and $[B]+[C]+G$, will be developed accordingly.

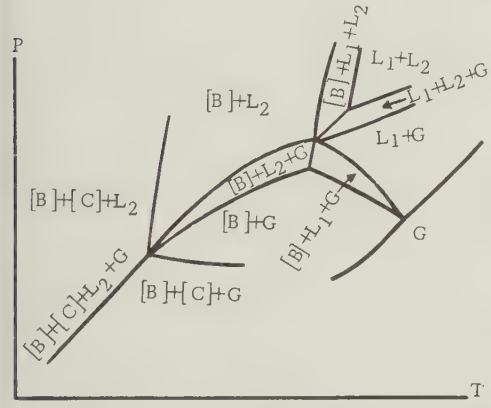

FIGURE 7. Pressure-temperature diagram of a three-component system with liquation phenomena

It become clear, on comparison of figures 6 and 7, in what manner heterogeneous equilibria undergo change on transition from 2-component to 3-component system.

PT Profiles for Ternary Systems of Nikolayev's Mixed Type at Constant Composition

A ternary system of Nikolayev's mixed type may be regarded most rationally as the prototype of typical magmatic systems. The TX projection of Nikolayev's 3-component system is represented in figure 8. The ternary system has the following components:

A - the volatile component (H_2O); B - the non-volatile component (a rock-forming silicate); C - the "special" component (alkali silicates, alkali sulfides and halogen compounds, halides and sulfates of alkaline-earth and of heavy metals).

Marginal systems: System AB, Type III (with a single critical point P); System AC, Type I, with unlimited mutual solubility of its components, and with maxima on the 3-phase curve; System CB, with eutectics.

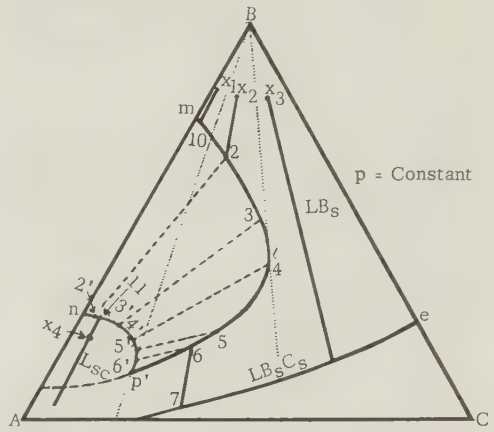

FIGURE 8. Isobar diagram of a ternary system with the "special Nikolayev component C"

The following should be represented by the diagram for a ternary-system of Nikolayev's Mixed Type:

1. The principle of limited volatility, within marginal system AB, which exerts a strong influence on the entire ternary system.

2. Presence of "special" component C which, together with A (the volatile component), forms a marginal system, Type I.

We must direct our attention now to the role of "special" component C. An increase in C concentration, to a certain level, changes the entire character of the system by transforming it from Type III (water - a rock-forming silicate) into Type I, with a maximum on the 3-phase curve and without interruption by any critical phenomena of the 3-phase equilibrium $[B]+L+G$.

Following this, changes begin in the sequence of heterogeneous equilibria. When A:C is high in systems rich in the B component (composition x_1, fig. 1 [Ed: fig. 8]), the magmatic stage L will be separated from hydrothermal phase L' by pneumatolitic stage $[B]+F$ (G); when A:C is low (composition x_2 and x_3, figure 8), there exists even the possibility by analogy with the well-known generalization by Niggli (the Type I diagram), of gradual transition from melt L to hydrothermal solution L', with concurrent gaseous-phase separation. The possibility that the liquid phase exists continually throughout the crystallization temperature range with gradual transition from melt L to hydrothermal solution L' is considered by V. A. Nikolayev as the most important conclusion obtained by analysis of ternary systems of mixed type.

Proceeding from the TX diagram for a

ternary system of Nikolayev's Mixed Type, we may construct a series of PT profiles for its individual components (x = constant). We constructed PT profiles of three typical cases. The profiles serve to characterize fully these typical cases, as well as the course of crystallization studied by V. A. Nikolayev in his TX diagram.

PT profiles may be constructed only for confined systems, however (distillation Type I), because constancy in the system's composition is their absolute prerequisite. Let us consider then, some individual cases in the construction of the diagram:

Composition x, Close to B, between Segments of Bm and B'p Straight Lines (A:C High; Figure 8)

Analogous to the Nikolayev's successions: with decreasing temperature, in our PT diagram at x = constant, equilibrium is shifted from the B+L field to the 3-phase-equilibrium field (fig. 9a) (provided that external pressure against the system exceeds maximum pressure on the 3-phase curve in system AC and, on eutectic curve LBC). Distillation takes place first, followed by condensation of the gaseous phase and by transition of the system, at temperature point 11, to the super-critical saturated-phase field with solid B: [B]+F ($L_{sc.}$).

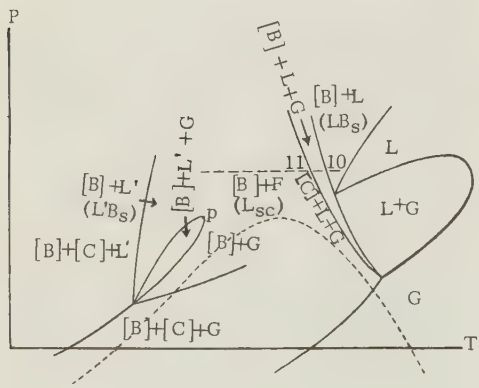

FIGURE 9a. Pressure-temperature profiles of a ternary system of Nikolayev's mixed type, at constant composition (x_1 = constant); confined systems (distillation type I)

On the whole, this diagram is analogous to the PT diagram for binary systems of Nikolayev's Type III [34, 35]. Thus, we are dealing with the hydrothermal-solution field and 3-phase equilibria, [B]+L+G (the binary equilibrium) pivoted at critical point P; the system passes into the saturation field with respect to "special" component C, where corresponding monovariant equilibrium already is represented by curve [B]+[C]+L'+G. The saturated melt with gaseous phase [B]+L+G, becomes separated from the hydrothermal-solution area [B]+L'+G by the super-critical saturated-phase field [B]+F. The tri-phase equilibrium band]B]+L+G has no maximum. Transition from first liquid phase L (the melt) to second liquid phase L' (the solution) is continuous throughout the super-critical phase area F, by analogy to the typical diagram: (water - a rock-forming silicate).

Composition x_2 $(A:C)_2 < (A:C)_1$. Composition Point Lies Between B^1p and BL Segments of the Straight Lines (Fig. 9b).

This diagram changes its character abruptly; it assumes the appearance of a typical PT diagram (a volatile, a sparingly volatile component) at constant composition, with a definite maximum in the 3-phase equilibrium band [B]+L+G. The influence of "special" component C is quite noticeable in the PT profile; increase in concentration of this component is followed by complete change in character of the diagram. We are dealing here with gradual transition from liquid phase L to solution L'.

For x_2, 3-phase equilibrium [B]+L+G reaches higher concentrations of volatile component A. For x_3, where C > A, pressure falls abruptly (fig. 9b).

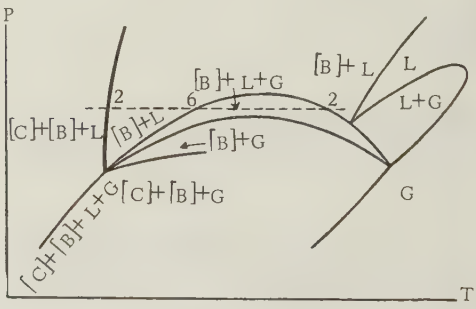

FIGURE 9b. Pressure-temperature profiles of a ternary system of Nikolayev's mixed type, at constant composition (x_2 = constant); confined systems (distillation type I)

At composition x_2 (isobaric temperature decrease), transition takes place through 3-phase-equilibrium area [B]+L+G. For case x_3, at the same pressures, the gaseous-phase area remains unaffected by decreasing temperature, inasmuch as it occurs at significantly lower pressures because of lowered volatile-substance concentration.

The diagram represented in figure 9a, reflecting ternary systems of mixed type, characterizes typically primary magmatic systems. This diagram is not particularly interesting to us; diagrams representing residual magmatic

systems (hydrothermal) are far more important (figs. 9b, 9c, and 10).

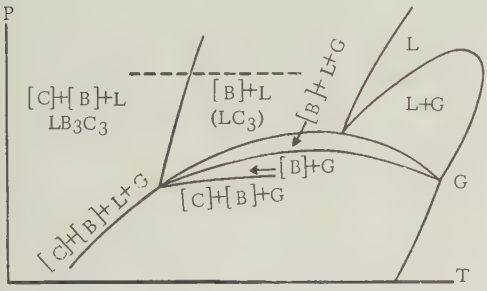

FIGURE 9c. Pressure-temperature profiles of a ternary system of Nikolayev's mixed type, at a constant composition (x_3 = constant); confined systems (distillation type I)

Let us consider the case of super-critical phase separation from solid phase [B], by using PT profiles for a 3-component system of Nikovayev's Mixed Type (fig. 8, at x_1 [35, p. 71]), with its constancy having continuous duration. At certain relatively high magnitudes for P and T, composition x_4 will represent unsaturated critical-phase relatively high in volatile component A (the prototype of hydrothermal systems). This particular case will be typical of Type II distillation, according to V. A. Nikolayev [35]. Like the preceding ones, a diagram of this type may be constructed from the well-known profiles of Smith's and White [75], with composition remaining constant, analogous to the Smiths' profile, as represented by Niggli. An example of Type II distillation is given in figure 10 analogous to the lower left part of the diagram in figure 9a.

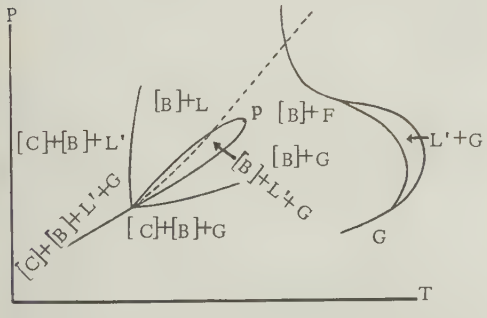

FIGURE 10. Pressure-temperature profile for residual composition x_4 = constant, after distillation type II (separation of gaseous phase in an open system at the original composition x_1; the hydrothermal stage)

Saturated systems [B]+F become undersaturated with respect to their [B] component only in high temperature fields.

Generalized PT Diagram for a 5-Component System; its Use in Interpretation of Thermometric Measurements

Complete PTX diagrams may be constructed only for one-component systems. For systems with a larger number of components, all constructions must be transferred into a higher dimensional space. Using only an areal PT diagram, however (without considering individual phase concentrations), it is possible to represent ternary as well as multi-component systems involving marked volatility differences between principal solvent and solutes, provided their composition remains constant. Such diagrams (corresponding to PT profiles for binary and ternary systems) are well adapted for theoretical interpretation of diverse cases involving thermometric measurement by homogenization method.

Let us consider now a generalized diagram (fig. 11) of a 5-component system probably analogous to hydrothermal quartz-forming systems investigated by us (relatively high solution concentrations; saturation curve for solutions having a gaseous phase is analogous to Type I diagrams; no critical phenomena in saturated liquid phases).

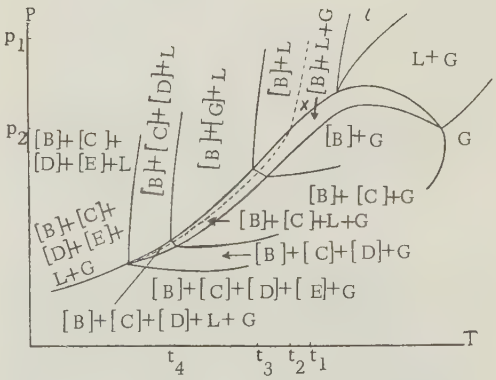

FIGURE 11. A generalized pressure-temperature diagram of a five-component system of the quartz-forming type.

The diagram for a 5-component system represented in figure 11 was derived from a simpler 3-compnent diagram (analogous to the profile in (fig. 9b); supplemented only by appearance of new solid phases at decreased temperatures. Accordingly, both number of components and of curves defining areas of heterogenous equilibria were augmented. Monovariant equilibrium here is at (n+1) phases (n = number of components; n-1, = number of solid components. The monovariants for our 5 component system is 6-phase equilibrium, [B]+[C]+[D]+[E]+L+G. Bivariant and multivariant systems shall be composed of fewer than n phases (in our case the number of

equilibrium phases is less than 5). A diagram of this kind may be derived for any multicomponent system analogous to our construction.

Let us consider now an example of crystallization with inclusion formation. A solid phase separating from the H_2O- B, C, D, E system will capture an inclusion at certain definite P and T parameters (p_1 and t_1, respectively). At temperature t_2 (after cooling) a gaseous phase will form in the system; trend of the isochore representing the given system will change abruptly. At the temperature t_3, the given system becomes saturated with respect to second component C, and, the solid phase makes its appearance in the inclusion. At t_4, another solid phase appears in the inclusion. Most systems in the inclusion do not reach this latter stage; they remain unsaturated with respect to dissolved constituents (temperature of observation somewhere between t_2 and t_3).

In the case most typical of mineral formation, analogous to 2-component systems, thermometric-measurement error depends on the isochore slope, $\Delta p/\Delta t = \tan\alpha$. Magnitudes of these errors may be determined, in practice, only by experimental studies of isochore positions in the PT diagrams for concrete systems analogous to the quartz-forming systems of our interest. Of course, first approximation may be guided by corrections deduced for water, previously discussed.

It becomes possible, therefore, to maintain confidently our conclusions based on studies of PTX diagrams for 2-component systems will remain unchanged, in principle, and that they are valid for multicomponent system diagrams.

CONCLUSIONS

1. Investigations of mineral-forming systems (concentration, temperature, pressure) are of cardinal importance in research on prospecting criteria and general theory of genetic mineralogy. Studies of mineral inclusions constitute one of the principal aids to our understanding of these systems.

2. Studies of the chemical composition of included liquids in quartz indicate preponderance of chlorides, sulfates, and other salts. In all probability, these constituents tend to increase solubility of more sparingly soluble substances. Preponderance of Na, K, Ca, and Cl is significant indeed; moreover, the solution reaction is alkaline. Extremely high solution concentration (40 to 50 percent) were reported only by certain investigators, and, only in isolated cases.

3. Our studies of solution composition in secondary quartz inclusions (quartz-healing solutions) show that Na^+, K^+, Ca^{2+}, Mg^{2+}, Al^{3+}, Fe, and, on occasion Mn and Cl^-, SO_4^{2-} BO_3^{3-} are the principal cations and anions present in dissolved state. We note for the first time presence of boron in quartz-forming solutions; moreover, its presence in relatively high amounts is very characteristic for all quartz forming solutions. The following series of certain dissolved constituents is established by quantitative analysis: Na> K> Ca (rarely K> Na) and Ca > Mg. Total dissolved-salt concentration may be as high as 30 to 35 percent, according to our calculations. Such magnitudes also are suggested by presence of only two phases in inclusions examined by us.

In our view, Si transfers in solution are due chiefly to metasilicate-type anions: SiO_3^{2-}; $Si_2O_5^{2-}$; hydroxyl, OH^-, is present also in solution as a result of metasilicate hydrolysis accompanied by formation of SiO_2+OH^- and small amounts of CO_3^{2-}. SiO_3^{2-} concentration in such solutions may be as high as 6 to 12 percent. OH^- concentration must be relatively low, of necessity, as we have no evidence that Ca, Mg, Fe, Al hydroxides are present.

4. An integrated method (including aqueous-extract analysis, of spectrographic analysis of powdered materials, and a preliminary microscopic study of the inclusions) was employed in chemical studies of the liquid phase. Optical-spectrographic analysis, using copper electrodes, and the microchemical (microturbidimetric) qualitative and quantitative methods, proved to be particularly useful under the conditions imposed by our work (small amounts of solutions; highly dilute solutions).

5. Through use of PTX and VTX diagrams for binary systems, mineral-formation possibilities may be gaged, in cases where their 3-component fields have the following phase composition: a) saturated solution ([B]+L); b) Saturated solutions having a gaseous phase ([B]+L+G); c) Saturated gaseous solutions ([B]+L).

6. On thermometry of inclusion homogenization, one may note that measurement errors and, consequently, appropriate temperature corrections, are determined by isochore slopes in PT diagrams for our systems ($\Delta t/\Delta p = \cot\alpha$).

Theoretically, single-phase inclusions should be present only in crystals forming at low temperatures and high pressures; or else, when observed temperature [Tr. : of homogenization - VPS] exceeds formation temperature of the crystal. This theoretical pattern is distorted significantly by metastability phenomena especially characteristic of low-temperature formations. Consequently, one may discuss low-temperature formations, in the presence of single-phase inclusions, while not losing sight of probability that cases where single-phase inclusions may indicate temperatures higher than the low temperatures repre-

sented by two-phase inclusions.

7. Two-dimensional PT diagrams for multicomponent systems may be employed in theoretical interpretation of principal physicochemical aspects of mineral-formation in general and, in particular, of homogenization thermometry. Such diagrams should be based on simpler two-component diagrams of Type I with their unbroken, 3-phase equilibria curves. The two-dimensional diagram for systems of our type, as compared to 2-component systems, is complicated only by phase-saturation fields, with respect to remaining components. Phase Rule should be used as a guide in determining susceptibility to variation at given phase equilibria.

8. Research on mineral-forming systems, based on liquid-inclusion studies in minerals, needs refinements in the near future, subsequent to development of methods best suited to chemical analysis of inclusion composition. Physicochemical studies on properties of systems in question should be expanded to include construction of appropriate 2-dimensional PT diagrams; this should make it possible, accordingly, to interpret the most complicated aspects of mineral formation in general and, particularly, of thermometric data.

REFERENCES

1. Belyankin, D. S., NASKOKO V DEYSTVITELNOSTI RASTVORYAYETSKA KREMNEKISLOTA V VODYANOM PARE NIZHE KRITICHESKOY TEMPERATURY? [TO WHAT EXTENT DOES SILICIC ACID INDEED BECOME DISSOLVED IN WATER VAPOR BELOW THE CRITICAL TEMPERATURE?]: Sovetskaya Geologiya, 1944, no. 3.

2. Berch, Fr., J. Sherer, and G. Spayser, SPRAVOCHNIK DLYA GEOLOGOV PO FIZICHESKIM KONSTANTAM [HANDBOOK OF PHYSICAL CONSTANTS FOR GEOLOGISTS]: Izdatelstvo Inostrannaya Literatura (translated from English), 1949.

3. Vernadsky, V. I., ISTORIYA MINERALOV ZEMNOY KORY [HISTORY OF MINERALS OF THE EARTH'S CRUST]: v. 1, no. 1, 1925; v. 2, 1933.

4. Vulchin, Ye. I., FIZIKO-KHIMICHESKAYA INTERPRETATSIYA TERMOMETRICHESKIKH ISMERENY METODOM GOMOGENIZATSII VKLYUCHENY [PHYSICO-CHEMICAL INTERPRETATIONS OF THERMOMETRIC MEASUREMENTS BY THE METHOD OF HOMOGENIZATION OF INCLUSIONS]: Lvovskoye Geologicheskoye Obsh-vo., Mineralog. Sbornik, 1951, no. 5.

5. _____, RASCHET KRIVYKH V_{zh}/V_p TEMPERATUR GOMOGENIZATSII I OPREDELENIYE KHARAKTERA GOMOGENNYKH FAZ PO DIAGRAMMAM TV [CALCULATION OF THE V_{liquid}/V_{vapor} HOMOGENIZATION TEMPERATURE CURVES AND DETERMINATION OF THE KIND OF HOMOGENEOUS PHASES FROM TV DIAGRAMS]: Lvovskoye Geologicheskoye Obsh-vo., Mineralog. Sbornik, 1952, no. 6.

6. Belyankin, D. S., ed., VOPROSY FIZIKO-KHIMII V MINERALOGII I PETROGRAFII [PHYSICO-CHEMICAL PROBLEMS IN MINERALOGY AND PETROGRAPHY]: Sb. Statey Pod Red. Akad., Izdatelstvo Inostrannaya Literatura, 1950.

7. Garrison, J., R. Lord, and Dzh. Lufburov, PRAKTICHESKAYA SPEKTROSKOPIYA [PRACTICAL SPECTROSCOPY]: Izdatelstvo Inostannaya Literatura, 1950.

8. Gillinkhem, T. Ye., RASTVORIMOST I PERENOS KREMNEKISLOTY I DRUGIKH NELETUCHIKH VODYANYM PAROM [SOLUBILITY AND TRANSFERS OF SILICA AND OTHER NONVOLATILE SUBSTANCES IN WATER VAPOR]: Sb. Voprosy Fiziko-Khimii v Mineralogii i Petrografii, Izdatelstvo Inostrannaya Literatura, 1950.

9. Grigoryev, D. P., K VOPROSY O RAZLICHENII PERVICHNYKH I VTORICHNYKH ZHIDKIKH VKLYUCHENY V MINERALAKH [ON THE SUBJECT ON IDENTIFICATION OF PRIMARY AND SECONDARY LIQUID INCLUSIONS IN MINERALS]: Lvovskoye Geologicheskoye Obsh-vo., Mineralog. Sbornik, 1948, no. 2.

10. Yermakov, N. P., ISSLEDOVANIYA MINERALOOBRAZUYUSHCHIKH RASTVOROV [INVESTIGATIONS OF MINERAL-FORMING SOLUTIONS]: Kharkov, 1950.

11. _____, PROISKHOZHDENIYE I KLASSIFIKATSIYA ZHIDKIKH VKLYUCHENY V MINERALAKH [ORIGIN AND CLASSIFICATION OF LIQUID INCLUSIONS IN MINERALS]: Lvovskoye Geologicheskoye Obsh-vo., Mineralog. Sbornik, 1948, no. 2.

12. _____, KRITERII POZNANIYA GENEZISA MINERALOV I SREDA RUDOOBRAZOVANIYA [CRITERIA FOR UNDERSTANDING ORIGIN OF MINERALS IN REFERENCE TO THE ENVIRONMENT OF ORE FORMATION]: Lvovskoye Geologicheskoye Obsh-vo., Mineralog. Sbornik, 1949, no. 1.

13. Yermakov, N. P., and Ye. M. Lazko, ZHIDKIYE VKLYUCHENIYA V GEO-

LOGICHESKOY TERMOMETRII [LIQUID INCLUSIONS AS GEOLOGIC THERMOMETERS]: Lvovskoye Geologicheskoye Obsh-vo., Mineralog. Sbornik, 1949, no. 3.

14. Yermakov, N. P., and R. F. Sukhorskiy, KRIVAYA DLYA VIZUALNOGO OPREDELENIYA TEMPERATUR OBRAZOVANIYA GIDROTERMALNOGO KVARTSA [CURVE FOR VISUAL ESTIMATION OF TEMPERATURES OF HYDROTHERMAL QUARTZ FORMATION]: Lvovskoye Geologicheskoye Obsh-vo., Mineralog. Sbornik, 1949, no. 3.

15. Zavaritskiy, A. N., FIZIKO-KHIMICHESKIYE OSNOVY PETROGRAFII IZVERZHENNYKH POROD [PHYSICOCHEMICAL PRINCIPLES OF IGNEOUS-ROCKS PETROGRAPHY]: Akademiya Nauk SSSR, Izd., 1926.

16. _____, OSNOVNOY VOPROS FIZICHESKOY KHIMII PROTSESSA OBRAZOVANIYA PEGMATITOV [THE FUNDAMENTAL PROBLEM IN PHYSICAL CHEMISTRY OF PEGMATITE FORMATION]: Akademiya Nauk SSSR, Izvestiya, Seriya Geologicheskaya, 1944, no. 5.

17. Zakharchenko, A. I., REZULTATY IZUCHENIYA ZHIDKIKH VKLYUCHENY V GORNOM KRUSTALE PAMIRA [THE RESULTS OF LIQUID-INCLUSIONS STUDIES IN QUARTZ FROM PAMIR]: Lvovskoye Geologicheskoye Obsh-vo., Mineralog. Sbornik, 1950, no. 4.

18. _____, K VOPROSU O PRIRODE GIDROTERMALNYKH RASTVOROV [ON THE PROBLEM OF THE NATURE OF HYDROTHERMAL SOLUTIONS]: 1952.

19. Ivantishin, N. M., GALENITOVYYE RUDOPROROYAVLENIYA NA PODOLSKOY PALEOZOYSKOY POLOSE [EXPRESSIONS OF GALENA ORES IN THE PALEOZOIC BELT OF PODOLIA]: Akademiya Nauk SSSR, Geolog. Zhurnal, v. 7, no. 3, 1947.

20. Indichenko, L. N., RASSHIFROVKA SPEKTROGRAMM RUD I MINERALOV [INTERPRETATION OF SPECTROGRAMS OF ORES AND MINERALS]: Gosgeolizdat, 1951.

21. Komarovsky, Poluektov, MIKROCHEMIE [MICROCHEMISTRY]: 1934, no. 14, p. 317.

22. Karpinsky, A. P., In: Gornyy Zhurnal, v. 11, nos. 4-5, p. 96, 1880.

23. Kertman, L., KACHESTVENNYY KHIMICHESKY POLUMIKROANALIZ [QUALITATIVE CHEMICAL SEMIMICROANALYSIS]: Goskhimizdat, 1949.

24. Kliya, M. O., NEKOTORYYE VOPROSY OBRAZOVANIYA ZHIDKIKH VKLYUCHENY V KRISTALLAKH [CERTAIN PROBLEMS ON FORMATION OF LIQUID INCLUSIONS IN CRYSTALS]: Akademiya Nauk SSSR, Inst. Kristallografiya, 1952 (abs.).

25. Korenman, I. M., KOLICHESTVENNYY MIKROKHIMICHESKY ANALIZ [QUANTITATIVE MICROCHEMICAL ANALYSIS]: Goskhimizdat, 1949.

26. Kuznetsov, V. I., K METODIKE NABLYUDENIYA ZHIDKIKH VKLYUCHENY V PROERACHNYKH MINERALAKH S POMOSHCHYU IMMERSIONNYKH ZHIDKOSTEY [ON METHODS OF OBSERVATION OF LIQUID INCLUSIONS IN TRANSPARENT MINERALS, WITH THE AID OF IMMERSION LIQUIDS]: Lvovskoye Geolgicheskoye Obsh-vo., Mineralog. Sbornik, 1949, no. 3.

27. Lemmleyn, G. G., SEKUNDÄRE FLÜSSIGKEITSEINSCHLUSSE IN MINERALIEN [SECONDARY LIQUID INCLUSIONS IN MINERALS]: Zeitschrift für Kristallographie, 1929.

28. _____, PROTSESS ZALECHIVANIYA TRESHCHINY V KRISTALLE I PREOBRAZOVANIYE FORMY POLOSTEY VTORICHNYKH ZHIDKIKH VKLYUCHENY [THE PROCESS OF HEALING OF A CRACK IN A CRYSTAL AND TRANSFORMATIONS OF THE SHAPE OF CAVITIES CONTAINING SECONDARY LIQUID INCLUSIONS]: Akademiya Nauk SSSR, Doklady, v. 78, no. 4, 1951.

29. _____, O SOOTNOSHENII SOVREMENNOGO I PERVONACHALNOGO OBYEMOV ZHIDKIKH VKLYUCHENY V MINERALAKH [ON THE RATIO OF PRESENT TO ORIGINAL VOLUME OF LIQUID INCLUSIONS IN MINERALS]: Akademiya Nauk SSSR, Doklady, v. 72, no. 4, 1950.

30. Lemmleyn, G. G., and M. O. Kliya, NOVYYE DANNYYE OB OTLOZHENII VESHCHESTVA KRISTALLA NA STENKAKH POLOCTI ZHIDKOGO VKLYUCHENIYA [NEW DATA ON THE DEPOSITED CRYSTALLINE MATERIAL ON THE WALLS OF SECONDARY LIQUID INCLUSIONS]: Akademiya Nauk SSSR, Doklady, v. 82, no. 5, 1952.

31. Malyarov, K. L., KACHESTVENNYY

MIKROKHIMICHESKY ANALIZ [QUALITATIVE MICROCHEMICAL ANALYSIS]: Moskovskaya Universiteta, Izd., 1951.

32. Morey, Dzh. Ch., ZAMECHANIYA K STATYE F. G. SMITA "PERENOS I OTLOZHENIYE NESULFIDNYKH ZHILNYKH MINERALOV. III. FAZOVYYE OTNOSHENIYA V PEGMATITOVUYU STADIYU" [REMARKS ON THE ARTICLE BY F. G. SMITH. ENTITLED "TRANSFERS AND DEPOSITION OF NONSULFIDE VEIN MINERALS. III. PHASE RELATIONSHIPS DURING THE PEGMATITIC STAGE]: In: Voprosy Fiziko-khimii v Mineralogii i Petrografii[Physicochemical Problems in Mineralogy and Petrography]: Sbornik Statey, Izd. In. Lit., 1950.

33. Niggli, P., MAGMA I YEYE PRODUKTY [MAGMA AND ITS PRODUCTS]: Gosgeolizdat, 1946.

34. Nikolayev, V. A., DIAGRAMMY RAVNOVESIYA BINARNYKH SISTEM TIPA SILIKAT-VODA I OTDELENIYE LETUCHIKH SOYEDINENY IZ MAGMATICHESKIKH RASPLAVOV [EQUILIBRIUM DIAGRAMS OF BINARY SYSTEMS OF SILICATE-WATER TYPE AND SEPARATION OF VOLATILE COMPOUNDS FROM MAGMATIC MELTS]: ZVMO, v. 72, no. 2, 1945.

35. _____, O TROYNYKH SISTEMAKH S LETUCHIMI KOMPONENTAMI I ETAPAKH GLUBINNOGO MAGMATICHESKOGO PROTESSA [ON TERNARY SYSTEMS WITH VOLATILE COMPONENTS AND, ON STAGES OF THE DEEP MAGMATIC PROCESS]: ZVMO, v. 76, 1947.

36. _____, O FIZIKO-KHIMICHESKOY STORONE PROTSESSA LIKVASHCHII NA POZDNIKH ETAPAKH KRISTALLIZATSII MAGMY [ON SOME PHYSICOCHEMICAL ASPECTS OF LIQUATION PROCESSES DURING THE LATE STAGES OF MAGMA CRYSTALLIZATION]: ZVMO, v. 80, no. 1, 1951.

37. NOVYYE ISSLEDOVANIYA PO KRISTALLOGRAFII I KRISTALLOKHIMII [NEW RESEARCH IN CRYSTALLOGRAPHY AND CRYSTAL CHEMISTRY]: In: Sbornik II: Rost Kristallov, Izd. In. Lit., 1950.

38. Boky, R. B., ed., NOVYYE ISSLEDOVANIYA PO KRISTALLOGRAFII I KRISTALLOKHIMII [NEW RESEARCH IN CRYSTALLOGRAPHY AND CRYSTAL CHEMISTRY]: In: Sbornik III: Kristallicheskiye Struktury, Izd. In. Lit., 1950.

39. O Nil, T. F., GIDROTERMALNOYE IZMENENIYE POLEVYKH SHPATOV PRI TEMPERATURAKH 250°-400°C [HYDROTHERMAL ALTERATIONS OF FELDSPARS AT 250°-400°C]: Voprosy Fizikikhimii v Petrografii i Mineralogii: Sbornik Statey, Izd. In. Lit., 1950.

40. Ostrovsky, I. A., DIAGRAMMA OBYEM-TEMPERATURA-SOSTAV V SISTEME TIPA SILIKAT-VODA DLYA SLUCHAYA ORGANICHENNOY SMESIMOSTI V ZHIDKOY FAZE [THE VOLUME-TEMPERATURE-COMPOSITION DIAGRAM OF A SILICATE-WATER TYPE SYSTEM FOR THE CASE OF LIMITED MISCIBILITY IN THE LIQUID PHASE]: Akademiya Nauk SSSR, Doklady, v. 74, no. 5, 1950.

41. _____, DIAGRAMMA RAVNOVESNYKH SOSTOYANY V SISTEME SILIKAT-VODA DLYA SLUCHAYA OGRANICHENNOY SMESIMOSTI I VOZMOZHNOYE ISTOLKOVANIYE DANNYKH GORANSONA [EQUILIBRIUM DIAGRAMS OF SILICATE-WATER SYSTEM, LI ITED MISCIBILITY CASE, AND POSSIBLE INTERPRETATION OF GORANSON'S DATA]: Akademiya Nauk SSSR, Doklady, v. 72, no. 3, 1950.

42. _____, O DIAGRAMME VTX DLYA PROSTEYSHEGO SLUCHAYA V SISTEME SILIKAT-VODA [ON THE VTX DIAGRAM FOR THE SIMPLEST CASE, THE SILICATE-WATER SYSTEM]: Akademiya Nauk SSSR, Izvestiya, Seriya Geologicheskaya, 1950, no. 5.

43. Ravich, M. I., OB USLOVIN SUSHCHESTVOVANIYA KRISTALLICHESKIKH SOLEY V PRISUTSTVII VODYANOGO PARA [ON THE PREREQUISITES FOR EXISTENCE OF CRYSTALLINE SALTS IN THE PRESENCE OF WATER VAPOR]: 4th Soveshchaniya po Eksperimentalnoy Mineralogii i Petrografii, Trudy, 1950.

44. Rusanov, A. K., SPEKTRALNYY ANALIZ RUD I MINERALOV [SPECTROGRAPHIC ANALYSIS OF ORES AND MINERALS]: Gosgeolizdat, 1948.

45. Samoylov, Ya., MATERIALY DLYA GEOLOGII ROSSII [DATA ON THE GEOLOGY OF RUSSIA]: v. 23, 1908.

46. Smit, F. G., PERENOS I OTLOZHENIYE NESULFIDNYKH ZHILNYKH MINERA- I. VVEDENIYE. II. FAZOVYYE OTNOSHENIYA V PEGMATITOVUYU STADIYU [TRANSFER AND DEPOSITION OF NONSULFIDE VEIN MINERALS. I. INTRODUCTION. II. PHASE RELATIONSHIPS DURING PEGMATITIC STAGE]. Voprosy fiziki-khimii v Petrografii i Mineralogii: Sbornik Statey, Izd. In. Lit., 1950.

47. Syromyatinkov, F. V., K. VOPROSU O GAZOVOM PERENOSE KREMNEKISLOTY [ON THE PROBLEM OF GASEOUS TRANSFER OF SILICA BY WATER VAPOR]: 4th Soveshchaniya po Eksperimentalnoy Mineralogii i Petrografii, Trudy, 1950.

48. _____, THE PROBLEM OF TRANSFER OF SILICA BY WATER VAPOR: Econ. Geology, v. 30, p. 89-92, 1935.

49. Sendel, Ye. B., KOLORIMETRICHESKOYE OPREDELENIYE SLEDOV METALLOV [COLORIMETRIC DETERMINATION OF TRACES OF METALS]: Goskhimizdat, 1949.

50. Tamman, G., RUKOVODSTVO PO GETEROGENNYM RAVNOVESIYAM [MANUAL OF HETEROGENIC EQUILIBRIA]: ONTI, 1935.

51. Tredvell, F. P., and V. T. Goll, KACHESTVENNYY ANALIZ [QUALITATIVE ANALYSIS]: Goskhimizdat, 1946.

52. Tuttle, O. F., and I. I. Freedman, NESMESIMOST ZHIDKOSTEY V SISTEME H_2O-Na_2O-SiO_2 [IMMISCIBILITY OF LIQUIDS IN THE H_2O-Na_2O-SiO_2 SYSTEM]: Voprosy Fiziki-khimii v Petrografii i Mineralogii: Sbornik Statey, Izd. In. Lit., 1950.

53. Khitarov, N. I., O SOSTOYANII OSTATOCHNOGO MAGMATICHESKOGO RASTVORA (PO EKSPERIMENTALNYM DANNYM) [ON THE STATE OF RESIDUAL MAGMATIC SOLUTION (BASED ON EXPERIMENTAL DATA)]: Sovetskaya Geologiya, 1939, no. 7.

54. Khitarov, N. I., and L. A. Ivanov, PAROVAYA I GAZOVAYA FAZA SISTEMY KREMNEZEM-VODA [STEAM AND GASEOUS PHASE OF SILICATE-WATER SYSTEM]: Sovetskaya Geologiya, 1944, no. 2.

55. _____, ISSLEDOVANIYA V OBLASTI KRITICHESKIKH TEMPERATUR VODNYKH RASTVOROV [INVESTIGATIONS ON THE CRITICAL TEMPERATURE FIELD OF AQUEOUS SOLUTIONS]: 2nd Soveshchaniya po Eksperimentalnoy Mineralogii i Petrografii, Trudy, Izd. Akademiya Nauk SSSR, 1937.

56. _____, EKSPERIMENTALNYYE DANNYYE PO KHARAKTERISTIKE VODNYKH RASTVOROV V OBLASTI KRITICHESKIKH TEMPERATUR V PRILOZHENII K VOPROSAM GEOLOGII [EXPERIMENTAL DATA ON CHARACTERISTICS OF AQUEOUS SOLUTIONS IN THE CRITICAL TEMPERATURE FIELD IN APPLICATION TO GEOLOGIC PROBLEMS]: 17th Sessii Mezhdunarodnogo Geologicheskogo Kongressa, Trudy, v. 5, 1940.

57. Khitarov, N. I., L. A. Ivanov, and L. E. Rotman, K POZNANIYU KRITICHESKIKH YAVLENY V PRIRODNYKH PROTSESSAKH [A CONTRIBUTION TO THE UNDERSTANDING OF CRITICAL PHENOMENA IN NATURAL PROCESSES]: Sovetskaya Geologiya, 1939.

58. Khrushchev, K. V., In: Mineral. Petrograf. Mitt. Wien, 1882.

59. Chaykovsky, S. A., YAVLENIYA PEREGREVA ZHIDKIKH VKLYUCHENY V MINERALAKH [SUPERHEATING PHENOMENA IN LIQUID INCLUSIONS IN MINERALS]: Akademiya Nauk SSSR, Doklady, v. 76, no. 3, 1951.

60. Bowen, N. L., GEOLOGIC THERMOMETRY: In: Laboratory Investigation of Ores, E. E. Fairbanks, ed., 1928, p. 172-199.

61. Brewster, D., In: Edinburgh Society, Trans., v. 10, p. 141, 1823; v. 10, p. 407-427, 1826; v. 16, p. 7-8, 1849, v. 23, p. 39-44, 1861.

62. _____, In: Philosophical Magazine, ser. 15, 1853, p. 235-236.

63. Davy, H., In: Philosophical Transactions, 1822, p. 367-376.

64. Konigsberger, J., and W. Muller, ÜBER DIE FLÜSSIGKEITSEINSCHLÜSSE IM QVARTZ ALPINER MINERALKLUFTEN [ON LIQUID INCLUSIONS IN ALPINE QUARTZ MINERAL CLEAVAGES]: Centrlbl. für Mineralog, 1906, no. 71-72, p. 341.

65. Lasaulx, A., In: Niederrein Gesell. Zitz. Berichte, Bonn, 1883.

66. Lindgren, W., THE GOLD-QUARTZ VEINS OF NEVADA CITY AND GRASS VALLEY DISTRICTS, CALIFORNIA: U. S. Geological Survey 17th Annual Rept., v. 2, p. 1-262, 1895-1896.

67. Lindgren, W., and W. Whitehead, In.: Econ. Geology, v. 9, no. 5, 1914.

68. Newhouse, W., THE COMPOSITION OF VEIN SOLUTIONS AS SHOWN BY LIQUID INCLUSIONS IN MINERALS: Econ. Geology, v. 27, no. 5, 1932; v. 28, no. 8, 1933.

69. Nicol, W., In: Edinburgh New Philosophical Journal, v. 5, p. 95, 1828; v. 7, p. 111-113, 1829.

70. Pfaff, F., In: Poggend. Annalen, 1871, no. 143, p. 610-620.

71. Prinz, W., In: Soc. Belgique Mineralogie, Ann., 1882.

72. Sjögren, H., In: Upsala Geol. Inst., Bull., v. 1, no. 2, 1893.

73. Sorby, H. C., ON THE MICROSCOPIC STRUCTURE OF CRYSTALS, INDICATING THE ORIGIN OF MINERALS AND ROCKS: Geol. Soc. of London, Quart. Jour., v. 14, p. 453-500, 1858.

74. _____, In: Philosophical Magazine, v. 18, p. 81-91, 1859.

75. Wuite, J. P., PT-DURCHSCHNITTE [PRESSURE-TEMPERATURE AVERAGES]: Zeitschrift für Physikalische Chemie, v. 78, 1912.

76. Zirkel, N., DIE MIKROSKOPISCHE BESCHAFFENHEIT DER MINERALE UND GESTEINE [THE MICROSCOPIC CHARACTERISTICS OF MINERALS AND ROCKS]: 1873.

77. _____, LEHRBUCH DER PETROGRAPHIE [MANUAL OF PETROGRAPHY]: v. 1, p. 162, 1893.

78. Roozeboom, H. W. B., DIE HETEROGENE GLEICHGEWICHTE VON STANDPUNKTE DIE PHASENLEHRE [HETEROGENEOUS EQUILIBRIA FROM THE STANDPOINT OF PHASE RULE]: 1904.

PRINCIPAL GEOLOGIC AND METALLOGENIC FEATURES OF THE MOUNTAINOUS TAYMYR[1]

by

M. G. Ravich and F. G. Markov[2]

• *translated by Research International* •

ABSTRACT

Within the mountainous Taymry the oldest formations are highly metamorphosed sedimentary and extrusive rocks of Proterozoic age, overlain by less altered rocks of the Sinian complex. These in turn are overlain with angular unconformity by Lower Cambrian deposits, whose age has been determined on the basis of fossils. Paleozoic rocks are widespread, and all systems of the era are represented. Proterozoic rocks occur on the northern coast of the peninsula. The younger Sinian and Paleozoic formations are south and southeast of these. Mesozoic rocks constitute small areas in depressions. Quaternary sediments, consolidated by permafrost, are widely distributed throughout the area. Magmatic activity is well developed. The lower Proterozoic magmatic cycles began with intrusion and extrusion of basic rocks, and ended with granitoid injections accompanied by formation of pegmatitic zones. In the upper Proterozoic, magmatic activity is again characterized in early stages by extrusion and intrusion of basic rocks, and later by the formation of granitic intrusions and their facies, as well as by extrusion of felsite porphyry towards the end of the era. Intrusions of granitoids appeared in the middle Paleozoic. The upper Paleozoic was marked by the formation of traprock and sulfide mineralization. In the early Mesozoic, the occurrence of small subalkaline intrusions resulted in the formation of ores of various types.

INTRODUCTION

The Taymyr peninsula can be sharply divided into two nearly equal parts: the northern, mountainous region, mainly composed of Paleozoic and Precambrian rocks, and the southern lowlands, composed of Quaternary deposits and rare Mesozoic outcrops. The northern, mountainous territory is part of the Taymyr folded region. Until the 1930's, this region had not been explored. The ideas of the geologic structure of the Taymyr mountains was based on meager information supplied by individual investigators. Currently, a geologic mapping at a scale of 1:1,000,000 is being conducted for the entire area. Larger scales are being employed for certain localities.

In this article, F. G. Markov describes the geologic structure of the mountainous Taymyr, and M. G. Ravich describes the magmatic activity and metallogeny of the area, based on data available to January 1, 1958.

GEOLOGIC STRUCTURE

The Taymyr peninsula is composed mainly of Proterozoic and Paleozoic rocks, all systems of the latter era being present. Mesozoic rocks are limited in extent, occurring in low-lying sections of the region. Friable Quaternary deposits are widespread.

The oldest rocks are Proterozoic and occupy the entire northern margin of the peninsula. Towards the south, in the direction of the continent, Paleozoic formations extend to the margin of the Byrrang mountains, which are primarily composed of folded Permian rocks.

Two fairly distinct complexes of strongly faulted rocks occur in the Proterozoic formations. The older is composed of garnet-biotite, garnet-biotite-hornblende, garnet-hornblende, enstatite-pargasite, amphibole, cordierite, sillimanite, and other plagioclase. Within this series, more than 7,000 meters (m) thick, are found metamorphosed gabbroid rocks, porphyritic granite-gneisses and two mica granites, surrounded in many places by a rather wide migmatic zone. The rocks of the upper complex, which rest unconformably on the gneiss series, are composed of actinolite-epidote, amphibole-biotite, epidote-amphibole, epidote-chlorite-quartz, chlorite-sericite, chloride-sericite-quartz schists, quartzites, some metamorphosed arkosic sandstones, and marbles. The thickness of this complex, including sills formed by repeated intrusions of basic rocks (later metamorphosed) and dome-shaped granitoid intrusions, reaches 6,000 m.

Field studies conducted in 1957 by members of the Arctic Geological Institute resulted in the identification of Sinian formations. These formations previously had been assigned to either the Proterozoic or the Cambrian. The clearest stratigraphic relationships were found in the basins of the Lenivoy and Shrenka rivers, in their upper reaches. Here, the observed

---

[1] Translated from Osnovnyye cherty geologii i metallogenii Gornogo Taymyra: Sovetskaya Geologiya, 1959, no. 5, p. 11-24.

[2] Scientific Research Institute of Arctic Geology (NRIAG)

series, 4,000 m or more in thickness, consisted mainly of dolomites and limestones containing algal remains. The lower part contained siltstones, shales, and polymict sandstones, with conglomerate at the base of the section. Thin layers of basic extrusives were found in the carbonate rocks of the upper part of the series. The Sinian rests transgressively on upper Proterozoic rocks, and is overlain with angular unconformity by limestones containing trilobites of the Aldan stage of the Lower Cambrian. In the south, the Cambrian formations lie on the eroded surface of the contorted and faulted Precambrian. They are composed of limestones, dolomitic limestones, and dolomites containing varying amounts of terrigenous material, either interbedded calcareous-argillaceous shale or, more rarely, arenaceous rocks. The thickness of the Cambrian ranges from 600 m to 1,400 m. All three divisions of the Cambrian can be distinguished by the presence of organic remains.

Ordovician formations occur in isolated sections comprising a relatively wide belt in the central zone of the mountainous Taymyr. Ordovician rocks lie conformably on the Cambrian formations. In the eastern zone, local transgressions on the Cambrian have been noted. Limestones, dolomitic limestones, and dolomites are interbedded with argillaceous and calcareous-argillaceous shales. It is characteristic of the Ordovician formations that shales increase in volume eastward from the Pripyansky region. The thickness of the Ordovician formations ranges from 500 m to 1,800 m.

Silurian rocks have a rather wide distribution, similar in extent to Ordovician rocks which they overlie conformably or transgressively. The stratigraphic boundary between the Ordovician and the Silurian formations can be distinguished fairly clearly by fossil content. A Silurian section usually begins with sandy-argillaceous shales or sandy limestones, at the base followed by limestones and dolomitic limestones, alternating with argillaceous and calcareous-argillaceous shales. These rocks contain an abundance of fossil ramains. The limestones contain some bitumen. In the northern part of eastern Taymyr, the carbonate series is replaced by calcareous-argillaceous graptolite shale facies. The thickness of the Silurian is 750 m to 1,500 m.

Devonian rocks comprise small, isolated sections within areas of Silurian rocks and outcrop at the crests of anticlinal structures in the Byrrang mountains. There is a gradual transition from Silurian to Devonian rocks. All three divisions of the Devonian were identified on the basis of fossil content, though in places, deposition was interrupted toward the end of the Lower Devonian and the beginning of the Middle Devonian. Devonian rocks are mainly limestones, dolomitic limestones, and rarely dolomites. In the western part of the peninsula these rocks are infrequently interbedded with argillaceous and calcareous-argillaceous shales. The upper Lower Devonian in this area contains considerable gypsum. In the central Byrrang mountains, bitumen-bearing limestones occur in Middle and Upper Devonian carbonate rocks. A gypsum-bearing Middle Devonian series 100 m thick outcrops at the southeast margin of the Taymyr (Belaya and Seraya volcanos). The thickness of the Devonian formations is 950 m to 2,200 m.

Carboniferous rocks occur in some localities, outcropping from beneath Permian rocks or preserved in troughs formed by middle Paleozoic formations. They rest conformably, and in places transgressively, on Devonian rocks in the eastern part of the peninsula. Lower Carboniferous rocks are most widely distributed; they are composed of limestones, dolomitic limestones, and, more rarely, dolomites interbedded with calcareous-argillaceous shales. The amount of terrigenous rock increases sharply in the middle Carboniferous and in the tentatively identified upper Carboniferous formations of western Taymyr. Lower Carboniferous carbonate rocks in eastern Taymyr are typically overlain by a siltstone and argillite series containing rare plant remains and spore-pollen complexes of the lower and middle horizons of the Kuznets basin Balakhonskaya suite. The thickness of the Carboniferous rocks is 750 m to 1,700 m.

Permian formations occupy a large area comprising the Byrrang mountains. The terrigenous series, 4,000 m to 4,500 m thick, has several different stratigraphic relationships with the underlying rocks. In western Taymyr, there is a gradual transition from lower Carboniferous carbonates to the Permian terrigenous series; in other parts of the peninsula, Permian formations rest transgressively on Carboniferous and older rocks. Formations of both divisions are present, consisting of sandstone, siltstones, argillites, argillaceous and carbonaceous-argillaceous shales, and conglomerates. In the lower parts of the lower and upper Permian formations, concentrations of limestone occur; in the upper parts, coal seams frequently of workable thickness, are present. The Taymyr peninsula can thus be considered a favorable prospective coal region. Permian formations contain numerous traprock sills.

In the Taymyr area the Paleozoic section is capped by a traprock series composed of several sheets of basic rocks and tuffs. The relationships of these rocks vary from region to region. The thickness of the volcanic series ranges from 100 m to 150 m in some areas and from 800 m to more than 1,000 m in others. Concentrations of sandy-argillaceous rocks containing remains of terrestrial flora and fresh-water fauna can be found in the volcanics. In places, the volcanic series progressively altered the underlying terrigenous Permian strata, or is distributed over the partially eroded surface of these rocks. Volcanism occurred from the end of the upper Permian to the Lower

Triassic. At Cape Tsvetkova, near the Laptevyy sea, faunally determined formations of the Indskean stage of the Lower Triassic, overlie the volcanic series conformably; farther west in Taymyr, the upper parts of this series consist of Middle Triassic rocks lacking a Mesozoic cover.

As previously mentioned, Mesozoic formations cover an insignificant area in low-lying regions of the Taymyr mountains. Marine Triassic sediments have been identified only at the southeastern margin of the Byrrang mountains. A complete section is developed only at Cape Tsvetkova, where all three faunally determined divisions, totalling 1,250 m in thickness, can be distinguished. They are composed of sandstones interbedded with concentrations of argillaceous shales and argillites. The extrusive-agglomerate beds, preserved in depressions of the central Byrrang mountains, are Lower Triassic, or possibly Middle Triassic.

Jurassic formations are limited; the most complete section occurs at Cape Tsvetkova, where a sandstone and argillaceous-shale series outcrops. It contains faunal remains of all three divisions and has a thickness of 1,400 m (excluding the lower Lias). Jurassic rocks lie with angular unconformity on Triassic formations. In other parts of the Taymyr mountains, Upper Jurassic sediments predominate, progressively replaced by Lower Cretaceous marine formations whose thickness does not exceed 100 m.

Cretaceous formations have a somewhat larger extent that the Jurassic. They compose small, isolated sectors. Lower Cretaceous formations predominate. The lower part of this section consists of sandy-argillaceous rocks containing a Valanginian marine fauna; the upper, terrigenous rocks contain layers of brown coal and anthracite. The Lower Cretaceous strata are as thick as 600 m. Upper Cretaceous sediments occur only in isolated eroded areas on the northern shore of western Taymyr where individual layers of sandy-argillaceous rocks outcrop from beneath friable Quaternary deposits.

Tertiary rocks have not yet been observed in the mountainous territory of Taymyr.

Quaternary deposits are relatively widespread; the greatest volumes occur in low-lying areas. Marine, glacial, and lacustrine-glacial, as well as Recent eluvial, diluvial, and alluvial sediments, form a mantle of varying thickness. The Taymyr peninsula was subjected to two periods of glaciation, each followed by marine transgression. Permafrost is widespread, and fossil ice is encountered almost everywhere. A small glacier presently exists in eastern Taymyr.

The Taymyr folded structures of different ages form a large crescent convex to the southeast. Its inner zone is composed of highly faulted Proterozoic rocks forming a system of complex contorted and isoclinal folds which resulted from both lower and upper Proterozoic tectonic activity. These folds strike approximately eastward in western Taymyr but their strike is progressively more northward in the north (Chelyuskin peninsula). The folded structures composed of Sinian and Paleozoic rocks extend along the southern and southeastern margins of the middle Proterozoic massif and maintain approximately the same strike. The rocks of the Sinian complex lie transgressively on rocks of various Proterozoic suites. The Sinian folds are less intensively developed than the Proterozoic folds. Lower Paleozoic formations lie unconformably on the Sinian complex. They form a similar series of folds which dip more gently than the Precambrian structures. Near the Precambrian massif, these linear folds are intermittent; asymmetrical brachyfolds with relatively steep dips are common. Locally, lower Paleozoic rocks form monoclines above the highly faulted Precambrian series (Chelyuskin peninsula).

The middle and upper Paleozoic formations form a system of parallel folds, typically broader and of greater extent along the strike. They border ancient folded structures and extend along their southern and southeastern peripheries. These folds are quite different in form from the older folds. Commonly, Permian formations and the volcanic series covering them form large similar folds.

Alpine tectonic movements, which formed folded structures in the Mesozoic (Jurassic and Cretaceous) in the adjoining Taymyr depression to the south, caused widespread multiple fracturing in the previously consolidated Taymyr folded region; these movements caused the relocation of individual blocks within the region. In the mountainous region of Taymyr, Jurassic and Cretaceous formations lie either almost horizontally or form sloping folds with dips of several degrees. It is possible that the appearance of the sloping folds was caused by the relocation of individual blocks. Similar heterogeneous movements also occurred in the Cenozoic.

MAGMATIC ACTIVITY

Four tectonic-magmatic cycles in the Taymyr fold region can be distinguished on the basis of uniform distribution of magmatic activity in space and time.

Magmatic activity in the lower Proterozoic began with basic flows which were subsequently metamorphosed into garnet amphibolites. The surrounding sedimentary rocks were metamorphosed into various gneisses. Sills of basic composition, composed mainly of orthoamphibolites, olivine gabbro-norites, and gabbros with

relict drusy and gabbro-diabase texture, were also subsequently converted into lenticular bodies.

At the very end of the lower Proterozoic, intrusion of high-silica magma in the form of deep-seated injections occurred during folding. These injections were of considerable extent, approximately concordant with folds within the gneisses and schists. Similar intrusions, surrounded by migmatites, are composed of pophyroblastic biotite granites-gneisses and partly granosyenite-gneisses locally tending in composition toward granodiorites and quartz diorites. The dike facies is represented by aplites and biotite pegmatites, commonly gneissic. The deep-seated ultrametamorphism of ancient geosynclinal formations had a great influence on the formation of the magmatic melts which formed both the intrusive and migmatitic dike material. Crystallization of these magmas continued during tectonic movements related to fold formation. As a result, multiple intrusions frequently formed individual migmatite plutons. Almost simultaneously with biotite granite-gneiss formation, or somewhat later, thin sills, branching phacolithic and flat batholithic bodies of two-mica granite formed within upper parts of the gneiss and schist complex. In the uppermost horizons, discordant intrusions occurred along fractures, and stocks of muscovite granite formed. Abundant muscovite pegmatite dikes were concentrated either in individual fields around two-mica granite bodies or nonuniformly in the contact zone of individual batholithlike bodies. Due to autometamorphism and, mainly, hydrolysis of feldspar, the granites were significantly enriched in muscovite. The accompanying muscovite pegmatites were also formed by autometamorphic processes due to recrystallization of granite dikes and aplites.

Extrusion of much basic magma forming basalt sheets and tuff initiated upper Proterozoic magmatic activity. The green-schist series lying at the base of the upper Proterozoic is the result of regional metamorphism of these basic extrusives. Multiple sills of diabase and gabbro-diabase, transformed during regional metamorphism into greenstone of the orthoamphibolite type, were emplaced contemporaneously with the deposition of terrigenous rocks in which they now occur; the enclosing rocks were converted to phyllites, quartzites, and marbles.

Formation of granitoid domes and arching structures near stocks and multiple dikes of granitoid porphyry terminated upper Proterozoic magmatic activity. Granitoids, more common in these intrusions than grano-diorites and quartz diorites, are highly fractured, even mylonized. The concordant arching granitoid intrusions formed during the last stage of folding, continued after their crystallization; thus, the protoclastic structures of the rock are thoroughly developed. Locally, granite magma penetrated the surface through fractures; sheets of felsite porphyries and albitophyres occur capping Proterozoic formations. Although these extrusions were small, they are widely distributed throughout the Taymyr. Such sheets, in individual instances, are directly related to domed granitoid intrusions which may be considered subvolcanos.

The conglomerate at the base of the Sinian commonly contains pebbles of metamorphosed granite, felsite-porphyry, and albitophyre. The earliest indications of Paleozoic magmatic activity occur in the Cambrian; they are basic lavas and their tuffs, including sheets of spilite. Laccolithic intrusions, generally concordant, and gabbro-diabase dikes, both relatively weakly metamorphosed (not completely schistose), and similar to analogous intrusions in the upper Proterozoic, occur in the upper part of the Cambrian section. In the middle Paleozoic, during a late Caledonian folding phase, high-silica magma was intruded through fractures. This magma formed domes and stocks, and, in rare instances, penetrated Upper Silurian rocks. These intrusions are many-phased composites. Earlier phases are characterized by normal granites and granitoids; later, by porphyritic granosyenites and syenite-diorites; and, finally, by fine-grained aplitic granites or syenites. The vein facies is completely developed. It is represented by two dike types: one composed of granite and granosyenite porphyries; the other composed of lamprophyres of the spessartite odinite and minette-kersantite types. Some dikes acquired exceptionally large amounts of kaolin and carbonate during autometamorphism. The intrusions are surrounded by thick accumulations of cordierite, andalusite, and biotite-staurolite hornfels. It can be inferred from the properties of the intrusions that the formation of spaces which facilitated the intrusions is related to the extension of primary post-folding fractures resulting from intensive block movements in the enclosing rocks.

It should be mentioned that eight different absolute age determinations by the argon method gave identical data for all four intrusive cycles. Thus, the age of the porphyroblastic granite-gneiss; the metamorphosed, cataclastic, two-mica granites; and the porphyritic granosyenites taken from various regions and formations is 230 million to 240 million years, as determined from weight composition and 225 million to 270 million years, as determined from biotite of the corresponding granitoids. Such a discrepancy between the geologic position of the individual granitoids and their absolute age can be explained by the superposition of the tectonic processes, which affect the retention of radiogenic argon; the actual age of the mineral formation cannot be determined. The Precambrian central massif, which contains almost all of the Taymyr granitoid formations, was subjected to repeated orogenic movement; thus, absolute age will correspond only to the time of the latest tectonic processes which acted upon the granitoids.

Upper Paleozoic magmatic activity is evidenced by traprock, developed widely throughout Taymyr as extrusive-pyroclastics or intrusives. These rocks play a considerable role in the composition of the Permo-Triassic series. Tuffites lie at the base of the effusive series. Higher in the section, basaltic tuffs are interbedded with basaltic lava. The uppermost part of the section, and the thickest, is composed of basalt sheets with significant amounts of amygdules. These tend in composition toward picrite in one direction and andesite in the other. The intrusive-trap facies is composed of numerous sills and, very rarely, dolerite and gabbro-dolerite dikes which, as is usually the case, serve as feeders for the sills. The sills are distributed more or less uniformly throughout the Permian terrigenous formations and comprise 15 to 20 percent of the total Permian thickness (measured at 5 kilometers). The sills are usually several dozen meters thick, and are rarely as much as 100 m thick. One exception is a sill 900 m thick; but even this one is highly differentiated. The sill has an anisotropic structure. It is composed of a series of different compositions from amphibole peridotite at the base to alaskite granites at the top. Gabbro-dolerites, becoming typical diorites in gradual transition and with low olivine and pyroxene content, predominate. Thick beds of cordierite and pyroxene hornfels formed, particularly at the base of this intrusion, as a result of the introduction of magnesium, calcium, and iron into the enclosing rocks by the magma. The magma became enriched in silica as a result of gravitational-kinetic differentiation in the basic magma (which had been enriched by silica during crystallization). Rocks of varying composition, including alaskite granites formed a layer 300 m thick at the top of the intrusion.

The small subalkalic and alkalic intrusions, whose formation is related to post-folding fractures, developed during the final stages of the Hercynian tectogenetic cycle, are of early Mesozoic age, if the tectonic activity continued in the Triassic. The small intrusions are planar structures, deformed domes, and stocks, as well as typical filled fractures, flattened lenticular forms with sharp terminations extending normal to the strike of the enclosing rocks. They range from one to dozens of square kilometers in size. As yet, only about 20 such intrusions have been found, primarily among the Permian formations of the western Byrrang mountains. Small intrusions intersect the Permo-Triassic tuff-lava series, as well as traprock dikes and sills. Fragments of the small intrusions have been found in the Lower Cretaceous conglomerates. This is why the age of the intrusions has been established as Upper Triassic to Lower Cretaceous. The small intrusions are the youngest manifestations of magmatic activity in Taymyr. They are subdivided into two types: subalkalic and alkalic, which are almost never found together. Granosyenites and granodiorites predominate in the subalkalic rocks; diorite syenites and monzonites are rare. Syenites and the rarer nepheline syenites predominate in the alkalic rocks. Granites occur only rarely; they are represented by porphyritic varieties, which also occur among the subalkalic types. The numerous dikes (dike facies of the small intrusions) are composed of granite porphyries or lamprophyres. The former are thicker than the latter, but occur less frequently. Locally, radiating dikes can be seen 1 to 2 km from the intrusions. Layers of biotite-cordierite hornfels surround almost all of the small intrusions; their thickness is nearly proportional to the size of the intrusion.

BASIC FEATURES OF METALLOGENY

The numerous ore formations of the Taymyr peninsula are directly related to the very extensive and varied magmatic phenomena of this region. Polymetallic and, in part, mercury and molybdenum deposits, clearly related to the post-Hercynian low-alkali and subalkalic intrusions, deserve the closest attention. All other ore deposits related to Proterozoic and Paleozoic intrusions (with the exception of the abundant dikes of muscovite pegmatites) have been little studied until recently.

The fields of pegmatite dikes containing muscovite are related to the Proterozoic two-mica granitoids. The Birulinskoye deposits, on the Zarya peninsula near the shore of the Karsk sea, have been studied more thoroughly than the other fields. Here, the great number of pegmatite dikes occurs most commonly in plagioclase-gneisses. Those dikes which are situated directly in the granites and determine zonal structure, are the ones which usually contain mica. Muscovite in triangular, hexagonal, and lenticular crystals dozens of square centimeters in size occurs in the central parts of the dikes and at the margins of feldspar and quartz zones. The largest and most valuable deposits of muscovite form in swellings of lamellar dikes or in oval dikes. Beryl, as elongated prismatic crystals, is found in some dikes. Small concentrations of scheelite are found in the "zahlbands".[1] Muscovite from the Biryulinsk formation is not commercially usable because of its fractured structure, due to cataclasis. In spite of the relatively low quality of the mica, the pegmatite fields deserve close scrutiny as areas for prospecting and exploration. A study of the pegmatite dikes at depth for the purpose of testing and determining their composition more thoroughly is particularly necessary.

[1] Side surfaces separating veins from enclosing rocks; also the mineralized or ore-bearing parts of the enclosing rocks.

A separate mineralization is related to the Caledonian formation of subalkalic granitoids. Metallic disseminations are scattered throughout the graptolite series of siltstones and shales surrounding the granitoid intrusions. Gold, copper, molybdenum, vanadium, zinc, and other elements are more highly concentrated in breccias composed of graptolite-shale fragments or in highly kaolinized porphyry and lamprophyre dikes. Primary minerals, originally mostly sulfides, were not preserved due to intense alteration in the zone of leaching. Extensive aggregates and concretions of marcasite formed in their places. Chemical analysis shows that considerable amounts of zinc, copper, molybdenum, and vanadium are components of unknown compounds in the breccias.

Iron, copper, and nickel sulfides are related to the Permo-Triassic traprock formation. Of great interest is the thick differentiated intrusions in the Tulay-Kiryaka-Tas plateau (southeastern Taymyr). At the base of these intrusions (near the porphyritic olivine-dolerite horizon which is 12 m to 15 m thick), disseminated pyrrhotite and chalcopyrite, as well as massive lenticular ore bodies, were found.

Three main ore belts exist in Taymyr (in paragenetic relationship with the small intrusions): 1) tungsten-molybdenum; 2) lead-zinc; 3) arsenic-mercury, extending 100 km and nearly concordant with the strike of the linear fold structures. The lead-zinc and the arsenic-mercury belts are located in the Byrrang mountains; the lead-zinc primarily in the eastern half and the arsenic-mercury in the western. These belts almost merge in the center of the Byrrang mountains (upper reaches of the Verkhnaya Taymyra river), where a mixed-ore assemblage can be observed. The tungsten-molybdenum belt is located north of the Byrrang mountains; it is associated with contact zones of small alkalic intrusions.

The most significant molybdenum occurrence has been found in remnants of the upper part of a syenite intrusion on Ostrov Morzhovyy, which is the western extreme of the Ostrov Kamennyye archipelago. Far to the east of this archipelago, near the lower course of the Lenivaya river, disseminations of molybdenum have been found in massive blocks of faulted vein quartz. Still farther to the east, between the upper reaches of the Mamonta and Kolomeytseva rivers, disseminations of molybdenum in remnants of ancient quartz veins are even more common. Stocklike syenite bodies, situated mainly among the large Precambrian granitoid massifs, are found in the same areas. According to geologic data, these bodies are always associated with the small intrusions. Finally, considerable amounts of molybdenum have been detected (by chemical analysis) in the southern Chelyuskin peninsula in the middle reaches of the Leningradskaya River. They have been found in highly fractured mineralized breccias of the graptolite shales in the contact aureoles of the small alkalic intrusions. These are located at the margin of the large Caledonian granitoid massif. The heavy-mineral residue from alluvial deposits contain considerable traces of scheelite. If the individual points where molybdenum and scheelite have been found were connected, they would form a belt stretching for several hundred kilometers. Within this belt, in contact zones of the small alkalic intrusions, it is quite possible that potential tungsten-molybdenum deposits exist.

The Taymyr occurrences are a product of one of the early molybdenum-ore complexes which developed in the later stages of fold formation; the multiple fracturing and magmatic activity in the form of small intrusions are related to the later stages. The complexes are also related to the earlier-formed syenite bodies which occur at relatively greater depths than the other small intrusions within mountainous Taymyr. The ore occurrences belong to two main types: 1) skarn rocks situated in Paleozoic carbonates, and 2) vein-quartz occurring in the Precambrian rocks and the terrigenous Paleozoic strata. Few of these have been studied; those deposits discovered during small-scale surveying are generally quite insignificant. Nevertheless, that molybdenum has been found in contact zones of small alkalic intrusions is very promising. Prospecting and exploratory work in the contact aureoles of these intrusions is recommended.

The polymetallic belt, trending east, can be traced for 120 to 130 km. It is situated 20 to 30 km from the northern shore of Lake Taymyr. If the polymetallic occurrences in the upper reaches of the Bootankag river (Verkhnaya Taymyra river basin) and those west of it are considered, then the length of this belt can be doubled. Outcrops and alluvial detritus from dozens of ore veins and metamorphosed breccias have been found within the ore belt. The ore bodies within the polymetallic belt are confined, as is usually the case, to two perpendicular fracture systems: one trending northeast and the other northwest. The ore belt itself, which is 2 to 10 km wide, is characterized by a system of east-trending fractures within one of the largest anticlinal structures in Taymyr. Breccia zones, composed of hydrothermally altered fragments of dolerite and sandstone cemented by calcite (and, more rarely, by quartz), are developed along the fractures to a thickness of 50 m. Disseminated sphalerite and fine-grained granular quartz veins are found in the cement. The Lake Surovoye occurrence, near the crest of the large anticline, extends along the northern shore of Lake Taymyr. Thirty-two veins, for the most part vein-like breccias, contained within the east-trending fractures, were found in an 8-km^2 sector of Permian terrigenous rocks cut by dolerite dikes and sills. Veins, commonly

deformed and practically vertical, can be traced for distances from hundreds of meters to three kilometers. Their thickness ranges from 40 to 60 centimeters to 2 meters. The main ore minerals are sphalerite and galena; the zinc content is twice that of lead; their combined content is from 10 to 20 percent.

The Partizan stream occurrence is located along a vertical fracture in the contact between a dolerite dike and a Permian sandstone-siltstone series. It has been traced for 1.5 km and is 1 to 1.5 m thick. The ore body is actually a belt of mineralized breccia between the surrounding rocks. Galena and sphalerite comprise the bulk of the breccia cement and, in rare instances, form separate lenses and veins (particularly galena). The lead and zinc content is almost constantly 15 to 20 percent. The Partizan stream occurrence is as large as the Lake Surovoy occurrence.

The polymetallic ores of Taymyr are mesothermal lead-zinc deposits related to ore complexes of similar designation which are characteristic of the late stages of fold-belt development. Locally, they are accompanied by considerable concentrations of pyrite. Although no direct spatial relation has been observed between these occurrences and the small intrusions, they resemble the so-called telethermal occurrences. Their paragenetic relationship with the small intrusions is supported by the following: 1) the similarity of the structural-geotectonic elements which control both the ore bodies and the small intrusions and their dikes, 2) the abundance of sphalerite as an accessory mineral in the small intrusions, and 3) similarity in the geochemical properties of postmagmatic processes related to the small intrusions and accessory alteration of country rocks. If the tungsten-molybdenum ores are contained directly within the contact zones of the early-stage small intrusions, the lead-zinc ores are paragenetically related to the late-stage small intrusions. It can only be concluded from this that the ore occurrences have a final, common parent source situated at relatively low depths; this is characteristic of the development of late magmatic stages.

Insufficient study of the lead-zinc deposits makes it impossible to estimate their industrial value at this time. However, as a result of geologic environment, particularly in relation to structural-tectonic elements, the development of prospecting and exploration in the polymetallic belt of the Byrrang mountains can be recommended.

The arsenic-mercury belt is located in the western half of the Byrrang mountains. Until now, during small-scale geologic surveys, only two major ore veins have been found. These are situated on the flanks of this belt 350 km from each other. Between these two deposits cinnabar has been repeatedly found in heavy-minerals residues concentrated in contemporary alluvial deposits; however, no major concentrations have been found. The most important primary arsenic-mercury deposit was discovered in the upper reaches of Tari-Bigay river (Pyasina river basin), specifically, near one of its tributaries, the Izvilistaya river. Here, in an area of 6 km^2 are concentrated thin veins, lenses, nests, and networks of fine veinlets (Stockwerk). They are related to the fracture zones in lamprophyres and their contacts with limestones. As yet only two such zones, trending northwest, have been found, but there is a good possibility of finding a whole series of such zones. The largest zone has been traced along fine channels for 400 m, although it may extend for over 1 km. Mineralization of the fracture zone is exceptionally uneven; frequently the zone is barren. Lenses and nests of realgar, several dozen centimeters in size, intersected by veinlets of cinnabar, are common. Veinlets of realgar with finely disseminated cinnabar forming a fine network are also common. Locally, country-rocks have been transformed into a finely ground friable mass in which numerous small lenses and veinlets of realgar and stibnite, as well as finely disseminated cinnabar, are included. In rare instances, the realgar acts as a cement in the fractured limestone. More commonly, it is disseminated in calcite veins which pinch out sharply.

The only other known occurrences of primary cinnabar in Taymyr are located at the source of Malaya Uboynaya River in the extreme western part of mountainous Taymyr. Realgar-cinnabar mineralization is concentrated in an area of 5 or 6 km^2. The occurrence is related to a tectonic wedge of Upper Devonian and lower Carboniferous limestones formed by a system of diagonal normal and thrust faults in the center of the major anticline whose limbs are composed of Permian sediments. The ore occurs in breccias, especially where expanded longitudinally. Several similar zones are known and have been traced for hundreds of meters. Their maximum thickness is 20 m. The breccia is composed of quartzitic-limestone fragments cemented by a network of quartz veins whose drusy surfaces are filled with calcite, stibnite, realgar, and cinnabar. Only realgar is found in the calcite veins. The mercury content of the ore is insignificant.

The arsenic-mercury occurrences in Taymyr can be related to one type of arsenic-mercury-antimony mineralization which is one of the latest ore complexes formed during the latest period of folding. Typically epithermal, this occurrence approaches the arsenic type of mineralization in composition with admixtures of mercury and some antimony. Within the ore-bearing area, only the small-intrusion dike facies was encountered; this phase barely preceded ore mineralization. The practical value

of the arsenic-mercury occurrences in the Byrrang mountains is not clear, for these occurrences have been only superficially studied.

A description of endogenic mineralization related to small intrusions would not be complete without mentioning the fluorite mineralization encountered at several localities throughout the Byrrang mountains. The fluorite occurrences are related to limestone outcrops in Permian terrigenous rocks. The most extensive concentration of fluorite was found on the northern shore of eastern Lake Taymyr.

Those ore occurrences in mountainous Taymyr related to small intrusions differ from the later stage deposits formed during the development of other folded regions in the following manners: 1) the relatively low distribution of mineralization in the early ore complexes, absence of intermediate ore complexes, and maximum distribution of mineralization in the latest complexes (the limited development of tungsten-molybdenum deposits and the thoroughly intensive development of lead-zinc mineralization is quite typical for the Byrrang mountains); 2) absence of sulfide-cassiterite mineralization, characteristic of early silver-lead-zinc-tin ore complexes, thus relegating the lead-zinc ores of Taymyr to the end of the late stages of ore development; 3) incomplete development of the arsenic-mercury-antimony ore complex. Only the low-temperature types are encountered, distinguished by the predominance of realgar or the relative paucity of cinnabar. Thus, ore development in the later stages is far from representing all types of mineralization. In part, concentrations of tin, copper, gold, iron, and the clay minerals are lacking; concentrations of mercury and antimony are relatively low.

The Taymyr fold region, particularly its southern part (the Byrrang mountains, extending for more than 1,000 km) is a new Siberian metallogenic province. Rich deposits of lead and zinc, as well as indicative traces of molybdenum, mercury, and other valuable elements, and of nonmetallic minerals such as muscovite, and fluorite take on even greater significance in the light of abundant workable coal seams in the same region. The development of shipping along the northern sea routes, along the northern coast of Taymyr, and the proximity of the main Siberian water route, the Yenisei river, will greatly facilitate the development of mineral resources in these regions.

REFERENCES

1. Anikeyev, I. P., A. I. Gusev, GEOLOGICHESKY OCHERK YUGO-ZAPADNOY CHASTI TAYMYRSKOGO POLUOSTROVA [GEOLOGIC DESCRIPTION OF THE SOUTHWESTERN PART OF THE TAYMYR PENINSULA]: Trudy Arkt. Inst., v. 140, 1939.

2. Bakar, V. A., GEOLOGICHESKOYE STROYENIYE TSENTRAL-NOY CHASTI VOSTOCHNOGO TAYMYRA [GEOLOGIC STRUCTURE OF THE CENTRAL PART OF EASTERN TAYMYR]: Trudy Instituta Geologiy Arktiki, v. 34, 1951.

3. Wittenberg, P. W., GEOLOGIYA I POLEZNYE ISKOPAYEMYE SEVERO-ZAPADNOY CHASTI TAYMYRSKOGO POLUOSTROVA [GEOLOGY AND THE MINERAL RESOURCES OF THE NORTHWESTERN PART OF THE TAYMYR PENINSULA]: Trudy Gorno-Geologicheskogo Upravleniya, v. 12, 1941.

4. Lyutkevich, Ye. M., D. K. Aleksandrov, PALEOZOY KARSKOGO POBEREZHYA I YENISEYSKOGO ZALIVA I YEGO UGLENOSNOST [PALEOZOIC OF THE KARSK COAST AND THE YENISEY GULF, AND ITS COAL RESOURCES]: Trudy Arkt. Inst., v. 121, 1939.

5. Markov, F. G., M. G. Ravich, V. A. Vakar, GEOLOGICHESKOYE STROYENIYE TAYMYRSKOGO POLUOSTROVA. SB. PO GEOLOGII SOVETSKOYE ARKTIKI [GEOLOGIC STRUCTURE OF THE TAYMYR PENINSULA. SYMPOSIUM ON THE GEOLOGY OF THE SOVIET ARCTIC] Trudy Instituta Geologii Arktiki, v. 81, 1957.

6. Migay, I. M., GEOLOGICHESKOYE STROYENIYE RAYONA MYSA TSVETKOVA NA VOSTOCHNOM TAYMYRE [GEOLOGIC STRUCTURE OF CAPE TSVETKOVA IN EASTERN TAYMYR]: Trudy Instituta Geologii Arktiki, v. 36, 1952.

7. Mutafi, N. N., GEOLOGICHESKOYE STROYENIYE I UGLENOSNOST NIZOV YEV REKI PYASINY [GEOLOGIC STRUCTURE AND COAL RESOURCES OF THE LOWER REACHES OF THE PYASINA RIVER]: Trudy Arkt. Inst., v. 126, 1939.

8. Obruchev, V. A., DOKEMBRY TAYMYRSKOGO KRAYA I SEVERNOY ZEMLI. STRATIGRAFIYA SSSR. [PRECAMBRIAN OF THE TAYMYR REGION AND SEVERNAYA ZEMLYA. STRATIGRAPHY OF THE U. S. S. R.]: Izd. Akademii Nauk SSSR., v. 1, 1939.

9. Ravich, M. G., GEOLOGICHESKOYE STROYENIYE SEVERNOY CHASTI TAYMYRSKOGO POLUOSTROVA [GEOLOGIC STRUCTURE OF THE NORTHERN PART OF THE TAYMYR PENINSULA]: Trudy Instituta Geologii Arktiki,

v. 6, 1950.

10. Ravich, M. G., DOKEMBRY TAYMYRA [PRECAMBRIAN OF THE TAYMYR]: Trudy Instituta Geologii Arktiki, v. 76, 1954.

11. Urvantsev, N. N., TAYMYRSKAYA GEOLOGICHESKAYA EKSPEDITSIYA 1929 G. [TAYMYR GEOLOGICAL EXPEDITION OF 1929]: Trudy Glavnogo Upravleniya, issue 65, 1931.

12. Shvedov, N. A., KHARAKTERISTIKI SVIT VERKHNEGO PALEOZOYA TSENTRALNOY SIBIRI PO ISKOPAYEMOY FLORE [DESCRIPTION OF THE UPPER PALEOZOIC SUITES OF CENTRAL SIBERIA BY FOSSIL FLORA]: Trudy Instituta Geologii Arktiki, v. 53, 1953.

A SCHEME FOR GENETIC CLASSIFICATION OF ENDOGENIC ORE-FORMING PROCESSES[1]

by

V. K. Chaykovsky

• *translated by Research International* •

ABSTRACT

Classification of endogenic ore-forming processes is based on relations existing between mineralization products and intrusions of different composition. Occurrences of contact and near-vein metamorphism are similar. By generalizing information obtained on near-vein alteration and fissure development within intrusion fields, it is possible to conclude that granitoid magmatic source of mineralization, as it grows more basic with depth, approximates gabbrodiorite in composition. Development of ore-body groups within such a field depends upon three independent phenomena: fissure-aureole, mineralization, and magmatic zoning. The classification scheme for ore-forming stages associated with magma indicates close relationship between ore occurrences and granitoid magmas of particular composition, either at the surface or at depth. --Research International.

Long ago, certain investigators suspected magmatogenic heavy-mineral deposits to be related to definite types of magmatic rocks. S. S. Smirnov has shown various heavy metals in ore nodes of a given intrusion, actually to result from successive intrusions of various magmas, in direct genetic relation to the ore deposits. In one of his articles, Smirnov [12] wrote, "even in relatively narrow compositional ranges of granite, the differentiation process related to tectonic activity can produce considerable differences in metallogeny of individual, derived mineralization products: i. e., the need for more precise mineralization-product classification, related to intrusions of varying composition and to various conditions of deposition, is quite apparent."

Over the past 20 years, Smirnov's conclusions have been confirmed repeatedly in the Transbaikal region and the Far East. Extensive geologic and petrographic investigations in the Severo-Vostok [Tr.: the northeast] also have led to similar results. Thus, two cycles of Mesozoic ore deposition were determined in the axial region of Koly-Yano-Chukotka geosyncline. The first, related to Middle or Upper Jurassic tectono-magmatic activity is characterized by dike formations of intermediate granodiorite and diorite; also, the well-known Severo-Vostok sulfide deposits are related to this cycle. The second, also well known and related to Upper Cretaceous granitic intrusions, constitutes a widely developed rare-metal source, predominantly silicic in composition. A Lower Cretaceous intermediate intrusive phase has been noted in the axial zone of Kolymo-Yano-Chukotka geosyncline. Analogous magmatic and ore relationships of the Hercynian were described by B. M. Kupletsky [8] for the eastern slope of the Urals.

Upper Cretaceous magmatic activity throughout Kolymo-Yano-Chukotka geosyncline is represented by leucocratic granite intrusions with corresponding rare-metal deposits in the axial zone, and toward the margins (fig. 1), a more basic granite showing more prominent sulfide mineralization.

The Chinese geologist, Ven Guan [Tr.: Wen Haun?] [3], recently has published data on metallogenic granitoid specialization in western China. He presents 41 chemical analyses of 10 deposits of tin, tungsten, molybdenum, copper, and iron ores. His conclusions regarding genetic relationship between these metals and on their occurrence in various types of granitoids are given in figure 2. Numerical relationships of quantitative indicators, are given, according to A. N. Zavaritsky, for various types of metallogenic granites.

Differences in types of ore deposition are determined by magmatic-differentiation processes (and, naturally, by tectonic processes); extremely well demonstrated in mobile belts of the earth's crust. It is well known that mineralization products or types of deposit vary in different intrusions; they differ also within a single ore node related genetically to a single intrusive body.

Endogenetic ore mineralization can be considered a stage in contact-metamorphic alteration which occurs in the intrusive aureole. In order to establish relationships between various mineralization types in ore nodes and genetically related intrusions one may employ the results of studies on contact-metamorphic phenomena.

Magmatic and postmagmatic mineralization are differentiated in magmatic processes.

---

[1]Translated from Skhema geneticheskoy sistematiki protsessov endogennogo rudoobrazovaniya: Sovetskaya Geologiya, 1959, no. 5, p. 81-95.

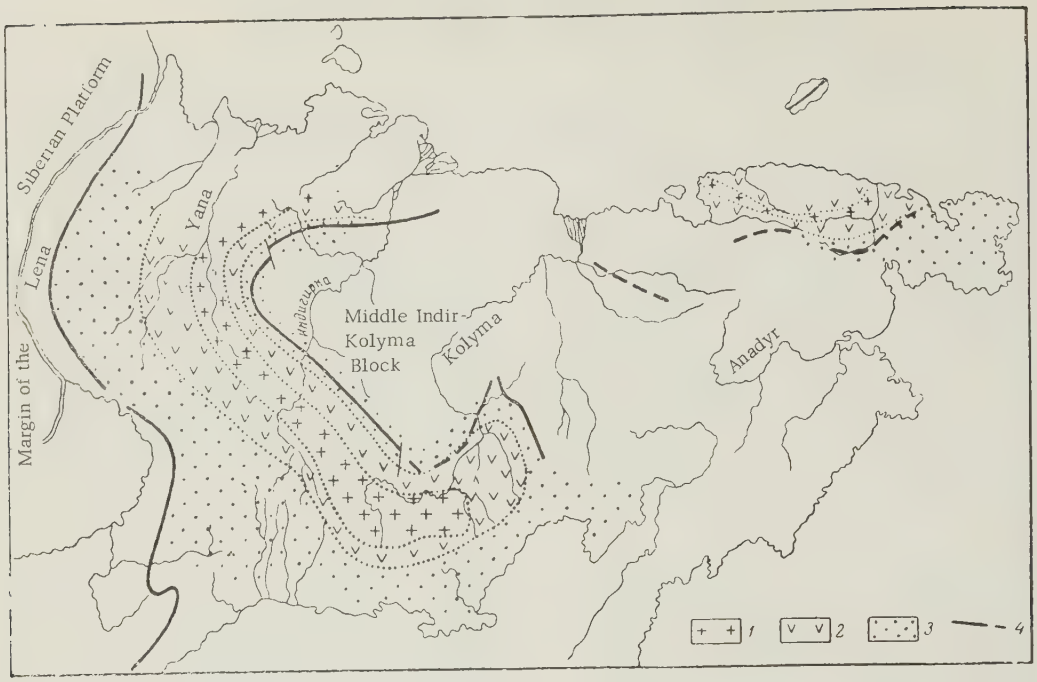

FIGURE 1. Map indicating distribution of post-Upper Jurassic mineralization in the Northeast (Severo-Vostok)
Zones with predominant pegmatite and greisen mineralization: 1) tourmaline, 2) quartz-sericite, 3) sulfide, 4) border between platform and geosynclinal regions.

According to A. S. Korzhinsky [4], post-magmatic mineralization encompasses early alkalic, later alkalic, and final alkalic stages. Appearance of alkalic stages generally corresponds in time and type to pegmatitic and skarn mineralization stages distinguished by high formation temperatures; the nature of pegmatite and skarn development reflects their origin. Most geologists agree that pegmatites are end products of silicic and ultrasilicic magmas; and, that skarns are related to granitoid magmas of varying composition. Pegmatites are located most frequently in axial regions or, in those adjoining the axes, or paraxial regions of geosynclinal zones displaying features typical of deep-seated tectonic activity; skarns are restricted to geosynclinal margins (eastern Transbaikal, the northeast).

Pegmatites and skarns differ from one another in their development: Pegmatites are greisenized and albitized during the course of further mineralization; the ore is composed, for the most part, of metal oxides and molybdenite. Skarns are subjected to hydration, carbonization, and chloritization; heavy-mineral oxides and sulfides are formed. In places where both skarns and pegmatites occur, pegmatites are commonly contained within the skarns as younger, or intersecting formations. G. A. Ivankin and other investigators encountered this phenomenon in skarns of the Khakassin region. Moreover, N. M. Uspensky has noted that skarns in one magmatic complex contain polymetallic and copper ores almost exclusively and, that tungsten and molybdenum ores are present in pegmatites and aplites.

Many examples of pegmatites intersecting skarns and skarn ores were noted by Kh. M. Abdullayev; in his opinion, skarn-ore deposits, very similar in form, to intrusives, in themselves initiate an entire genetic order; thus, they occupy a definite and natural position in relation to dikes. Post-intrusive dikes (aplites, pegmatites) and partly syn-intrusive dikes obviously can intersect skarns; these dikes undergo skarnization through original- or later-postmagmatic solutions [1].

According to several investigators, therefore, mineralization products related to two phases of granitoid magmatic activity, can occur in skarns or contact-metamorphic formations. The first, or earlier phase frequently is characterized by iron, polymetallic, and gold ores; the second, or later phase, related to more silicic granitoids, frequently is distinguished by rare-metal ores. This is in complete agreement with theories on the progression of levels of differentiation in magmatic mineralization sources.

Major metasomatic processes of the post-

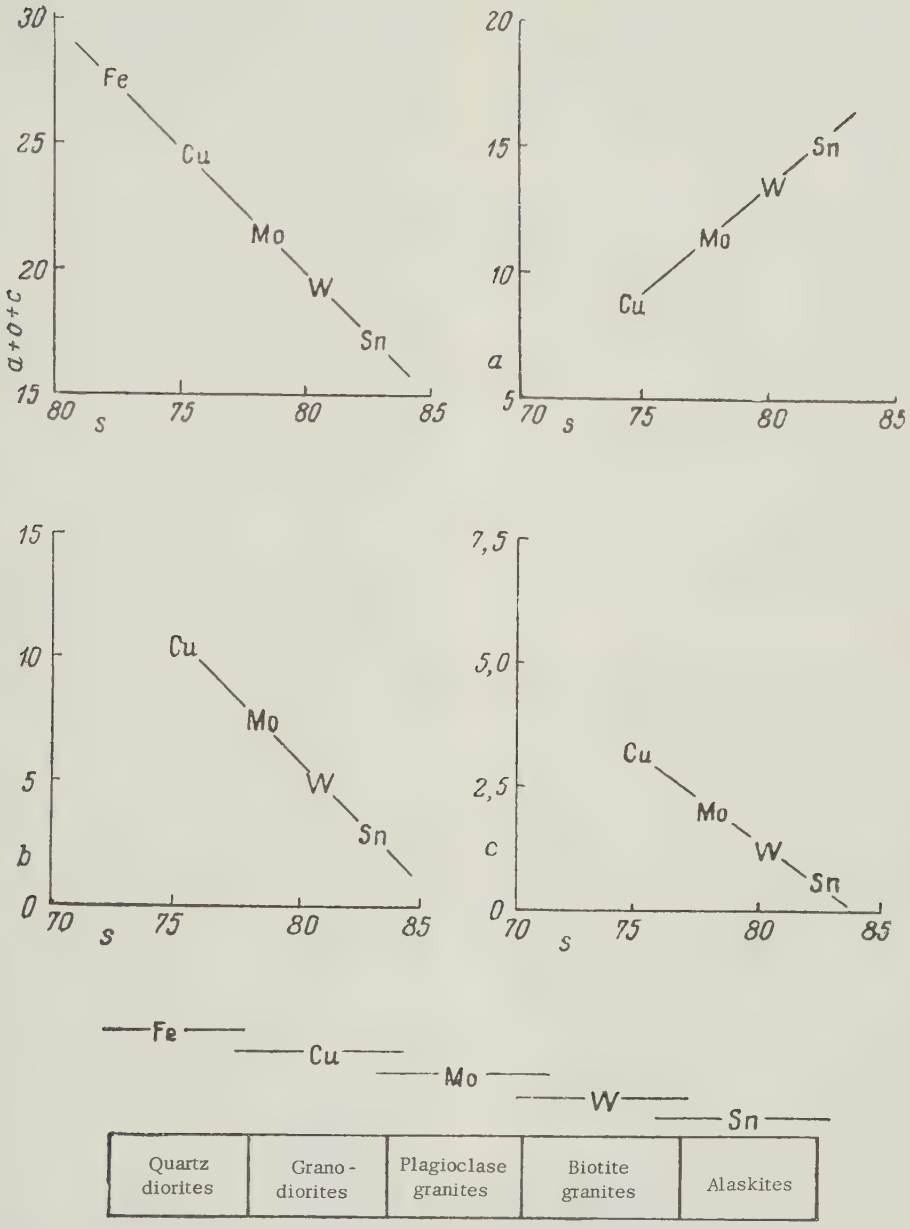

FIGURE 2. Diagram representing relationships between ore deposits and granitoid intrusions of varying composition in eastern China after Ven Guan. (Tr.: Wen Huan).

magmatic acidic stage are greisenization, tourmalinization, quartzitization-sericitization (a single phase, most frequently including quartzitization and sericitization, analogous to designation of the greisenization process to include quartzitization and muscovitization), and propylitization, named in order of their occurrence in progressively more basic intrusive rocks (i. e. , from acid granites through diorites to gabbros).

Greisenization, obviously the best-known and most sharply developed metasomatic process, is characterized by intensive removal of alkalines and by its quartzitization of rock by acid postmagmatic solutions [1]. Principal ore minerals formed exclusively in greisens are cassiterite, wolframite, and molybdenite; the light elements beryllium and lithium are characteristic for this rock type.

Tourmalinization and greisenization are similar in many respects; however, tourmalinization always occurs somewhat later than

greisenization. Frequently, tourmalinization conceals greisenization products; also, it differs from greisenization by its unique distribution. Greisens, or greisenized rock, do not always contain tourmaline; greisenization is not prerequisite for tourmalinization.

It is interesting to note that the primary tourmaline-mineralization area in the northeast is somewhat removed toward the margins, from the axial zone of the geosyncline; greisenization has occurred in the axial zone (fig. 1). Spatial disjunction of these fields is not accidental: Geologic literature contains many indications that tourmalinization is related genetically to less silicic magma than is greisenization [4]. From repeated observation in the northwest, it was established that tourmalinization is not accompanied by any significant metallogenesis in monomineralic media; however, a considerable number of ore formations have been found in tourmaline-rich veins. In the majority of cases, these ore formations are not related to tourmalinization; rather, they appear to be associated with some other phase of postmagmatic activity.

The most widespread postmagmatic process is quartzitization [Tr.: silicification?]-sericitization; in the northwest, this process has occurred after greisenization and tourmalinization, and, represents an early phase only where other processes had not developed. The nature of quartzitization-sericitization occurrence varies; for this reason, possibly, geologists are not able to assign it definitely to contact-metamorphic or ore-forming processes. Subregional, quartz-sericite metasomatism develops in hypabyssal environments, in more or less permeable rocks having considerable extent. Rocks referred to somewhat erroneously [9], as "secondary quartzites," are formed by this process in the presence of silicic postmagmatic solutions. Under near-surface conditions, or, in highly fractured zones which form porous leached rock, it is possible that clay minerals may predominate (argillitization).

According to N. I. Nakovnik [10], secondary quartzites have a clearly expressed, genetic relation to silicic rocks and surface volcanic processes. Typically, they form definitive mineral complexes composed mainly of quartz-sericite, alunite, kaolinite, andalusite, diaspore, and pyrophyllite; secondary minerals are corundum, dumortierite, topaz, zunyite, and tourmaline. The minerals constitute a facies and form in definite sequence, locally displaying sharp zoning.

From Nakovnik's study, the following points were determined: 1) secondary quartzites are derived from a series of solutions originating successively from a progressively more basic source; 2) quartz-sericite facies of secondary quartzite is related genetically to intermediate-silicic rocks, locally forming polymetallic, molybdenum, and gold-silver ores; 3) quartz-sericite facies of secondary quartzites are very similar to beresite rocks, a widely distributed type of vein alteration product.

Propylitization is the next type of post-magmatic activity in time and in degree of solution activity. According to Korzhinsky [4], propylitizing solutions are less active, or less acid, because for the most part, they are generated in more basic magmas of granodiorite type, rather than in granites. Propylitized rocks are intersected by quartz and quartz-epidote veins containing ore minerals, principally chalcopyrite; in some areas, this association has economic potential. Some of these minerals formed during propylitization; others, later. Later quartz veins frequently contain rich gold and silver ores.

According to Korzhinsky, greisenization, quartzitization-sericitization, and propylitization are contact-metamorphic in subregional extent; however, it is possible to argue that analogous metasomatic-mineralization complexes can be observed in vein alteration related directly to analogous ore formations and representing a stage of contact-metasomatic mineralization.

Both greisens of similar composition and vein-associated greisens having some areal extent are common. Alterations in vein-associated rock related to ore-bearing-solution activity along fractures, are analogous to subregional tourmalinization, quartzitization, and sericitization. Mode of occurrence of the linear and areal groups depends upon distribution of mineral solutions and development of metasomatic processes, determined by different types of tectonic structures. Under conditions of sufficiently high temperature, fine fractures implement uniform areal distribution of metasomatism; larger fractures direct development of metasomatism along definite, linear structures.

Great similarity between mineralogic and chemical features of subregional or vein-associated mineralization of a given type indicates that solutions of analogous composition serve as their formation source and, consequently, as their magmatic source. This conclusion is very important: If subregional metasomatism indicates directly how acid or basic the post-magmatic mineralization source was, then vein-associated alterations are observable with a single ore node and are represented by a series of successively altered types of mineralization; this indicates that these solutions do not remain constant. Alterations in vein-associated mineralization are very regular. If these conclusions on magmas and contact metasomatism are correct, the character of

these alterations invariably points to increasingly basic magmatic sources.

A great deal of factual material, obtained by the author (1940-1941) during his investigation of mineral occurrences in Yano-Adychausky basin (Severo-Vostok), demonstrates continental intrusions not only formed ore-bearing solutions, but fractured the country rock as well, allowing these solutions to circulate in upper layers of the lithosphere. As a rule, in plan and in horizontal projection, ore-bearing fractures open during periodic occurrences of tectonic activity, toward the periphery of an intrusive. Qualitative evolution of fractural deformations proceeds as progressive spatial displacement: tension fractures in intrusive domes give way to shear fractures along the periphery. Mutual distribution and qualitative characteristics, as well as growth direction of fractures, are in complete agreement with accepted theories as to time, location, substance, and fracture-filling processes. Similar ideas were expressed by A. V. Korolev [5] who termed this "centrifugal" mineralization.

An excellent example of fracture distribution and ore formation of this type (around a complex leucocratic-granitoid intrusive, forming a series of ore nodes) occurs in Severo-Vostok. Lazo ore node in the silicic granitoid intrusive belongs to this formation type. Greisens, quartz, and quartz-tourmaline veinlets occur in the arched area of the massif; their areal extent is limited by contact of massif with surrounding rock (fig. 3). Numerous tension-fracture veins containing conspicuous tourmaline mineralization are located in the inner contact zone. In the outer contact zone (the practically unmetamorphosed country rock), extensive shear zones are characterized by chlorite-sulfide mineralization.

According to I. Ya. Nekrasov, in an extreme northern region of the U. S. S. R. the tourmaline, quartz, sulfide, tin suite is replaced from the center of the node outward toward the periphery, first by a chlorite, quartz, and sulfide suite; then, by sulfides containing increasing amounts of lead and zinc and decreasing amounts of tin. Several interesting lead deposits were found at ore-node margins. This zoning, as explained by Nekrasov, resulted from gradual growth of fractures away from the center and, from the multiple-staged fracture-filling process. The later-formed fractures (those farthest from the center) were filled by minerals precipitated from later solutions. Many such instances can be cited: the Zapadnoverkhoyansk region (fig. 4), described by Smirnov [11], is analogous.

Smirnov observed, "high-temperature molybdenum and copper-zinc deposits are found exclusively in hornfels; polymetallic deposits are distributed considerably further

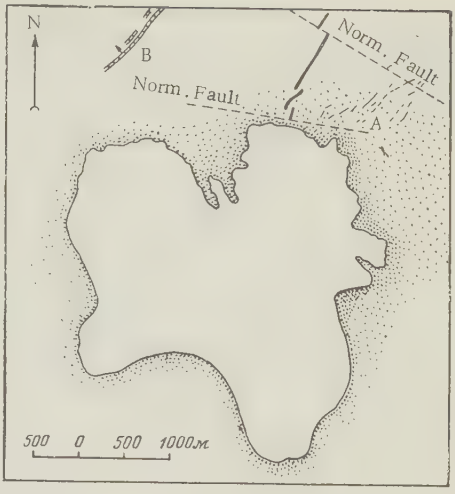

FIGURE 3. Ore lode in Lazo granitoid massif A) region of quartz-tourmaline veing development, B) zone of chlorite-sulfide mineralization.

outward." Naturally, such a situation could not be understood, were no direct genetic relationship between fractures described and ore-bearing solutions of the intrusive established instead of an indirect or paragenetic relationship.

Mineralization aureoles are not always completely developed: for instance, it is possible, depending on fracture types, to find sulfide zones in the central intrusive; although if they are at all possible, aureoles have not been observed indicating fracture formation and mineralization of a given stage to have formed at intrusive-field margins, then to have proceeded toward the center. Thus, fractures formed in an intrusive field during a single ore-formation process, vary. Distribution of veins and metasomatic formations in an ore node is the spatial reflection of temporal change in mineralizing agents; this change (during a single magmatic phase) always occurs as though mineralizing-solution sources within a single intrusive front were characterized by a gradual magma shift to basic. Change in silicic dikes is an even better indicator of increasingly basic mineralization. According to petrographers, these dikes originite in relatively deep horizons. Geologists in studying ore deposits know that leucocratic dikes usually precede (though they be nearly contemporaneous) metallic-ore deposition in acidic veins. Analogous relationships have been observed repeatedly in corresponding phenomena of intermediate magmas (Primorye, Severo-Vostok). That this analogy occurs not only in time but also in space is interesting; with passage of time, ore and dike bodies tend to

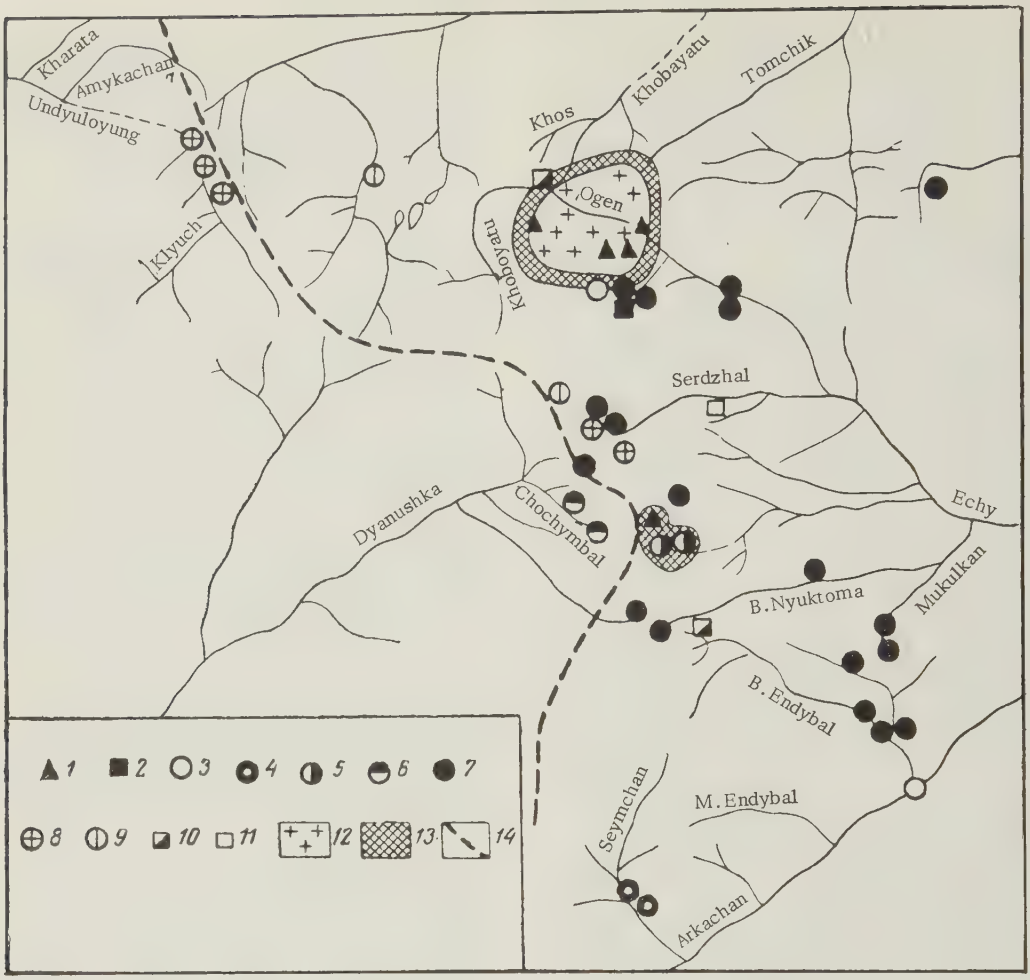

FIGURE 4. Ore deposits in western Verkhoyansk range
1) molybdenum, 2) tin, 3) arsenic, 4) copper-arsenic, 5) copper-zinc, 6) arsenic-polymetallic, 7) polymetallic, 8) pyrite, 9) copper, 10) polymetallic ore fragments, 11) Permian sandstones and shales, 12) granite, 13) contact (sulfide-altered) hornfels, 14) main-watershed line.

migrate toward intrusive-field margins.

Arga-Ynnakhkhay intrusive field (Severo-Vostok) illustrates ore-body and dike migration; there changes have occurred over both space and time: 1) in intrusive rocks, pegmatites and greisen types; 2) in outer-contact hornfels, cassiterite-quartzite and quartz-tourmaline types; and 3) in the inner portion of outer contact zones, sulfide types. Dike composition also changes from leucocratic in the center to mesocratic at the margins.

"It becomes apparent," writes M. B. Borodayevskaya [2], "that both are characteristic of formations having their sources at different depths. The pegmatite-granite series of vein rocks obviously represents outliers situated relatively close to cooling intrusives; the various porphyrites originated at deeper horizons." V. S. Koptev-Dvornikov [6] remarked on a region in Kazakhstan: "if rocks of the first type (aplites, aplitic granites - V. V.) are related spatially only to intrusive bodies, vein rocks of the second type (granite-porphyry, diorite-porphyrites, gabbro-diabase, gabbro-porphyrites, and lamprophyres-V. V.) actually originate from more deeply seated magmatic sources." This is evidenced by considerable deviation of rocks beyond confines of the intrusion.

Quartz-ore veins containing gold and polymetallic sulfides constitute a vein-rock series of the second granodiorite stage. Formations of rare-metal sulfides containing cassiterite or

wolframite correspond to this formation type for intrusions in Siberia (for example, formations characteristic of the inner portion of outer contact zones).

Doubtlessly, relationships observed between dikes and ore-formation processes originate from some common cause: an uninterrupted differentiation in magmatic source. As, during renewed tectonic activity fractures increase vertically and magma composition within one intrusive field changes, given steady decrease in continuous activity level for the fracture-forming and mineralizing source, the direct consequence is a shift to basic. This approach seems to raise the question involving organic relationships of increase in fracturing to cooling of an intrusive, put forth by Smirnov. "It may be," he wrote [13], "that renewed fracturing, uncovering new passages for new solutions, is related to further evolution of a cooling intrusive."

Therefore, two rather opposite tendencies are observed in development of mineralization. One corresponds to Smirnov's suggestion that deposition of various heavy metals in an intrusive field, is the result of consecutive injections and post-intrusive activities of magmas grown progressively acid with passage of time. Obviously, this happens only when large fractures form during the time interval between injections; this interval is marked also by considerable periods of relative inactivity. A completely opposite development however, can be observed: these phenomena, quite well known to geologists, develop throughout each individual magmatic phase; they can be observed readily in ore nodes and deposits where mineralization is accompanied by silicic to basic-magma transitions and concomitant fracture development within the intrusive field.

O. V. Olsner [15] has found mineral paragenesis to have occurred in identical sequence for each of 18 regions of the Rudnyye mountains. He explains the sequence by the relation of mineralization to multiphased Variscan granites: Sudetic, Asturic, and Salic. Only the youngest Variscan magmas are characterized by high lead, tungsten, and bismuth content; older magmas are distinguished by predominance of cobalt and nickel: in this manner, developing concurrent to a sequence of magmatic-differentiation phases, a progressively more silicic mineral paragenesis can occur.

In the same article, Olsner indicated another type of ore development: "According to its distance from the pluton, mineral paragenesis begins with a pegmatitic-pneumatolitic casserite or tungsten association. Subsequently, high-temperature polymetallic paragenesis can be observed everywhere. After a certain transitional period, quartz-gel containing hematite, barite, or even fluorite occurs throughout. This is followed, although developed extensively only locally by carbonates containing silver-antimony compounds, barite veins containing lead-silver ores, and cobalt-nickel-ore associations with quartz. After this, silver, arsenic and antimony ores again are formed with carbonates."

On the basis of material examined, a definite idea may be formed on postmagmatic-process development. Actually a single granitic intrusion, in composition is a multiple magmatic complex whose individual components can become mineral-solution sources, under favorable conditions, during a single phase; moreover, composition of these sources becomes progressively basic. Transition from upper, more silicic, to lower, more basic horizons of a cooling intrusive is reflected in zonal distribution of various mineralization types or, in dikes of varying compositions within a single intrusive field. Regular (centrifugal) fractures in the intrusive field form space for equally regular (in composition) ore-solution complexes. With cooling of the intrusive and passage of the active magmatic front to lower horizons, these regular sequences support the notion that ore-forming melt composition within an individual node becomes progressively more basic (independently, or almost independently, of country rock).

"The mechanism of this differentiation," Yu. A. Kuznetsov stated [7], "is not completely understood, but the possibility exists that differentiation of magmatic solutions by specific gravity, analogous to differentiation of aqueous salt solutions determined experimentally by A. M. Kuzmin, occurs here." This does not constitute complete refutation of paragenetic relationships between intrusions and mineralization, demonstrated by Smirnov, Yu. A. Bilibin, and F. K. Shipulin. The relationships do exist and their presence in certain mineralized areas is admitted by geologists. Sharp distinction between metals related to definite intrusive bodies and those of another, or different substratal or subformational origin, is untenable. The possibility of "paragenesis" of lead-, lead-zinc-, and gold-type metallic deposits, in our opinion, should be considered a consequence of potential capacity of corresponding ore-bearing solutions to migrate over great distances from the parent source, as compared to solutions containing tin- or tungsten-type metals.

Table 1 indicates relationships between composition of magmas and of ore-forming solutions. It should be noted that this table presents only certain average indicators for deposit formation and mineralization, most typical of a given magmatic composition. Genetic stages of mineralization are only conditional; and, are based primarily on relative distances of postmagmatic solutions from

TABLE 1. Classification of ore-deposit mineralization

Chemical Characteristics of Magma	Genetic stage of mineralization	Mineralization stages	Near-vein alteration	Probable principal mineralization agents
Acid	Pegmatitic	Aplite-pegmatitic	Granitization, usually concealed by later alteration	Alkaline magmatic residue
	Pneumatolitic	Gneiss-quartzitic (quartz, cassiterite)	Muscovitization, quartzitization (greisenization)	H_2O, fluorine chlorine
	Pneumatolitic-hydrothermal	Tourmaline	Tourmalization, chloritization	H_2O, bromine carbonic acid
		Quartz-sericite	Quartzitization, sericitization, kaolinization, chloritization, albitization, carbonatization (beresitization)	H_2O, fluorine, carbonic acid, sulfur, arsenic
Intermediate	High-temperature-hydrothermal	Sulfide	Sulfization, chloritization, carbonization	H_2O, sulfur, carbonic acid
	Intermediate temperature-hydrothermal	Carbonate polymetallic (late sulfide)	Carbonization, chloritization, sulfidization, propilitization	H_2O, carbonic acid, sulfur
	Low-temperature-hydrothermal	Gold quartzitic	Hornfels, alunitization	H_2O, carbonic acid, sulfur

magmatic sources.

Features of genetic stages in mineralization always can be distinguished in skarn deposits if country rock composition is considered. Ore-formation stages for granitoid magmas are shown in sequence as they develop during a single magmatic phase (from earliest to latest mineralization stages). In a given ore node, although any of these stages may be absent, the general course of development is always retained. Telescoped deposits are marginal cases of an abbreviated type where a series of mineralization stages for a given sequence, occurs during a single uninterrupted stage.

From the table it is apparent that quantitative relationships for mineral combinations undergo definite change for each of the mineralization stages. Tin (and tungsten) is metal typical in leucocratic mineralization; that is, mineralization related to acid magmas rarely, or very rarely, encountered in later stages of the process (last item in the table). Molybdenum is similar genetically to tin and tungsten, but because of its great affinity for sulfur, it displays definite deviation toward chalcophilic elements; both acid and intermediate magmas are sources of molybdenum.

Most geologists (including A. Ye. Fersman, Smirnov, Bilibin) relate gold mineralization to diorite, although some investigators admit that it can be derived from more silicic magmas. Understandably, as in all works of this sort, certain generalization of known factual material

stages with respect to acid and intermediate magmas

Degree of concentration of principal metals				Supposed phase of magmatic differentiation	Position of vein in relation to intrusion	Ore body form
Tin	Molybdenum	Polymetals	Gold			
Avg.	Almost none	Almost none	Almost none	Very acidic granites	Varied	Irregular planar bodies
Avg.	Avg.	Almost none	Almost none	Very acidic and acidic granites	Domes and mantles of intrusions	Stockwerk (fine networks of veins), parallel veinlet systems
Small amounts	Almost none	Almost none	Almost none	Intermediate acidic granites	Inner- and outer contact zones of granitoid intrusives, distributed throughout cupola region	Parallel systems of veinlets, groups of veins, rarely individual ore bodies
High	High	Avg.	Small amounts			
Small amounts	Avg.	Above avg.	Small amounts	Granodiorites	Inner portions of outer contact zones	Same as above, or individually mineralized zones minutely fractured at outer portions of outer contact zones
Almost none	Small amounts	High	Avg.	Quartz diorites	Outer portion of outer contact zones	Individual veins in outer portions of outer contact zones
Almost none	Small amounts	Small amounts	High	Diorties and gabbro-diorite	Metalliferous origin often only assumed	Morphology of ore body closely related to regional structure

is unavoidable; a good example of this is the series of diagrams by the Chinese geologist, Ven Guan [Tr: Wen Haun] (fig. 2).

From the table, it is clear that the greisen mineralization stage, poor in iron, is replaced by an iron-rich tourmaline stage, replaced in turn, by a quartz-sericite stage almost completely devoid of iron; this, is followed by an iron-rich sulfide stage (mostly pyrite). The described fluctuations are rhythmical and undoubtedly reflect corresponding composition changes in the ore-forming front. A genetic stage of mineralization is not, in concept, synonymous with a deposit type. Usually, a deposit encompasses several stages and periods of mineralization, superimposed one upon the other following the sequence of the table; principal stages define a given type of deposit.

CONCLUSIONS

A chemically definitive type of ore formation corresponds to a chemically definitive metal-bearing solution, regardless of internal mineralization conditions. This conslusion is supported by Smirnov's well-known assumption regarding relationships between deposit types and of ore-forming magma compositions.

Ore formation is a process defined by a cycle of consecutive mineralization stages whose development is parallel to differentiation in magmatic ore-solution source and fracturing process. Three types of simultaneously developing zonal phenomena occur within a single intrusive field;

fracturing, ore formation, and magmatic activity.

In a given magmatic phase, once an ore-forming process has begun, it can proceed in only one direction. In the case of granitoid magmas, active mineralization sources of a single magmatic front becomes progressively more basic.

Change over a time interval in mineralization stages corresponds in ore-forming fronts, to definite displacement from upper to lower (from more silicic to more basic) intrusive-complex horizons.

Minerals deposited during mineralization process follow a zoning pattern owing to alternate enrichment of petrogenic elements (silicon, calcium), and metallogenic elements (iron, copper, lead, etc).

REFERENCES

1. Abdullayev, Kh. M., DAYKI I ORUDENIYE [DIKES AND ORE FORMATION]: Gosgeoltekhizdat, 1957.

2. Borodayevskaya, M. B., NEKOTORYYE VOPROSY GEOLOGII PETROGENEZISA I METALLOGENII MALYKH INTRUZIY POZDNYKH ETAPOV RAZVITIYA TEKTONO-MAGMATICHESKOGO TSIKLA [SOME PROBLEMS ON THE GEOLOGY, PETROGENESIS, AND METALLOGENY OF SMALL INTRUSIONS IN THE LATE STAGES OF THE TECTONO-MAGMATIC CYCLE]: In: Magmatizm i Svyaz s Nim Poleznykh Iskopayemykh, Akademiya Nauk SSSR, Izd., 1955.

3. Ven Guan (Tr.: Wen Haun), O METALLOGENICHESKOY SPETSIALIZATSII GRANITOIDOV [METALLOGENIC SPECIALIZATION IN GRANITOIDS]: Science Record, New Series, v. 2, no. 11, Peking, 1958 (reprinted in Russian).

4. Korzhinsky, D. S., OCHERK METASOMATICHESKIKH PROTSESSOV. OSNOVNYYE PROBLEMY V UCHENII O MAGMATOGENNYKH RUDNYKH MESTOROZHDENIYAKH [AN OUTLINE OF METASOMATIC PROCESSES. BASIC PROBLEMS IN THE STUDY OF MAGMATOGENIC ORE DEPOSITS]: Akademiya Nauk SSSR, Izd., 1953.

5. Korolev, A. V., ZAVISIMOST ZONALNOGO ORUDENENIYA OT POSLEDOVATELNOSTI RAZVITIYA STRUKTUR RUDNYKH MESTOROZHDENY [RELATIONSHIPS BETWEEN ORE FORMATION AND THE SEQUENCE IN THE DEVELOPMENT OF ORE-DEPOSIT STRUCTURES]: Akademiya Nauk SSSR, Izvestiya, Seriya Geologicheskaya, 1949, no. 1.

6. Koptev-Dvornikov, V. S., K VOPROSU O NEKOTORYKH ZAKONOMERNOSTYAKH FORMIROVANIYA INTRUZIVNYKH KOMPLEKSOV GRANITOIDOV [SOME LAWS GOVERNING THE FORMATION OF INTRUSIVE GRANITOID COMPLEXES]: Akademiya Nauk SSSR, Izvestiya, Seriya Geologicheskaya, 1952, no. 4.

7. Kuznetsov, Yu. A., PROISKHOZHDENIYE MAGMATICHESKIKH PORODOV [ORIGINS OF MAGMATIC ROCKS]: In: Magmatizm i Svyaz s Nim Poleznykh Iskopayemykh, Akademiya Nauk SSSR, Izd., 1955.

8. Kupletsky, B. M., GRANITNYYE INTRUZII VOSTOCHNOGO SKLONA SREDNEGO URALA. VOPROSY MINERALOGII, GEOKHIMII I PETROGRAFII [GRANITIC INTRUSIONS OF THE EASTERN SLOPE OF THE CENTRAL URALS. PROBLEMS OF MINERALOGY, GEOCHEMISTRY, AND PETROGRAPHY]: Akademiya Nauk SSSR, Izd., 1946.

9. Loginov, V. P., ALYUMOSILITSITY KOLCHEDANNOGO MESTOROZHDENIYA [ALUMINUM SILICATES OF THE KABAN PYRITE DEPOSIT]: Akademiya Nauk SSSR, I. G. N., Trudy, 1951, no. 15.

10. Nakovnik, N. I., VTORICHNYYE KVARTZITY, IKH MINERALNYYE FATSII, GENEZIS I PRAKTICHESKOYE ZNACHENIYE [SECONDARY QUARTZITES, THEIR MINERAL FACIES, GENESIS, AND PRACTICAL IMPORTANCE]: Akademiya Nauk SSSR, Izvestiya, Seriya Geologicheskaya, 1947, no. 1.

11. Smirnov, S. S., METALLOGENIYA ZAPADNOGO VERKHOYANYA [METALLOGENY OF WESTERN VERKHOYANSK]: Problemy Sovetskoy Geologii, 1934, no. 4.

12. _____, SKHEMA METALLOGENII VOSTOCHNOGO ZABAYKALYA [OUTLINE OF METALLOGENY IN EASTERN TRANSBAIKAL]: Problemy Sovetskoy Geologii, 1936, no. 4.

13. _____, K VOPROSU O ZONALNOSTI RUDNYKH MESTOROZHDENY [ZONALITY IN ORE DEPOSITS]: Akademiya Nauk SSSR, Izvestiya, Seriya Geologicheskaya, 1937, no. 6.

14. Buddington, A. F., COINCIDENT VARIATIONS OF TYPES OF MINERALIZATION AND OF COAST RANGE INTRUSIVES: Econ. Geology, v. 22, 1927.

15. Olsner, O. W., DIE ABHÄNGIGKEIT DER PARAGENESEN ERZGEBIRGISCHER LAGERSTATTENEBEZIRKE VON INTRUSIONALTER DER ZUGERHORIGEN GRANITE: [RELATION OF HARZ MOUNTAIN PARAGENETIC DEPOSITIONAL REGIONS TO INTRUSION AGE OF GRANITE COUNTRY ROCK]: Die Bergacademie Freiberger Forschungheftes, 1951, no. 8.

SOME PROBLEMS ON THE ORIGIN OF FOLDING[1]

by

V. V. Ez

• *translated by Royer and Roger, Inc.* •

ABSTRACT

The mechanism of geosynclinal folding has been explained variously by vertical compression, wave motion, shearing action, competent folding, and laminar redistribution of material within beds. Theoretical objections to various aspects of the major hypotheses are reviewed. The two principal classes of folds, concentric and similar, grade from one to the other. Horizontal compression, applied not only to the edge of a belt of folding, but uniformly throughout the area of folding is a significant mechanism. No new hypothesis is proposed but rather the relationship of seemingly different phenomena of folding is emphasized. --M. Russell.

The mode of origin of folding has for a long time been one of the most interesting problems of tectonics. Many publications have been devoted to this question, to which varied answers have been given. At the same time it is quite obvious that one cannot provide a well-founded explanation of why folds are formed without first answering the question of how they are formed. Nevertheless, it appears that much more attention has been devoted to the second question than to the first.

In this connection, the author wishes to make certain observations on the phenomena that appear within the folds themselves during the process of their formation, namely the mechanism of formation of folds. The discussion will confine itself to folding of the type that it has been agreed to call complete or continuous folding, i. e., the folding most typical of geosynclinal regions.

M. M. Tetyayev [17] has suggested a hypothesis which considers vertical compression of the beds to be the direct cause of fold formation. The reasoning behind this hypothesis is as follows: the beds are compressed vertically and thus decrease in thickness; this decrease in thickness is inevitably accompanied by an increase in surface area. Because the area occupied by the beds, however, remains the same as before, the increase in the surface area of the beds must lead to their being squeezed into folds. It is easy to detect the error in this line of reasoning; if the surface of the beds is to be increased as a result of their vertical compression, it must also be possible to increase the area occupied by the beds; if this possibility does not exist, the surface area of the beds cannot be increased; there can be no formation of folds.

V. N. Danilovich [10] has suggested a "wave hypothesis" for the formation of folds. According to this hypothesis, folds are the result of friction between beds sliding against each other, just as waves on the surface of the sea are produced by the wind. Thus the folds, in Danilovich's opinion, run through a series of rock strata like the waves of the ocean. One need only recall, however, that large ocean waves do not arise immediately, but only after a long period of oscillation of large masses of water by the action of the wind, to see clearly that one cannot speak seriously of folding being produced in this manner within the earth's crust: in order to set in motion the enormous mass contained in folded rocks, such completely unrealizable relative displacements of the beds would be required as would immeasurably exceed the amplitude and length of the folds.

A completely different cause is suggested as the origin of so-called "shear folds". The term "shear folds" refers to folds produced as shown in figure 1, that is, by the shearing deformation of a series of layers in a direction perpendicular to that of the bedding, without any movement parallel to the bedding. Thus the bedding in this type of fold merely makes the folds more clearly distinguishable; in principle, however, the presence of bedding is not at all necessary for this process to take place.

Obviously, in individual cases, folded structures can actually be produced in such a manner, but one should not, as do some authors [1, 14], consider this to be the fundamental mechanism (or one of the fundamental mechanisms) of folding. This mechanism, in the first place, involves a necessary lengthening of the beds on the flanks of the folds, which, it is well known, is far from universal; in the second place, this mechanism can produce only strictly similar folding, and other processes must be called in to explain the origin of disharmonic structures.

---

[1]Translated from O nekotorykh problemakh proiskhozhdeniya skladkoobrazovaniya, in Lvovskoye Geologicheskoye Obshchestvo - Sbornik (Geological Society of Lvov - Symposium), No. 5-6, 1958, p. 462-478. Report presented at the session of the Lvov Geological Society devoted to problems of general and regional tectonics (January 23-27, 1957).

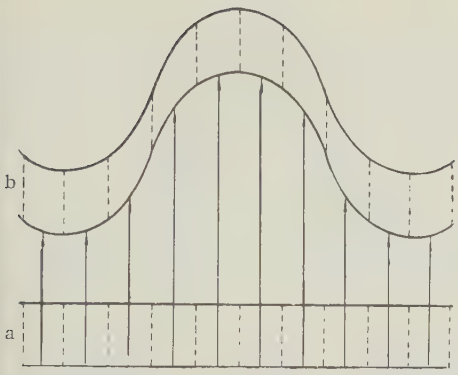

FIGURE 1. Suggested diagram of the formation of shear folds (the folds are formed through the parallel displacement of parts of the bed to different distances, in the direction perpendicular to the bed).

The most serious objection, however, is that this hypothesis fails completely (in fact, does not even attempt) to explain how irregularity of movements which produces folding can arise, folding which results in the appearance of great upward movements, corresponding to anticlines, and areas of lesser movement, corresponding to synclines. Thus the fundamental feature of folded structures, their rhythmic nature, remains the result of some irregularity in the external forces whose mode of origin is unknown.

The well-known hypothesis of "competent folding" was proposed before the turn of the last century [25]. The basic proposition of this hypothesis, which distinguishes it from those that have just been considered, is that folds are formed under conditions of horizontal compression, i.e., by shortening of the horizontal dimensions of the crumpled strata. This view of the conditions under which folding arises is shared at the present time by the overwhelming majority of geologists, although opinions as to the causes and nature of the horizontal compression diverge sharply.

According to the "competent folding" hypothesis, the leading role in the process of folding is played by rigid, "competent" beds, because only these are capable, of transmitting the externally applied horizontal pressure over a great area, while bending into folds, and, of upholding their own weight and that of the overlying rocks during the process of bending. The "incompetent" beds, according to this view, are incapable of transmitting the pressure over any considerable extent; thus they merely bend passively, are flattened out on the flanks of the folds between competent beds, and are pressed into whatever shape is dictated by the structure of the "competent" beds [15, 18].

A whole series of objections can be brought to bear against certain aspects of this hypothesis. It is not clear, for example, why only the so-called "competent" strata, and not all of the beds, can transmit pressure. The necessity of upholding the weight of the overlying rocks (in the exact sense of the word) must also not be considered as proven, since there are no gaps beneath the arches of anticlines.

Many investigators have brought forth other objections to this hypothesis. V. V. Beloussov [4, 6], for example, points out, in the first place, that within folds, rigid beds between more plastic strata are broken into separate blocks, which deprives them of their capability of transmitting horizontal pressure. In the second place, folding is, in his opinion, necessarily accompanied by regular changes in the thickness of all the beds (including the so-called "competent" beds); this is inexplicable in view of the hypothesis of "competent folding".

Relying to a considerable extent on these observations, V. V. Beloussov has proposed another hypothesis for the mechanism of continuous folding; the hypothesis of "laminar redistribution of material" as a result of vertical crushing. Where the hypothesis of vertical squeezing, proposed by M. M. Tetyayev, suggests that the vertical pressure is the direct cause of folding, V. V. Beloussov considers that vertical crushing at certain points produces horizontal compression of the beds, and that this leads to folding in other parts, although in many respects his hypothesis diverges essentially from that of horizontal compression.

The hypothesis of the laminar redistribution of material has had a large part in the development of the author's suggestions regarding the mechanism of folding, as it calls attention to the complexity and variety of the deformation in a stratum that has been compressed into folds; the bed is considered not just as material which deforms passively under the action of external forces, but as a medium that itself plays a large role in the distribution of these forces. This hypothesis, however, contains certain very important discrepancies; these must be examined in somewhat greater detail if they are to be distinguished and analyzed. Moreover, we are concerned not with the opinions of this or that author (which, naturally, will change with the course of time), but with the hypothesis itself in the form in which it appeared in geologic literature.

The laminar redistribution hypothesis [2, 3, 4, 5, 6, 13, 16] is based on the fundamental proposition that, in a typical, continuous, folded structure, there is a regular change in the thicknesses of all the beds: they are increased at the crests and troughs and decreased in the flanks, in comparison to the initial thicknesses. According to this hypothesis, the essence of the processes that take place within the fold itself is the following: irregularly distributed compression normal to the bedding squeezes the

material of the beds out of areas of heightened pressure, corresponding to the flanks of folds, and accumulates it in places where the pressure is less, where the crests and troughs of the folds are formed. Nevertheless the folding is closely associated with the appearance of lenses within the bedded strata, and each fold is viewed as an aggregation of lenticular bulges placed one above another.

From mechanical considerations alone it would, perhaps, be difficult to raise objections to the possibility of such a process of folding, if it is assumed that non-uniform vertical compression of the beds in folds is due to an unequal application of external forces to the dislocated stratum, creating a regular alternation of areas of greater and lesser compression, corresponding to the alternation of crests, troughs and flanks of folds. Such an assumption, however, is in opposition to the geologic data regarding the structure of areas of continuous folding. The adherents of this hypothesis proceed from an entirely different assumption, that the compression is produced by vertical forces applied outside the area where the folds are observed. The nonuniform pressure that is required for the material to flow arises within the dislocated stratum itself as a result of the specific nature of the process of folding. Thus, this hypothesis suggests that the determining factor in folding is "laminar redistribution" the displacement of particles within the beds and that the change of position of the beds in space is a secondary phenomenon, being merely the result of the redistribution of material. In accordance with this explanation, the supporters of this hypothesis believe that the leading role is played by the more plastic beds, in which there is a more intensive redistribution of the particles of matter.

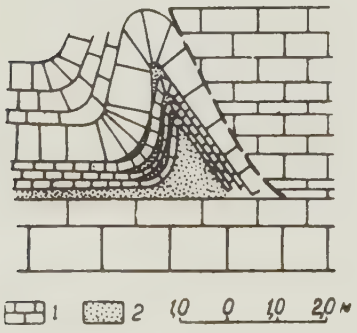

FIGURE 2. Diagram of the structure of disharmonic folds in the Turonian limestone -- Rion River, Georgia (after I. V. Kirillova); 1) limestone, 2) marl.

Disharmonic folding of the type depicted in figure 2 is often cited as one of the most convincing examples proving that the major role is played by the redistribution of the material within the beds in the process of fold formation. According to V. V. Beloussov, the shape of the fold is a clear indication of the "concentration of plastic material at one point (within the bed of marl -- V. Ez.) and explains the appearance of the fold" [6], whereas limestone beds merely bend passively to conform to the shape of the bulge in the plastic marl.

It is easy to see, however, that this same example can be used to support the opposite contention, that the swelling of the bed of marl was here caused by the bending of the more rigid limestone. The shape of the fold depicted in this illustration shows, actually, that there was a flow of the marl, apparently from points of greater to points of lesser pressure. But there is no basis for assuming that this pressure on the redistributed marl produced the bending of the overlying limestone beds. In reality, if the marl in the crest of the fold was under less pressure during the process of its formation than the adjacent areas, it would exert less and not more pressure on the beds of limestone. It is impossible to understand how the limestones beneath the marl could be pushed upward where the pressure on them was less, and downward where the pressure was greater, if this difference in pressure was the only cause of the bending. On the other hand, if one proceeds from another conception of the mechanism of folding, one which considers the formation of this fold to be the result of the bending of the upper beds of limestone by forces parallel to the original direction of the bedding, the source of the lower pressure in the crest of the fold which caused the marl to flow can be understood. Thus an explanation of the origin of folds based on the leading role played by the flow of material in the plastic beds turns out to be inadequate even in this very simple case.

Similarly, it may be shown that in a more complicated situation, in which the plastic layer does not have a flat bottom surface but is enclosed between two "rigid" strata that have been bent into a fold (see fig. 3), it is impossible to explain the separation of the "rigid" beds A and C at the crest and trough of the fold by the "passive" bending of the "rigid" strata resulting from the flow of material in the plastic beds. Actually, in this case also, the greater pressure was on the flanks of the fold and the lesser pressure at the crest and trough, to judge by the direction of flow of the material in the middle bed B. If the change in the distance between the two "rigid" beds is attributed only to nonuniform pressure from the plastic bed lying between them, the conclusion is inevitable that where the pressure was less (at the crest and trough) the rigid beds must come closer together, and be pushed apart in the flanks, where the pressure was greater.

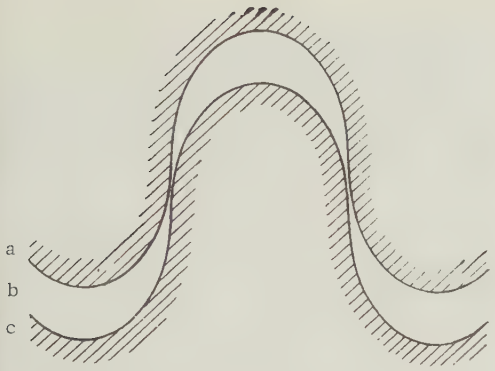

FIGURE 3. Diagram of a similar fold. The more plastic bed B is contained between the more rigid beds A and C.

That is, according to the principles of the laminar-redistribution hypothesis, the picture should be the opposite of what is actually the case. Thus, one cannot say that the thickness of the beds in the crests and troughs of folds increases because the plastic material tends to move in that direction; it is more correct to say that the plastic material is displaced into the crests and troughs because of the increase in the distance between the bedding planes at these points.

Let us consider a case in which a stratum subjected to complex dislocation lies above a slightly dislocated base, being separated from it by beds of more plastic rock (see fig. 4). Here also, one cannot say that a local concentration of plastic material produced the anticlinal folds in the overlying strata, because on this basis it is impossible to explain the presence of areas of lower pressure in which the plastic material accumulated. If, on the other hand, one considers that folding in the more rigid overlying strata (resulting, for example, from horizontal compression) was the cause of the squeezing-out of plastic material from under the synclines and its accumulation under the anticlines, this dilemma disappears; the required difference in pressure was produced by the crumpling of the more rigid layers into folds. One can easily see that in this process the plastic beds resist the bending of the more rigid beds above. But this being so, how can the force that resists the movement be considered the cause of the movement?

If the folding of this type under the influence of horizontal forces, as shown by numerous experiments [7, 17, 23, 25] and the theory of longitudinal bending [12], requires only a single movement, a general horizontal compression, the same folding by vertical forces requires as many points of application of external pressure as there are synclinal folds. Such as assumption is obviously not suitable as an explanation of the general case of continuous folding.

It is also easy to understand the reason for the contradictions in the hypothesis of laminar redistribution. This hypothesis, after stating that there is a redistribution of the material within the beds and concluding that this determines the difference in pressure, stops here and does not consider the causes, or movements, that might have produced this nonuniform pressure and maintained it during the entire process of folding. If, however, one considers the causes that might produce a cyclic nonuniformity of pressure coinciding with the rhythmic bending of the beds into folded structures, the conclusion is inescapable that the nonuniformity of the pressure is created by the bending of the beds.

It follows from all this that the redistribution of particles within the beds does not by itself produce a folded structure. To understand its origin, the nature of the movement of the beds themselves must also be taken into account.

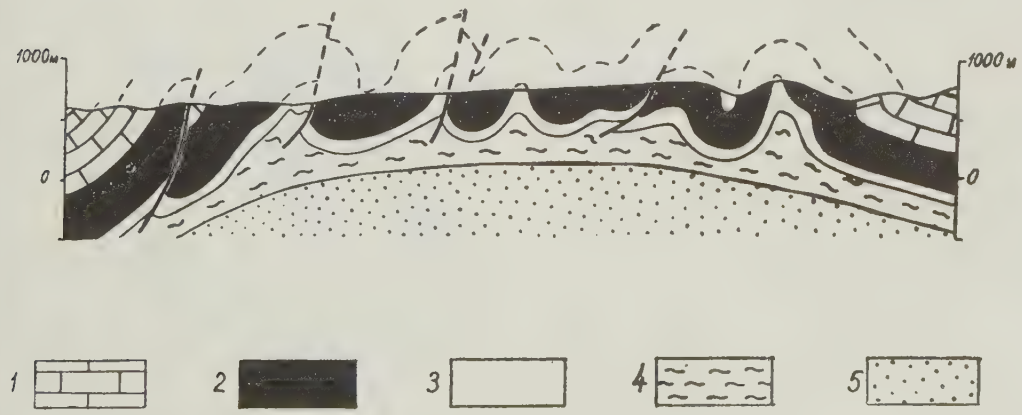

FIGURE 4. Section through a part of the Mirgalimsay anticlinal zone of the Kara-Tau ridge (Southern Kazakhstan): 1) limestone and dolomite; 2) thick-bedded dolomite; 3) thin-bedded dolomite; 4) argillaceous carbonate rocks; 5) sandstone.

Whenever one attempts to explain folding without considering this fundamental movement which produces the folds and without considering the diminution of the horizontal extent of the compressed layers, one comes up against unreconcilable contradictions.

Before proceeding to analyze the processes that take place within folds during their formation, the mechanics of folding, let us examine the basic morphologic features of folds.

Geologic literature has often divided the folds developed in areas of continuous folding into two basic morphologic types: concentric [Ed.: parallel?] and similar. Some authors also distinguish disharmonic folds in addition to these two types. The determining feature of concentric folds is the constant thickness of the beds that form them. Similar and disharmonic folds (which we shall combine under the general term "nonconcentric folds") are characterized by change in the thickness of the beds in the process of folding, i.e., by laminar redistribution of material. In similar folds, moreover, these changes are the same in all the beds, so that similar folds are merely a particular type of disharmonic folds.

Although the widespread development of nonconcentric folds is generally recognized, a number of authors doubt the existence of concentric folds, which has, in essence, been denied by the hypothesis of laminar redistribution [4, 13], this denial being one of the fundamental propositions of the hypothesis. On the other hand, practical field geology has revealed many folds in which there has been no increase in the thickness of the beds in the crests and troughs as compared to the flanks [21, 22, 24, 25].

The doubt that there could be a widespread development of concentric folds has apparently been determined to a great degree by their purely geometric properties; if concentric folds are geometrically extrapolated upward and downward, they must in practice, eventually fade out into completely flat beds [15, 19]. Actually, the existence of concentric folds which are totally suppressed upward and downward is improbable. But one must not lose sight of the very important circumstance that concentric folding, as Hills properly states [20], may be accompanied by non-concentric folds, into which they grade vertically. Since this eliminates the need to continue concentric folds upward and downward until they straighten out completely, it also answers all the objections to such a construction. Thus, there is no need to assert that folds with beds of unchanging thickness cannot exist; one should merely say that such folds cannot exist independently, without changing vertically into folds of another type. Many descriptions of folded structures actually do state that the beds forming concentric folds are underlain by beds that have been crumpled into folds of another type [22, 24, 25].

It is also clear from this why concentric folds need not always be gently dipping, as is commonly believed. Under favorable conditions, individual concentric folds might have very steep flanks, to the point of being almost isoclinal [21, 22].

The existence of folds of different types in a single vertical section is usually due to the different composition of the crumpled strata; more

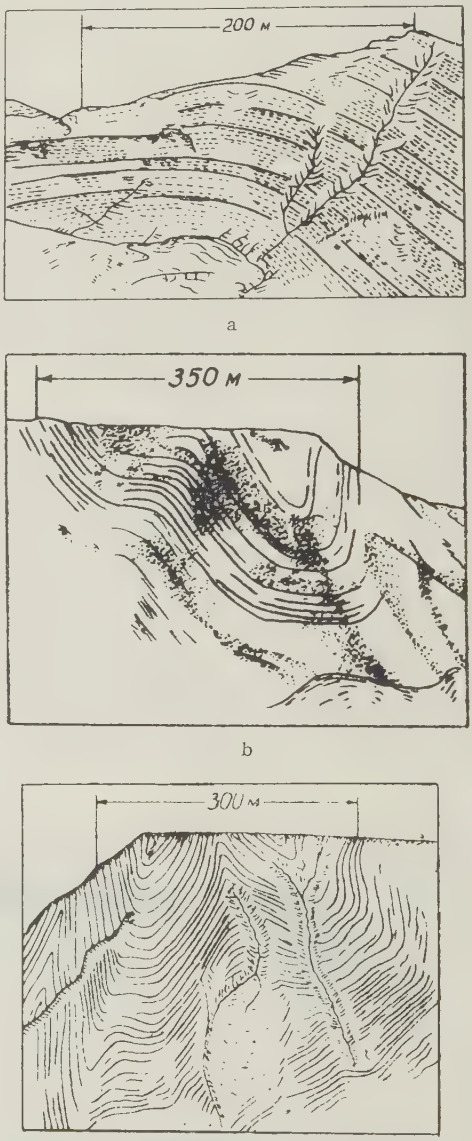

a

b

c

FIGURE 5. Folds in the Upper Tournaisian limestone of the Kara-Tau ridge (Southern Kazakhstan).

rigid, or, more specifically, less pliable groups of beds form folds that may be called concentric, whereas more pliable (more plastic) beds form nonconcentric folds. But if one compares the folds in various areas characterized by different structural conditions, it turns out that the same stratum will form concentric folds (see fig. 5a and 5b) in some places and nonconcentric folds (see fig. 5c) in others. The nonconcentric folds, moreover, are more tightly compressed and have steeper flanks than the concentric folds in the same stratum. Since complex, tight folds were at some time more gently dipping and less complex during the process of formation, the nonconcentric folds that are observed at the present time were concentric at certain stage of their development. That is, both types of folds are merely the results of arresting the process of folding at different stages. Between these stages, of course, there is a gradual transition rather than a sharp boundary.

At the same time, it has just been said that concentric folds cannot be formed without accompanying nonconcentric folds. Thus there is actually a parallel formation of both types of each particular place. The importance of the lithologic composition, the bedding and other factors that determine the mechanical properties of the crumpled stratum amounts to this, that less pliable beds under the same conditions as more pliable beds take longer to reach the stage of formation of nonconcentric folds. Special mention should also be made of the fact that the same rock will behave differently, according to the nature of the beds underlying and overlying it: it will behave more plastically when surrounded by more rigid beds, and more rigidly when surrounded by more plastic beds [22].

Similar results were obtained from experimental reconstructions of folds. Figure 6 shows the successive stages in the compression of a model composed of layers of uniform composition and subjected to horizontal pressure. It is quite clear that the concentric folds of stages a and b merge gradually into the nonconcentric folds of stages c and d. In layered models made up of groups of beds of different compositions, nonconcentric folds appear earlier in the more plastic beds than in the more rigid beds intercalated with them. As the degree of compression increases, the folds in all the beds gradually become nonconcentric through unequal changes in the thickness of the beds.

We may now draw conclusions regarding the most likely phenomena within folds during the process of their formation. Such phenomena include bending of the beds, slippage between the beds and complex nonuniform deformation of the beds leading to changes in their thickness. Numerous investigators have tried to distinguish these interrelated mechanisms of folding [1, 6, 8, 11, 20], but the exact nature of the interrelationship of these phenomena has either not

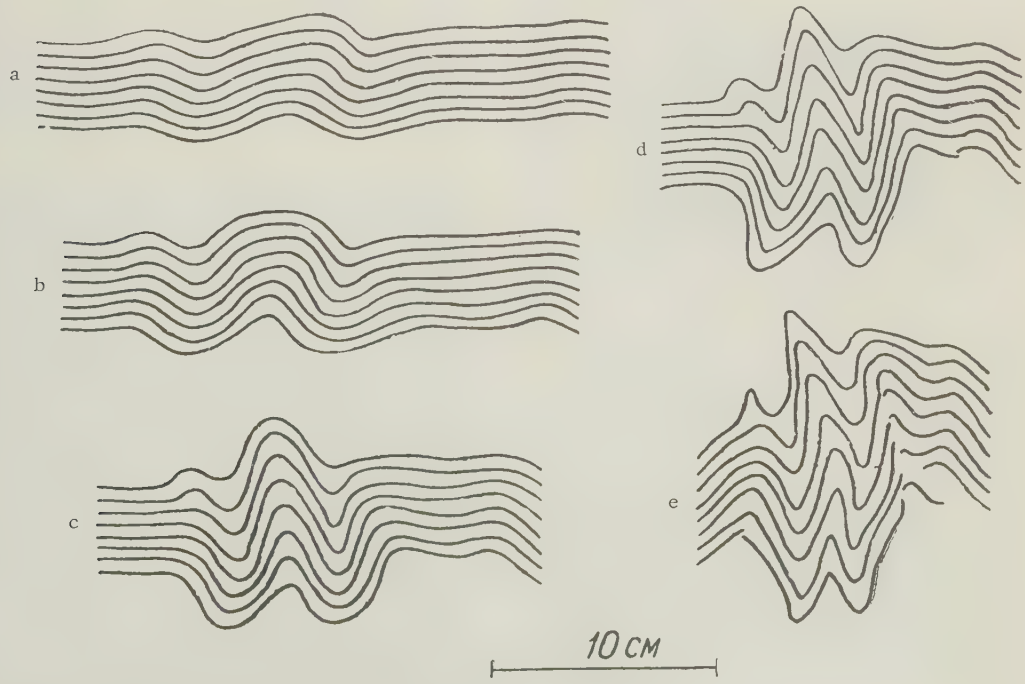

FIGURE 6. Successive stages in the development of folds in a group of layers composed of gun grease, compressed parallel to the bedding.

been considered or else has been treated in various ways.

Experiments have shown [2, 7] that bedding is a necessary condition for folding by horizontal compression. The main importance of the bedded structure is that it provides surfaces of weaker adherence between the strata. In actuality, the formation of concentric folds, in which the deformation of each bed is limited to bending, is impossible without slippage of the beds against one another [1, 6, 14, 20]. Bending and slippage between the layers apparently exhaust the basic features of the mechanism of such folding.

The presence of surfaces of division between the beds and longitudinal compression of the beds, as shown by experiments conducted by many investigators, are entirely sufficient conditions for the bending of the beds that accompanies their slipping against each other. Hence, it is easy to see why concentric folds are formed in the initial stage of folding.

It should be noted that in the formation of concentric folds, the most important thing is not so much the deformation of the beds as the change in their position in space. Strictly speaking, deformation of the beds is not required for such folding; this is shown by the existence of folds which have sharp, broken troughs, and crests and practically straight flanks (fig. 7).

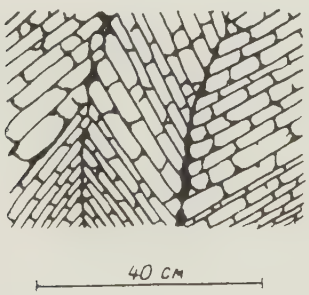

FIGURE 7. Small folds in thin-bedded limestones of the Famennian stage in the Kara-Tau ridge (Southern Kazakhstan).

Although this concept of bending and slippage of the beds under the conditions of horizontal compression is fully adequate for explaining the mechanics of concentric folding, not only gently dipping but of any degree of intensity, this is not true of nonconcentric folding, because neither slippage of the beds nor bending will account for the changes in thickness that are observed in them.

Let us note, first of all, that the local bulges and narrowings of the beds cannot be produced by forces parallel to the bedding, as is sometimes thought [9]. These could appear only when there were well-defined changes in the properties of the beds in the horizontal direction; bulges might appear in places where the given bed or the one that replaces it is more plastic than elsewhere throughout its extent. Obviously, however, such an explanation is not very useful, because it assumes the existence of such cyclic changes in the properties of the beds in the horizontal direction as would predetermine the positions of the folds.

It is much easier to explain the change in the thickness of the beds as an accompaniment of bending during the course of horizontal compression. What actually happens is that on the flanks of folds that have already been produced, because the beds here are at an angle to the direction of the compression (fig. 8), conditions are

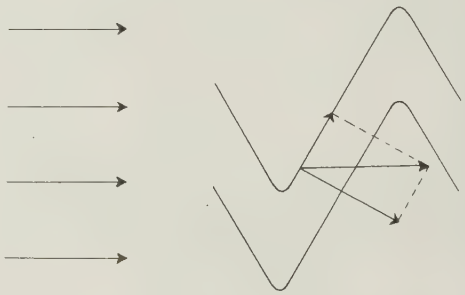

FIGURE 8. Resolution of the horizontal compressive forces in the flank of a fold.

created that tend to crush the beds and decrease their thicknesses (as P. N. Kropotkin, for example, has pointed out [14]). In the crests and troughs of the folds, where the bedding is for a certain distance parallel to the direction of compression, one would expect the reverse, an increase in the thickness of the beds. As the amplitude of the folds and the steepness of the flanks increase still further, the conditions for a change in thickness become more and more favorable, inasmuch as the component of the horizontal compression normal to the flanks becomes greater as this happens. This means that the inequality of the thickness between the flanks and the crests and troughs must increase with the increase in the degree of compression of the folds.

Thus, what has been called a laminar redistribution of the material is, under the conditions of continuous folding, nothing more than the result of the crushing of the beds on the flanks of the folds by horizontal compression. This being the case, beds of different composition will naturally be crushed to different degrees.

The formation of lenses within the beds and the breaking up of the more rigid beds into disconnected blocks are probably associated with this stage.

At the same time as the flanks become steeper, the conditions become less favorable for slippage between the beds, because the normal component pressing the beds together increases and the tangential component causing the beds to slip, decreases (fig. 8). When the flanks are at a certain angle, conditions may arise such that the amplitude of the fold will increase without any slippage of the beds, merely by further crushing during the overall compression of the strata crumpled into folds in the direction perpendicular to the axial plane of the folds [6].

From all this it is clear that the pressure arising within the folds and the flow of material produced by it is not the main question. The essence of the process of folding lies in the decrease in the horizontal dimensions and the corresponding increase in the vertical extent of the collapsed body [6]. In this process, the more rigid beds are primarily subjected to bending, while the bending in the more plastic beds is accompanied by complex nonuniform deformations leading to unequal changes in their thickness.

Thus, the concept of horizontal compression as the direct cause of folding also explains the origin of nonconcentric folds as either an accompaniment of the development of concentric folds or the result of their further growth. This agrees fully with the conclusions that were drawn earlier from the analysis of the morphology of the folds alone, that concentric folds may be considered as an earlier stage in the formation of nonconcentric folds.

In view of these concepts of the mechanism of folding, concentric and nonconcentric folds may be considered as two interrelated phases of the process of folding. One phase is the change in the position of the beds in space, associated with bending and slippage; the other phase is an extremely uneven deformation of the beds which produces changes in their thickness [6]. Both are closely interconnected: in the first place, bending and slippage between the beds at some points is inevitably accompanied by intraformational redistribution of the material at other points; in the second place, the bending gradually is accompanied by intraformational redistribution of material at the same point during the crumpling of the beds. The fundamental, most important phase, however, is still the bending of the beds.

What conclusions can be drawn from this brief examination of the problem of folding? First of all, it is evident that as long as one thinks only in terms of pressures or forces, one's line of reasoning will lead nowhere. The formation of folds does not involve the small deformations that are considered, for example, in the theory of elasticity, but enormous forces and enormous displacements. The forces that produce these deformations and displacements must not only have operated once but have been maintained somehow throughout the entire duration of this process. Nevertheless, the question of what movements could have produced these forces moves into the foreground.

The hypotheses of folding which do not associate the origin of continuous folding with horizontal compression cannot provide a satisfactory explanation of the basic structure of folds. This is also true of the "competent folding" hypothesis, in the form in which it was proposed by B. Willis [25]. Nevertheless, this hypothesis contains many sound observations, the most fundamental of which is that the direct cause of folding is the compression of bedded strata in a direction parallel to the bedding, i. e., that continuous folding is produced by a decrease in the horizontal dimensions of the dislocated strata. The concept of horizontal compression is the basis for explaining the basic features of the morphology of folds and for constructing a unified scheme of the mechanism of their formation.

None of these conclusions in principle depends on a solution to the question of the causes of the horizontal compression and the application of the forces that have created the folds. It must be stressed again that horizontal compression does not necessarily mean horizontal squeezing, as is often believed. The horizontally (or almost horizontally) acting forces may be applied not only to the edges of the dislocated strata but to the entire area of compression into folds (for example, through contraction, for whatever reason, of the surface of the basement complex). The forces might even be applied throughout the entire volume, as is suggested, for instance, by the gravitational folding hypothesis. Many phenomena, in fact, are much easier to explain on the basis of such a distributed, rather than of a concentrated, application of force.

The fundamental processes that take place during folding are, on the one hand, change in the position of the beds in space, accompanied by bending and slippage between the beds and, on the other hand, complex nonuniform deformation of the beds leading to unequal changes in their thickness. In some folds (concentric) only the first process takes place; in others (nonconcentric) both processes operate together. In addition, it has been seen that the redistribution of the material within the beds is a process subordinated to the movement and bending of the beds, and of essential importance mainly in the later stages of folding.

It has been seen that the author of this report

does not propose any new hypothesis of folding or any new solutions to the questions under consideration. The article is only an attempt to throw as much light as possible on the problem and to clarify the relationship between phenomena which are usually considered separately. It must not be thought, of course, that the particular explanation of the mechanism of continuous folding which has been mentioned as the one most probably correct exhausts all the possible cases and all the aspects of this phenomenon; the discussion was confined to some of the most general features of the basic trend of this process. In studying folding one must not unreservedly follow any one hypothesis; the possibility of various types of movements and deformations must always be kept in mind.

REFERENCES

1. Azhgirey, G. D., STRUKTURNAYA GEOLOGIYA [STRUCTURAL GEOLOGY]: Izd. Mosk. Un-ta, 1956.

2. Beloussov, V. V., OSNOVNYYE VOPROSY MEKHANIZMA SKLADKOOBRAZOVANIYA [FUNDAMENTAL PROBLEMS OF THE MECHANISM OF FOLDING]: Byull. Mosk. Ob-va Ispytateley Prirody, Otd. Geol., t. 22, no. 3, 1947.

3. _____, O PROISKHOZHDENII SKLADCHA TOSTI [ON THE ORIGIN OF FOLDING]: "Soviet Geology," no. 16, 1947.

4. _____, OBSHCHAYA GEOTEKTONIKA [GENERAL GEOTECTONICS]: Gosgeolizdat, M., 1948.

5. _____, POSLOYNOYE PERERASPREDELENIYE MATERIALA V ZEMNOY KORE I SKLADKOOBRAZOVANIYE [LAMINAR REDISTRIBUTION OF MATERIAL WITHIN THE EARTH'S CRUST AND THE FORMATION OF FOLDS]: "Sovetskaya Geologiya" no. 39, 1949.

6. _____, OSNOVNYYE VOPROSY GEOTEKTONIKI [FUNDAMENTAL PROBLEMS OF GEOTECTONICS]; Gosgeoltekhizdat, M., 1954.

7. Beloussov, V. V., Ye. I. Chertkova, and V. V. Ez, MODELIZOVANIYE SKLADCHATOSTI V USLOVIYAKH PRODOL'NOGO IZGIBA [EXPERIMENTAL MODELING OF FOLDING UNDER THE CONDITIONS OF LONGITUDINAL BENDING]: Byull. Mosk. Ob-va Ispytateley Prirody, Otd. Geol., t. 30, no. 5, 1955.

8. Billings, M. P., STRUKTURNOVYA GEOLOGIYA [STRUCTURAL GEOLOGY]: IL, M., 1959.

9. Gzovskiy, M. W., O ZADACHAKH I SODERZHANII TEKTONOFIZIKI [ON THE PROBLEMS AND SCOPE OF TECTONOPHYSICS]: Izv. Akademiya Nauk SSSR, Ser. Geofiz., no. 3, 1954.

10. Danilovich, V. N., O VOLNOVOY PRIRODE SKLADCHATOSTI NAPLASTOVANIY [ON THE WAVE-LIKE NATURE OF FOLDING IN BEDDED ROCKS]: Akademiya Nauk SSSR, Doklady, t. 66, no. 3, 1949.

11. _____, K VOPROSY O MEKHANIZME SPLOSHNOGO SKLADKOOBRAZOVANIYA [CONCERNING THE PROBLEM OF THE FORMATION OF CONTINUOUS FOLDS]: Izv. Akademiya Nauk SSSR, Ser. Geol., no. 4, 1953.

12. Dinnik, A. N., PRODOL'NYY IZGIB, GONTI [LONGITUDINAL BENDING, GONTI]: M.-L., 1939.

13. Kirillova, I. V., NEKOTORYYE VOPROSY MEKHANIZMA SKLADKOOBRAZOVANIYA [CERTAIN PROBLEMS OF THE MECHANISM OF FOLDING]: Tr. Geofiz. In-ta, no. 6 (133), Izd. Akademiya Nauk SSSR, 1949.

14. Kropotkin, P. N., O PROISKHOZHDENII SKLADCHATOSTI [ON THE ORIGIN OF FOLDING]: Byull. Mosk. Ob-va Ispytaley Prioridy, t. 25 (5), 1950.

15. Lizs, Ch. K., STRUKTURNAYA GEOLOGIYA, ONTI [STRUCTURAL GEOLOGY, ONTI]: M.-L., 1935.

16. Sorskiy, A. A., MEKHANIZM OBRAZOVANIYA MELKIKH STUKTURNYKH FORM V METAMORFICHESKIKH TOLSHCHAKH ARKHEYA [THE MECHANICS OF THE FORMATION OF SMALL STRUCTURES IN ARCHEAN METAMORPHIC ROCKS]: Tr. Geofiz, In-ta, no. 18 (145), Izd. Akademiya Nauk SSSR, 1952.

17. Tetyayev, M. M., OSNOVY GEOTEKTONIKI [FUNDAMENTALS OF GEOTECTONICS]: Gosgeolizdat, M-L., 1941.

18. Willis, B., and R. Willis, STRUKTURNAYA GEOLOGIYA [STRUCTURAL GEOLOGY]: Azerb. Gos. Izd-vo, Baku, 1932.

19. Usov, M. A., STRUKTURNAYA GEOLOGIYA [STRUCTURAL GEOLOGY]: Gosgeolizdat, M.-L., 1940.

20. Hills, E., OCHERKI STRUKTURNOY GEOLOGII [OUTLINES OF STRUCTURAL GEOLOGY]: IL, M., 1954.

21. Khorev, N. A., OSOBENNOSTI DORIFEYSKOGO SKLADKOOBRAZOVANIYA

[PECULIAR FEATURES OF DORIFEY-SKOGO FOLDING]: Izv. Akademiya Nauk SSSR, Ser.Geol., no. 2, 1955.

22. Ez, V. V., TEKTONIKA SEVERO-ZAPAD-NOY CHASTI TSENTRAL'NOGO KARA-TAU [THE TECTONICS OF THE NORTH-WESTERN PART OF THE CENTRAL KARA-TAU]: "Sovetskaya Geologiya," no. 41, 1959.

23. Daubree, A., ETUDES SYNTHETIQUES DE GEOLOGIE EXPERIMENTALE. Paris, 1879.

24. Heim, A., GEOLOGIE DER SCHWEIZ. Bd. 1, Leipzig, 1919.

25. Willis, B., THE MECHANICS OF AP-PALACHIAN STRUCTURE. 13th Ann. Report. U. S. Geol. Surv., pt. 2, 1893.

BRIEF GEOLOGICAL DESCRIPTION OF THE ZAPADNYYE (WESTERN) MOUNTAINS[1]

by

M. Blyakhu and R. Dimitrescu

• *translated by Research International* •

ABSTRACT

The crystalline basement is best exposed in the northern half of the Zapadnyye mountains. It consists of two large units, the Dzhileu and Aryesh suites, which differ in their lithology and development. These suites were metamorphosed in the Carboniferous, at which time the Peyushen formation was deposited. The Peyushen was metamorphosed during the Hercynian, simultaneously with formation of granite massifs. From the Hercynian to the end of the Cretaceous, three major areas of deposition were developed: 1) Bikhor, in which Triassic quartzites lie transgressively on the Dzhileu crystallines and Middle Triassic through Cenomanian limestones, dolomites, and flysch overlie the quartzite; 2) Kodru, characterized by a strong development of the Verrukano type underlain by Aryesh crystallines and overlain by the Bikhor-type Triassic sequence and Rhaetian clastics; 3) Meresh mountains, in which massive Malm limestones and Cretaceous through Cenomanian flysch overlie Paleozoic metamorphics. Magmatic activity occurred during the Permian, Triassic, Jurassic, and Cretaceous. The intrusions are primarily basic. In the Cretaceous, the Kodru formations were thrust northward over the Bikhor area forming the basic structure of the mountain. It is proposed that a bilateral orogeny caused the thrust structures of the Zapadnyye mountains. One orogeny arose in the Zapadnyye, the other in the southern Carpathians. The thrust sheets are therefore reverse displacements resulting from a convergent movement of separate autochthonous blocks.

INTRODUCTION

The Zapadnyye mountains, like the eastern and southern Carpathians, separate the Transylvanian basin from the Pannonian depression. Geologically, these mountains can be divided into two sharply differentiated parts. The southern part, comprising one-third of the Zapadnyye mountains, includes the Drocha, Metaliche, and Traskeu ranges, known collectively as the Meresh mountains. These are, for the most part, composed of Cretaceous flysch and Jurassic limestones and ophiolites. Small depressions filled with Miocene deposits are located along the margins of the Meresh mountains. Volcanic structures of Neogene age are distributed along the margins of the depressions. The northern part of the Zapadnyye massif consists of the Khigish, Kordu-Moma, Bikhor, Dzileu, Bledyasa, and Pedurya Krayuluy mountains. Crystalline schists, upper Paleozoic, Triassic, and Jurassic formations are widely distributed in this region; Cretaceous formations have a more limited distribution here than in the southern part. The northern part of the massif, according to several investigators, has a mantled structure; the presence of thrusts in the southern part of this massif is quite debatable. A fuller understanding of the geology of the Zapadnyye mountains was obtained in 1950 as a result of geologic surveys of the area.

CRYSTALLINE BASEMENT

The crystalline basement of the Zapadnyye massif outcrops over a considerable area, mainly in a sector between the Aryesh and Krishul-Repede rivers (Bikhor and Dzhileu mountains), north of this sector (Meresh and Rez mountains), as well as to the southwest and southeast (Traskeu, Khigish, and Kordu-Moma mountains) (fig. 1). Two major schist formations, the Dzhileu and the Aryesh, have been distinguished as a result of various studies of the metamorphic facies and tectonics of the crystalline basement. Although the differences between these two schists are less distinct than those between the Get and Duna (Danube) formations of the southern Carpathians, they still differ rather sharply. In both schists, the strongest possible regional metamorphism ("meso-" and "catogene"), as well as the weakest ("epizone"), are developed.

The Dzhileu schists are divided into the Somesh and Arada suite according to degree of metamorphism. The Somesh suite occurs along the northwestern slopes of the Muntele-Mare mountains; farther north in the Khuedin river basin, it is overlain by Paleozoic strata, and it outcrops in the Meresh mountains, continuing to the Rez massif. The area between the Rez massif and the northwestern Dzhileu mountains (Chucha region) is occupied by the Vledyasa banatite intrusions. Farther north, the Somesh suite outcrops among Tertiary sediments in the form of separate blocks (Byuk, Megura, Shimleul, Silvaniyev, Khegiyesh, Tikeu, and Preluke mountains) connecting the crystalline basement of the Zapadnyye mountains with the eastern Carpathians. The Somesh suite, as is

[1] Translated from Kratky ocherk geologii Zapadnykh Gor: Sovetskaya Geologiya, no. 5, p. 25-44, 1959.

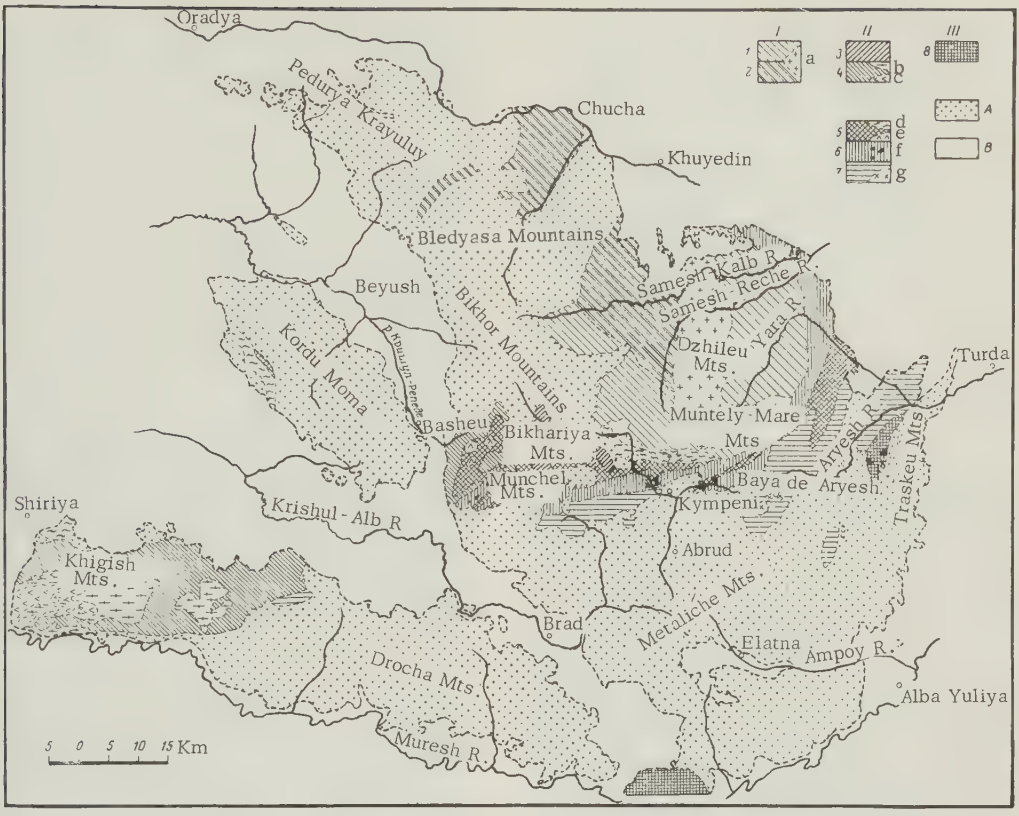

FIGURE 1. Crystalline suites of the Zapadnyye mountains

I. Dzhileu crystalline formation, 1) Arada suite, 2) Somesh suite, a) Muntele-Mare granite;
II. Aryesh crystalline formation, 3) green-schist suite, 4) Peyushen suite, 5) Bikhariya suite, 6) Munchel suite, 7) Baya de Aryesh suite, b) Khigish granite, c) metabasalts, d) Kodru intrusives, e) orthoamphibolites, f) lenticular gneisses (epigranites), g) pegmatitic granites;
III. Poyana-Ruska crystalline formation, A) Paleozoic and Mesozoic, B) Tertiary and Quaternary.

indicated by outcrops in the Preluka mountains, obviously corresponds to the suite of rocks composing the northwestern part of the Rodna massif and the Ineu mountains.

The Somesh suite is typically homogeneous in composition, thus allowing correlation with the Getskaya crystallines. It is composed, for the most part, of metamorphosed argillaceous-arenaceous sediments. The degree of metamorphism, according to Grubenman's classification, corresponds to the mesozone and, locally, the catozone. The rocks consist of a rather uniform muscovite schist which contains biotite, frequently considerable amounts of quartz, and quartz veinlets. The schists alternate with numerous bands of paragneiss, biotite schist, quartzite, and amphibolite. Crystalline limestone occurs only rarely. Several zones of metamorphism can be observed within the suite; their identification depends upon the amount of biotite, almandine, kyanite, or sillimanite present. The Somesh suite is distinguished by first-stage granitization and alteration of biotite to chlorite. Studies by T. Kreytner have shown that rocks of this suite compose the basement between the Krishul-Repede river and the lower reaches of the Somesh river.

The Arada suite covers less area. It appears only in the southwestern part of the Dzhileu mountains between the upper reaches of the Somesh-Kald and Albak rivers. For the most part, this suite corresponds to epizone metamorphism it is composed of quartzite-sericite schists; quartzites; and, more rarely, chlorite and amphibole schists.

Both the Somesh and Arada suites are cut by the Muntele-Mare granite massif. The massif is a typical "Delhi batholith." It is sharply distinguished from the Somesh and Arada suites and has a rather weakly developed thermal-

contact aureole (contact hornfels with biotite, garnet, and rather small zones of feldspar). The numerous pegmatites cutting the Somesh suite are related to this granite.

The Aryesh schists outcrop in the Bikhor massif; in southern and eastern Dzhileu mountains; in the Traskeu, Kodru-Moma, and Khigish mountains. Several suites are differentiated; their descriptions follow in order of their appearance from south to north, as well as in order of decreasing metamorphism:

1. The Baya de Aryesh suite is developed in the Traskeu mountains, southeastern Dzhileu massif, and Kympeni and Medrizeshti sectors (eastern Khigish-Drocha crystalline massif). It is composed of microblastic phyllites containing characteristic garnets; mica schists and paragneisses, also containing garnets and frequently staurolite; quartzite; plagioclase amphibolites; and marmarized limestones. Pegmatitic granites have also been found at the Baya de Aryesh outcrop. The feature which distinguishes this mesozonal suite from the others is its lack of pegmatite dikes.

2. The Munchel suite can be traced from southern Bikhor massif, across the Kympeni sector, to the eastern Dzhileu massif. It is composed of sedimentary rocks metamorphosed to quartzite-sericite, sericite, and blastopsammitic schists and quartzites. It also contains layers of tuffogenic schists with chlorite, albite, and epidote, as well as amphibole schists. Locally, in the upper Munchel, a horizon of black graphite quartzites occurs. In southern Bikhor massif, this suite is cut by numerous oval gneissic bodies (epigranites) and porphyries (metarhyolites and metadacites); here the suite is similar to the crystalline rocks of the Hemarides of Slovakia. Southward, in the direction of the Baya de Aryesh contact, the Munchel is interbedded with chlorite-sericite schists, some of which contain biotite.

3. The Bikhariya suite is a tuffogenic formation situated in the Kodru-Momu, Bikhor, and southern and eastern Dzhileu mountains. It is composed of chlorite schists containing albite porphyroblasta, or epidote and albite gneisses containing layers of muscovite schist. Limestones lenses and para-amphibolites are found among the crystalline schists. The para-amphibolites in the upper Bikhariya form an interrupted index horizon. The Bikhariya suite is very similar to the Leaota suite outcropping in the southeastern Carpathians and, to a certain extent, to the Dregshanu suite of the Dunay (Danube) formation, as well as to Lokva Banot) formation.

The first intrusive cycle, penetrating the Bikhariya suite, is found in the Kodru-Moma and Bikhor mountains and in the southeastern Dzhileu massif. It is composed of melanocratic metadiorites, metagabbros, and hornblendites. Its present appearance is that of an orthoamphibole schist containing hornblende, remnants of pyroxene, and acid plagioclase (albite through oligoclase). The second intrusive cycle (the Kodru intrusives) cuts crystalline schists and orthoamphibolites. The rocks are composed of plagioclase granites, granodiorites, and quartz diorites. Strong evidence of migmatism in relation to the intrusions of this cycle has been observed. Normal granites containing biotite and muscovite seemingly representing a new phase of magmatic activity, occur with the other intrusions. The Kodru intrusives are distributed in the southern Dzhileu massif (Albak), in the Kodru-Moma mountains, and in northwestern Khigish mountains (Shiriya).

The absence of reliable data prevents the accurate determination of the age of the schists in the Zapadnyye mountains. However, they are not younger than lower Paleozoic and actually appear to be even older (one school of thought relegates these formations to the middle and upper Paleozoic, another even to the Mesozoic). It is assumed that the mesozonal Somesh and Baya de Aryesh suites are older than the epizonal Arada, Munchel, and Bikhariya suites.

It should be mentioned that the locations of the crystalline schists within the crystalline massif is inversely proportional to the degree of their metamorphism; for example, the Baya de Aryesh suite rests on the Munchel suite. The Kodru intrusions penetrate only the epizonal schists. These data support the supposition that ancient thrusts existed here and that they preceded the Kodru intrusions. Field observations indicate that these thrusts, of rather small amplitude, were directed toward the south. Possibly, they can be correlated with tectonic movements in the Poyana-Ruska, which resulted in the southern mesocatazonal suite resting on a middle epizonal suite.

4. The Peyushen suite (Carboniferous) is younger than the other metamorphic units in the Zapadnyye mountains. The thicker Peyushen is composed primarily of blastopsephitic schists (metamorphosed conglomerates, serniphites) with layers of silvery sericite phyllites, lavender phyllites, chlorite or graphite phyllites, and occasional lenses of crystalline limestone. All schists are cut by sparse quartz veins. This suite is found exclusively in the southern Zapadnyye mountains: 1) in the Khigish mountains, it overlies transgressively the Baya de Aryesh suite (in Medrizesht); 2) in Bikhor, it overlies the Bikhariya suite; and 3) in the southern Dzhileu mountains, it overlies the Munchel suite (in the Bistra region).

The epizonal metamorphism of the Peyushen suite is related to the Hercynian orogeny. Its age is obviously Carboniferous. L. Pavelesku has recently described this suite from the southern Carpathians and named it the Tulisha suite.

In the Khigish mountains, the Peyushen suite is intersected by metabasaltic and metadoleritic rocks. Diorite and metagabbro intrusions are younger; the Rodna and Ivenuts granites are youngest.

The relationships between the Muntele-Mare granites in the Kodru intrusions and the Khigish granites have not been determined. If the Khigish granites are analogues of the Kodru intrusions, their age must be Carboniferous. The evolution of ancient magmatic activity in the Aryesh crystalline massif would then have occurred as follows: 1) pegmatitic granites at Baya de Aryesh are emplaced; 2) orthoamphibolites related to the Bikhariya suite are intruded; 3) epigranites of the Munchel suite, accompanied by hypobyssal porphyries, cut the Bikhariya in the southwestern Geyna mountains; 4) metabasalts, cut by the Peyushen suite (primary magmatic activity in the Hercynian), develop; and 5) granites of the Khigish mountains, possibly the Kodru intrusions also, representing synorogenic Hercynian plutonism, are emplaced. A somewhat later phase is represented by intrusions of acid two-mica granites, quite possibly related to the Muntele-Mare granites of the Dzhileu mountain region.

Accordingly, metamorphism of pre-Peyushen crystalline formations had taken place before the Carboniferous. Therefore, this metamorphism is apparently related to the Caledonian orogeny. The Peyushen suite was metamorphosed during the Hercynian orogeny. Judging from the geologic structure of the Zapadnyye mountains, the regional metamorphism continued until the granites were emplaced.

The following stages can be distinguished in the development of the crystalline formations of the Zapadnyye mountains: 1) metamorphism of the ancient crystalline formations and their accompanying intrusives; 2) thrusting of the Baya de Aryesh suite over the Munchel; 3) transgression, as a result of which the Peyushen suite was formed; 4) extrusion of metabasaltic magma; 4) metamorphism of the Peyushen and metabasalts; and 6) emplacement of the Khigish (Kodru?) intrusives.

Including this description of the metamorphic formations, mention of the green-schist suite found in the southern Bikhor mountains should be made. This suite is composed of blastopelitic chlorite-quartzite phyllites containing occasional layers of green sandstone and conglomeratic and amphibolitic lenses. The suite, undoubtedly Paleozoic, overlies the Bikhariya schists and, the Kodru intrusives, and underlies conformably lower Permian formations. Its relationship with the Peyushen is not clear; it may be different age or merely a different facies.

SEDIMENTARY ROCKS OF THE ZAPADNYYE MOUNTAINS

The sedimentary rocks of the Zapadnyye mountains do not form a continuous mantle but are confined to several mountain massifs separated by zones of crystalline rock, igneous massifs, or Tertiary basins. The paleogeographic development of the territory now occupied by the Zapadnyye mountains has resulted in special conditions of sedimentation in various tectonic zones. The sedimentary formations of the following tectonic regions are discussed below:

1. The Bikhor region is farthest north. To it belong, besides central Bikhor, the Pedurya-Krayuluy mountains.

2. The Kodru region occupies the southern area. Several tectonic zones can be differentiated within this region: 2) the Finnish zone occupying the western Kodru mountains, the southern Pedurya-Krayuluy mountains, the western Bikhor (Feriche region), and the southeastern Bikhor (Gyrda region); b) the Vyrful-Diyevy-Feriche-Ariyeshen zone occupying the eastern part of the Kodru mountains (Vyrful Diyevy), the western part of central Bikhor (Bokhodey region), and southern Bikhor (Ariyeshen region); c) the Moma zone situated south of the Kodru mountains, and d) the Bikhariya zone (southern Bikhor) extending to the southwest within the Khigish massif.

3. The Meresh mountain region includes the Traskeu and Metaliche mountains and the Drocha massif.

These sedimentary regions also differ in the structure of their crystalline basement. In the Bikhor region, the sedimentary cover is underlain by the Dzhileu crystalline formation, while in the Kodru region and in the Meresh mountains, by Aryesh crystalline schists.

Bikhor Region

The Permian rocks of this region outcrop in the Bretkutsa valley, along the Godinyasa and Shoymush rivers, in the Pedurya-Krayuluy mountains, and in the Megura-Vynete sector of central Bikhor. They are breccias composed of schist fragments cemented by a dark argillaceous material. A lens of quartz porphyry has been found in the upper breccia in the Megura-Vynete sector.

The base of the Triassic consists of 200 m of littoral-terrigenous clastics. A quartz conglomerate is generally overlain by quartzites and shales. The shales are more common in the upper part of the suite. These sediments are, for the most part, reddish violet in color; however, the quartzites may be yellowish, pink, gray, or greenish. The

quartzites are assigned to the lower Scythian stage.

The marine cycle proper begins with a fine-grained black limestone, weakly siliceous and dolomitic in places. Sections of dolomite of varying thicknesses are found at the base of the suite, as well as in its upper parts (lower and upper dolomites). The thickness of the dolomites, as well as their petrographic composition, indicates quite clearly that they are not major components of the suite. Thus, they are not classified as self-sufficient stratigraphic entities. Sections of white marble reef limestones overlie the black limestones and dolomites. Apparently, the upper dolomites formed within these limestones.

Upper Scythian fossils occur in the Pedurya-Krayuluy mountains, while some lower Ladinian fossils have been found in the white limestones of the Bikhor mountains. Therefore, the limestones containing the dolomite have been assigned to the upper Scythian and the lower Ladinian stages. In the Bikhor region, the remaining Triassic section is absent; at that time, the region was above sea level, as is indicated by the presence of lateritic weathering and karst-relief forms.

The Jurassic is represented in the Bikhor region by a basaltic conglomerate overlain by a continental-neritic series facially identical with the lower Scythian. The lower Lias consists of quartzitic sandstones and violet shales, which, in the Pedurya-Krayuluy area, include refractory clays. The middle Lias consists of dark-gray limestones and marl limestones; the upper Lias, gray marls. Southward (in the Bikhor mountains), the thickness of the middle and upper Lias decreases; the clastic facies of the lower Lias is interstratified with the upper Lias.

Although Dogger units in the Pedurya-Krayuluy area are thin, it was possible to distinguish all the ammonite zones. The Aalenian stage consists of marly limestones of a dark-gray color; the lower Bajocian, arenaceous marls and marly limestones; and the upper Bajocian and lower Bathonian, spar limestones, oölitic limestones, and arenaceous limestones (Klauss strata). In the Bikhor mountains, only spar [Ed.: crystalline?] limestones are found; the rest of the Jurassic section is usually faulted out.

The Malm is divided into marl limestones (Callovian), gray and black limestones (Oxfordian-Kimmeridgian), and marine white and gray reef limestones (Portlandian). The Portlandian concludes the Jurassic sedimentation cycle and marks the uplift of the Bikhor region above sea level. During the Valanginian, lateritic deposits, altered as a result of weathering to bauxite, formed on the Portlandian surface.

The sea again covered the Bikhor region during the Houterivian during which time dark-gray limestones containing Characeae and Ostracoda were deposited. It was also present in Barremian time and formed thick sections of gray and white limestone containing Pachydonta. These limestones are overlain by gray marls containing ammonites and Neohibolites belemnites and Aptian interbedded marls, sandstones, shales, and limestones. Cenomanian conglomerates and sandstones overlie the Aptian unconformably.

Kodru Region

Finnish-Gyrda Zone

The base of the Permian section is composed of a thick conglomerate and breccia containing crystalline rock fragments and argillaceous material; the cement is highly sericitized. The conglomerate pebbles show signs of strain. The conglomerates are rather strongly metamorphosed (seriphites). Frequently, they contain layers of mottled, light-violet, well-bedded sandstones and lustrous dark-violet shales. These conglomerates are distributed over the intrusive Kodru complex, both in southern Bikhor and in the Kodru mountains. In the upper conglomerate section of the Kodru mountains, a horizon of argillaceous-micaceous, dark-violet sandstones occur.

Transgressively overlying the conglomerates are greenish or reddish quartz porphyries interbedded, in the Kodru mountains, with pyroclastic rock (tuff and tuffaceous sandstone). In southern Bikhor (Gydra region), the tuffs overlie the porphyries.

Upper Permian formations are typically alternating brick-red shales, fine-grained conglomerates, and arkosic sandstone.

Triassic sediments can be traced throughout the Finnish-Gyrda zone. A quartzite suite (conglomerates, sandstones, and shales, similar to those of the Bikhor region) of lower Scythian age lies at the base of the Triassic section. It is overlain by a limestone-dolomite series very similar to the corresponding series in the Bikhor region. Many authors correlate these series, even though their stratigraphic sequence is different.

Above the lower Scythian quartzite are gray and black dolomites of upper Scythian and Anisian ages. These, in turn, are overlain by black, gray, pink, or white limestones interbedded with dolomites and marly shales (Ladinian stage), white sugary dolomites (Karnian stage), and white reef limestones (Norian stage). This suite, typical for the Kodru mountains (Finnish zone), in the southern

part of the Pedurya-Krayuluy area, consists of marly limestones, calcareous sandstones, and marls containing rich Ceratitoidaea fauna.

The Jurassic section lies conformably on the Triassic. Concentrations of various clastic rocks (sandstones; quartzites; and red, green, and black shales) cause considerable facial discontinuities. These rocks were apparently formed from the erosion products of a Paleozoic mountain chain. Black limestones containing Rhaetian fossils are infrequently encountered.

Above the clastics in the Kodru mountains are thick pink and white limestones, locally oölitic or ferrugenous. They contain a rich fauna indicating lower or, perhaps, middle Lias age. In the Pedurya-Krayuluy area, the lower Lias is underlain by quartzitic sandstone of [Tr.: gresten] facies, which is overlain by middle Lias limestones and marls.

The period between Lias and the Lower Cretaceous sea encroachment was one of uplift, resulting in a sedimentary hiatus. Sandstones and marls containing Aptychus are overlain by well-layered limestones cut by numerous calcite veinlets, very similar to the Sinayan beds of the eastern Carpathians. The Lower Cretaceous formations are developed both in the Kodru mountains and in the Pedurya-Krayuluy area, although in the latter the Sinayan formation is locally replaced by reef limestones.

This region was above sea level in Barremian time. It should be said that, in western Bikhor (Feriche region), the Permian and Triassic are developed through the Rhaetian stage inclusively; in southern Bikhor (Gyrda region), only the Permian is present. It is impossible to determine whether the absence of the remaining formations is a consequence of erosion or lack of sedimentation.

Diyevy-Bokhodey-Ariyeshen Zone

The Permian section in the Kodru mountains (Diyevy river region) begins not with a basal conglomerate but with a quartz porphyry horizon overlain by basic lava (diabase and green tuff) interbedded with red shales. In southern Bikhor (Ariyeshen region), its base is a violet cross-bedded conglomerate facies, similar to the conglomerates in the preceding zone. It is overlain by a series of violet micaceous sandstones with "hieroglyphic" cleavage planes. The sandstones alternate with dark-red argillaceous shales and mica-free sandstones. The micaceous sandstones contain small layers of extrusive material in the form of quartz porphyry and mixtures of tuffaceous and clastic material. In the upper part of the suite, the clastic material predominates over the tuffaceous.

In western Bikhor (Bokhodey region), sections similar to those of the Ariyeshen region are generally found. However, coarse-grained green quartzites interbedded with brick-red argillaceous shales substitute for the tuff suites; small lenses of quartz porphyry also occur, although infrequently.

The same quartzite complex described for the Bikhor and Kodru regions comprise the lower Scythian section. In the Diyevy region, the base of this complex is composed of a conglomerate series. Above the lower Scythian in the Kodru mountains the whole Triassic series is developed. It is composed, as in the Finnish zone, of gray dolomites, black and whitish limestones, saccharoidal dolomites, and white reef limestones. The uppermost part of the section is fossiliferous black Rhaetian limestone. In the Bokhor mountains, above the quartzite suite, only the first two horizons, the gray dolomites and black limestones, are present. These pinch out to the south.

Moma Zone

The base of the Permian section in the Moma zone is a cross-bedded violet conglomerate. The overlying horizon is volcanic, more basic than silicic. This series is sporadically developed. The complex is composed of red, green, and black shales and black quartzites, cut by many diabase dikes; spilosites (shales with patches of chlorite) have been developed at the intrusive contacts.

In the Moma zone, diabase occupies the position of the upper Permian and, quite possibly, the Scythian quartzite, which occurs only in the southern part of the zone, gradually pinches out toward the north; there, Anisian dolomites rest directly on the diabase.

The Mesozoic is represented by Triassic through Rhaetian sediments. Here, the Triassic facies differ sharply from those developed in the other parts of the Zapadnyye mountains. In the Moma mountains, the Triassic formations consist of extensive concentrations of massive limestones and smaller volumes of pink or red dolomites containing an abundant ammonite fauna. It is suspected that these limestones were developed in a "Hallshtadt" facies, a transition period between the Anisian and Rhaetian.

Bikhariya-Khigish Zone

In this zone, black argillites interbedded with black quartzites, or rarely conglomerates, rest conformably on the Peyushen suite. These rocks have been subjected to intensive hydrothermal metamorphism, as evidenced by the presence of greenish nests, belts, and veinlets of epidote, chlorite, and actinolite. The age of the black suite has not yet been determined.

Meresh Mountain Region

Only in the eastern part (Traskeu mountains) of the Meresh mountains do Malm sediments overlie the crystalline basement. Here are found siliceous limestones (Callovian), red limestones (Kimmeridgian), and massive coral limestones (Portlandian) containing Nerinea and Diceratidea. These limestones are of limited extent; the greater part of the Meresh mountains are occupied by the Cretaceous developed in a flysch facies.

The base of the Cretaceous section is composed of marls, sandstones, and limestones (Sinayan series) which are overlain by a thick concentration of conglomerate and sandstone interbedded with reef limestones (Urgon facies) of Barremian and Aptian age. After the Albian diastem, polymictic conglomerates and quartzitic sandstones of Cenomanian age were deposited and eroded. Basic igneous rocks, until recently assigned to the Triassic, but actually Upper Jurassic and Lower Cretaceous, occupy an important position in the Meresh mountain region.

The major tectonic phase in the Zapadnyye mountains occurred in the Cretaceous. After brief orogenic activity in the Cenomanian, a major transgression took place. Upper Cretaceous formations occur both in the Pedurya-Krayuluy mountains (Roshiya and Remetsi basins) and on both flanks of the Meresh mountains, in the northern part of the Baya de Aryesh basin (Kympen-Sokhodol-Bina) and in the southern part of the Deva basin. The present isolation of these formations can be explained by previous erosion resulting in erosion of these sediments from uplifted areas or by Tertiary subsidence during which these formations settled and were covered by Neogene formations.

The Upper Cretaceous is composed of conglomerates overlain by sandstones containing limestone bands of Actaeonella and Hippurites (Gosau facies). Above these are marls containing Inoceramus which, in the Meresh mountains, are replaced by marly sandstones. Occasionally, beds of agglomerates and tuffs, resulting from banatite extrusions, occur in the Upper Cretaceous.

During the upper Cenomanian, the Zapadnyye mountains were uplifted. The continental phase continued through the Paleogene; a series of basins appeared along individual faults in the Neogene. These basins separate the massifs of the Zapadnyye mountains (Borod, Beyush, and Zerand basins) or are situated in the interior parts of the mountains (Roshiya, Montana, Zlatna, Brad-Sekerymb basins).

In the intermontane basins, found also in the Metaliche mountains, sedimentation began in the second Mediterranean stage and continued with interruptions to the Pliocene. Clastics (Fatsa-Bey conglomerates and Almashul-Mare gravels), interbedded at depth with lavas and pyroclastic products of Neogene volcanism, comprise the Pliocene. The basins separating individual orogenic massifs are characterized by a more continuous sedimentation, which began in various periods. Thus, the Zerand basin includes Helvetian through Pliocene formations; the Beyush basin, Tortonian through Pliocene; and the Borod basin, Sarmatian through Pliocene.

In all these basins, Quaternary deposits consist of terrace formations and piedmont deposits, Diluvial formations are developed in the remaining parts of the Zapadnyye mountains. Glacial and paraglacial deposits occur at higher elevations. Eluvial formations appear on the karst platforms.

In general, the sedimentation cycle in these three regions of the Zapadnyye mountains evolved in a very similar manner. Thus, during the Permian and Triassic, the Meresh mountains had been uplifted, while the Bikhor and Kodru regions were areas in which sediments of the neritic-littoral and epicontinental types were being accumulated. During the Triassic, the Kodru region had been uplifted, while the Bikhor and Meresh regions were under an epicontinental regime. Finally, in the Lower Cretaceous, the Bikhor region had been uplifted, while sediments were being accumulated in the Kodru and Meresh regions.

Such differentiation in the course of sedimentation in these regions indicates that they developed independently of each other as sharply differentiated blocks in early Permian time. Moreover, their subsequent regrouping (in pairs) indicates that these blocks were subjected to intensive tectonic movements, after which common paleogeographic conditions prevailed. It is necessary to familiarize oneself with the general geotectonic evolution of the Carpathian-Dinaric Alpine geosyncline to understand these tectonic movements.

MAGMATIC ACTIVITY

Paleozoic

Extensive volcanic ejections, related to the subsequent Hercynian orogeny, occurred in the Zapadnyye mountains region during the Permian. In upper Permian time, extensive extrusions occurred in the Kodru mountains, in southwestern Pedurya-Krayuluy, and in central Bikhor. These formed quartz porphyries and were accompanied by deposition of tuff. The extensive porphyritic sheets interbedded with Permian sediments are indicators of the number of extrusions. In the Moma mountains, quartz porphyries are developed to a lesser

extent; diabase, from Permian to Lower Triassic, predominate.

Extrusions of granite and granite-porphyries containing tourmaline cut the black suite in western Khigish mountains and are probably related to the magmatic phase preceding the Permian extrusions.

Mesozoic

The initial ophiolitic magmatic activity of the Alpine orogeny had wide distribution within the Meresh mountains, from the Drocha mountains almost to the Turda. Here, two magmatic phases can be distinguished. The major phase, consisting of diabase and, to a lesser extent, of gabbro, developed through the Malm, or even Middle Jurassic (some authors assign them, without any reliable evidence, to the Triassic). The second phase, consisting of spilites and porphyrites, is Upper Triassic to Lower Cretaceous, including the Aptian, in age. These rocks are interbedded, locally, with quartz porphyries. Pyroclastics, as well as jasper containing radiolaria, are found in the basic rock complex.

Cenozoic

The first occurrence of magmatic activity subsequent to the Alpine orogeny was a banatite extrusion. The first phase of this extrusion is an upper Cenomanian andesite. It was followed by a hypabyssal phase, consisting, for the most part, of granodiorites accompanied by granites, diorites, granodiorite porphyries, rhyolites, and dacites.

The thickest banatite formation occurs in the Bledyasa massif where, according to D. Dzhushka, it is composed of taphroliths [Ed.: Formed by taphrogenesis?]. However, smaller bodies and veins are encountered in the Dzhileu, Bikhor, and Drocha mountains. Their age has been determined on the northern and northeastern flanks of the Dzhileu massif (apparently, two magmatic phases exist: one Cretaceous; the other younger, possibly lower Eocene).

Neogene igneous rocks, including rhyolites, dacites, and andesites, and their pyroclastic products are developed in the southeastern Zapadnyye mountains. They formed in the faults which caused the subsidence of the Miocene basins. According to the investigations of Gitsulesku, M. Sokolesku, and Mirchi Iliye, the sequence of intrusion was as follows:

1. The formation of rhyolites in the Roshiya-Montana and Beitsa sectors, and then of pyroxene andesites in the Fatsa-Bey sector, is

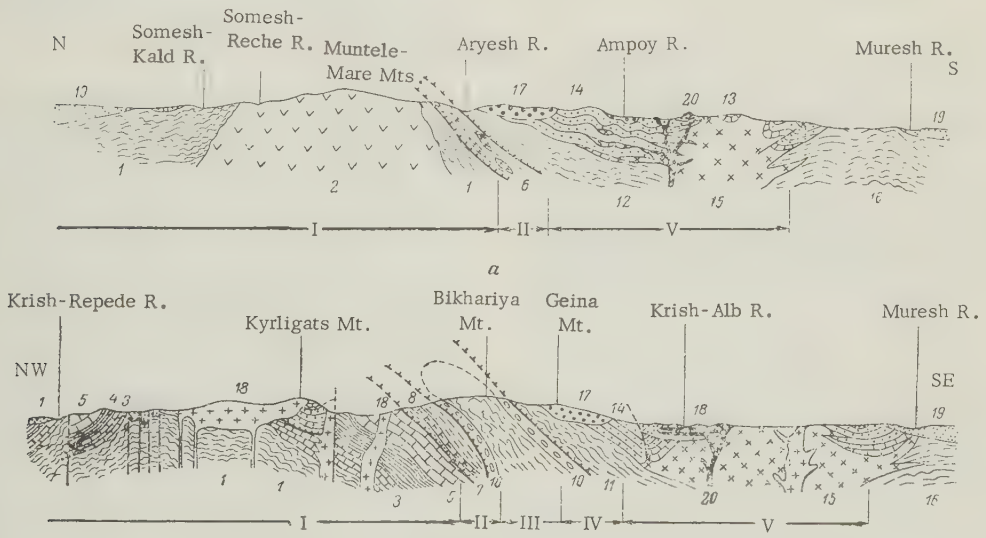

FIGURE 2. Geologic cross section of the Zapadnyye mountains (horizontal scale 1:500,000; vertical scale 1:100,000)

I. Dzhileu autochthon, 1) Dzhileu crystalline formation, 2) Muntele-Mare granite, 3) Triassic, 4) Lias, 5) Dogger-Malm-Neocomian;
II. Kodru thrust sheet, 6) Kodru intrusives, 7) Permian, 8) quartz porphyry;
III. Bikhariya thrust sheet, 9) Bikhariya crystalline formation, 10) Peyushen suite;
IV. Munchel thrust sheet, 11) Munchel crystalline formation,
V. Meresh mountain zone, 12) Baya de Aryesh crystalline formation, 13) Jurassic, 14) Cretaceous flysch, 15) ophiolites, 16) Poyana-Ruska crystalline formation; post-tectonic formations: 17) Upper Cretaceous, 18) banatite, 19) Tertiary, 20) Tertiary intrusives.

related to the first magmatic phase, assigned by M. Ilye to the Aquitanian stage. According to Gitsulesku and Sokolesku, the sequence is in reverse and the age of the entire phase is Tortonian. The differences in the age interpretation of the first phase is due to differences in age determination of the Fatsa-Bey conglomerates.

2. The second extrusive phase, of lower Sarmatian age, is composed of dacites occurring in Kyynel, Drayka, and Dyalul-Fety.

3. The major phase, which is responsible for the greater part of the ore deposits, consists of quartz andesites of the Barzc type (with pyroxene and amphibole), occurring in the Bryaza, Volkoy-Korabiya, and other sectors, as well as the Sekerymb-Porkurya type (with biotite), occurring in the dacites of Chertash and Baya de Aryesh. The volcanic formations of this phase cover upper Sarmatian sediments.

4. The lower Pliocene phase is composed of the Roshiya-Montana amphibole andesites. Iliye considers those rocks which Gitsulesku and Sokolesku relate to the second, third, and fourth phases to be contemporaneous.

5. The final extrusions of the Alpine orogeny consist of upper Pliocene basalt flows in the Detunata and Valya-Mureshuluy areas.

TECTONICS

The major tectonic development of the Zapadnyye mountains occurred in the Cretaceous. At that time, the foundations of the Kodru region (crystalline rocks, Permian or Lower Triassic formations) were thrust over the Bikhor region. The Kodru mantle had been previously fractured into several individual blocks, which were either thrust one upon the other or completely overthrust in respect to their former positions (fig. 2). At the same time, numerous radial fractures had formed.

The Bikhor autochthon consist of blocks cut by a system of faults. Grabens (at the headwaters of the Momeshul-Kald and Remecs rivers) and antithetical faults (in Pedurya-Krayuluy and central Bikhor) can be distinguished. The forward part of the Kodru thrust sheet[1] can be traced from Oradya mountain through southern Pedurya-Krayuluy to central Bikhor (Buduryasa region, fig. 3). Here, due to the subsidence caused by the taphrogenesis of the Vledyasa massif (between the Sokhodol and Bulz lines), it is impossible to trace the thrust front, because the autochthonous formations are completely missing. The same part of the thrust sheet reappears farther down in the Gyrda valley, where it is divided into two secondary sheets. It can be traced to east of Lupsha, and farther north. For the whole length from Oradya mountain to the Gyrda river, Permian rocks lie at the base of the sheet. East of the Gyrda river, the crystalline basement (Kodru intrusion) appears at the base of the sheet, overlying autochthonous Mesozoic formations; in eastern Albaka, it overlies autochthonous crystalline rocks.

The upper part of the Kodru sheet (Diyevy mountain sheet) appears in the eastern Kodru mountains where Permian formations are thrust over the Lower Cretaceous of the lower part of this sheet (Finnish valley). The same upper part (Feriche sheet) can be observed west of Bikhor where the Permian is thrust over the Triassic and Rhaetian. In southern Bikhor, this part of the sheet is very extensive (Ariyeshen sheet) and it can be traced from Tsapu mountain to Nyagra. Here, the sheets are composed of green schists at their base, and even crystalline rock in places; while in the western part, the base consists of Permian rocks.

The Moma thrust sheet is formed in the Kodru mountains only; here, the Permian formations are thrust over the Mesozoic sheet of Diyevy and Finnish mountains.

The upper part of the Kodru thrust sheet is of a different type structurally. Called the Bikhariya thrust sheet, it is found in the Bikhor massif (southern Bikhor). It is a crystalline series within the axial part of a recumbent fold; in both the normal and covered limbs, the Peyushen series covers the crystalline rocks. In the covered limb, the Peyushen series is covered by the black suite. This part of the Kodru thrust sheet is also found in the Khigish mountains. The singular tectonic characteristics of this part of the sheet suggest the possibility that it was formed in an older period of tectonic activity (Kimmeridgian).

A sheet composed of the Munchel crystalline series is thrust over the Carboniferous rocks of the Bikhor fold, as well as over the Permian rocks of the Kodru sheet. This sheet, having Bikhor crystalline rocks at its base, has been named the Munchel-Seketura sheet, after the two points located near its extremities.

The structures of the Meresh mountains form an anticlinorium. The axes are composed of crystalline and Jurassic rocks overlain by Lower Cretaceous sediments and ophiolites;

[1]The thrust structure of the Zapadnyye mountains is not distinguished by all geologists. The latest detailed geologic surveys do not indicate the numerous sheets described in the literature. These maps show traces of thrusts and numerous normal faults on a background of very simple folds.

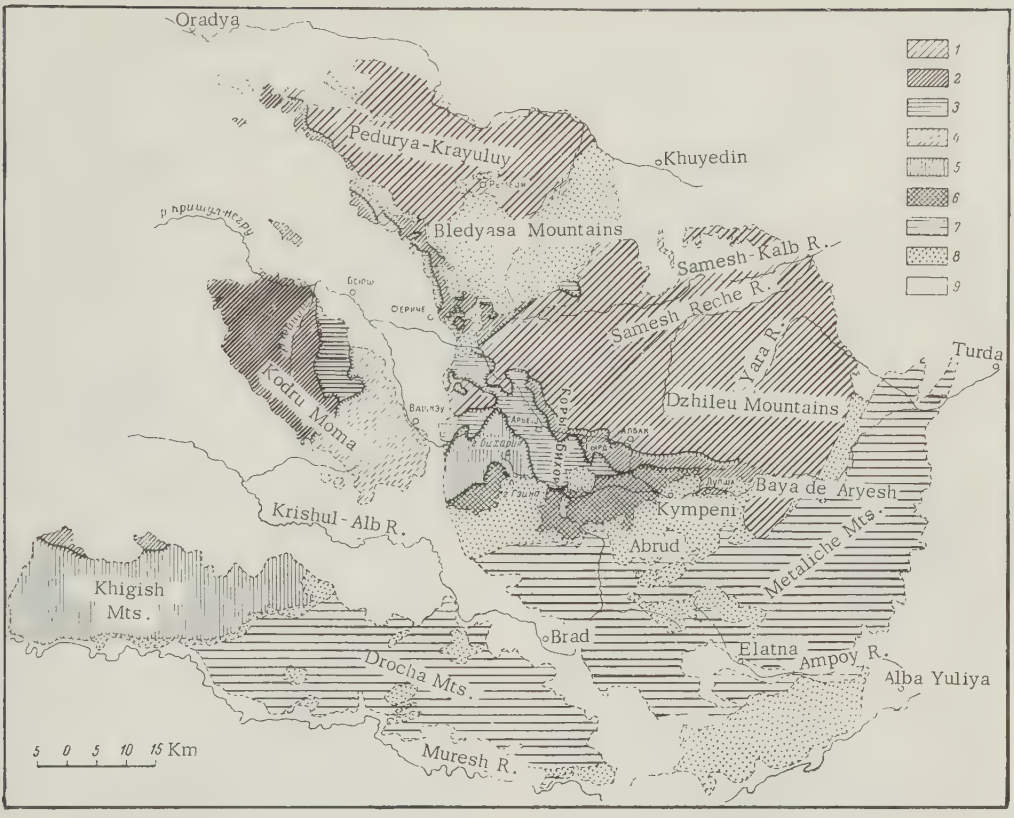

FIGURE 3. Tectonic scheme of the Zapadnyye mountains

1) Dzhileu-Bikhor autochthon, 2) Kodru thrust sheet, 3) Diyevy-Feriche-Ariyeshen mountains thrust sheets, 4) Moma thrust sheet, 5) Bikhariya-Khigish thrust sheet, 6) Munchel-Seketura thrust sheet, 7) Meresh mountain zone, 8) post-tectonic Senonian formations and banatite massifs, 9) Tertiary rocks (sedimentary and igneous)

the limbs of the anticlinorial elements are composed of Upper Cretaceous rocks.

The formation of the thrust sheet occurred during a subregional tectonic phase, according to information obtained from the youngest formations found under the thrust sheet. The Bikhor thrust sheet is an exception; it is unique in its tectonic characteristics and its forward part is acutely cut by the younger Munchel-Seketura thrust sheet (Kimmeridgian). It seems likely that the Ariyeshen sheet, during its movement, dragged along the already formed Bikhor fold.

It is apparent that, in the northern Zapadnyye mountains, the sheets have been thrust from the south to the north. It has been noted that in the eastern part the thrust sheets are composed of crystalline schists alone, while, in the west, of both crystalline schists and sedimentary rocks. Thus, in the east, the crystalline schists of the Munchel-Seketura sheet are thrust directly over the Kodru intrusives; the Kodru is, in turn, thrust over the Dzhileu crystalline schists. In the west, the Munchel sheet is thrust over the Peyushen series of the Bikhor sheet. This sheet, in turn, is thrust over upper Permian rocks of the Ariyeshen sheet, which cover the Kodru sheet. Autochthonous sedimentary formations, developed through Cenomanian time, underlie the Kodru sheet.

From these relationships it can be concluded that before the period of thrusting the eastern zone was an area of uplift, which, as the result of erosion, formed isolated sectors of sedimentary rock; the western zone was an area of submergence where the sedimentary cover was preserved (the process of sedimentation was almost continuous). The main tectonic deformations, corresponding to the maximum movement of the thrust sheets, occurred in this zone. The zone of subsidence was very stable; both Kimmeridgian and sub-Hercynian thrusts are typical for this zone. In the Neogene, the Beyush depression developed along this zone which later caused the formation of an east-trending synclinorium. The primary direction of the thrust movement, from south to north,

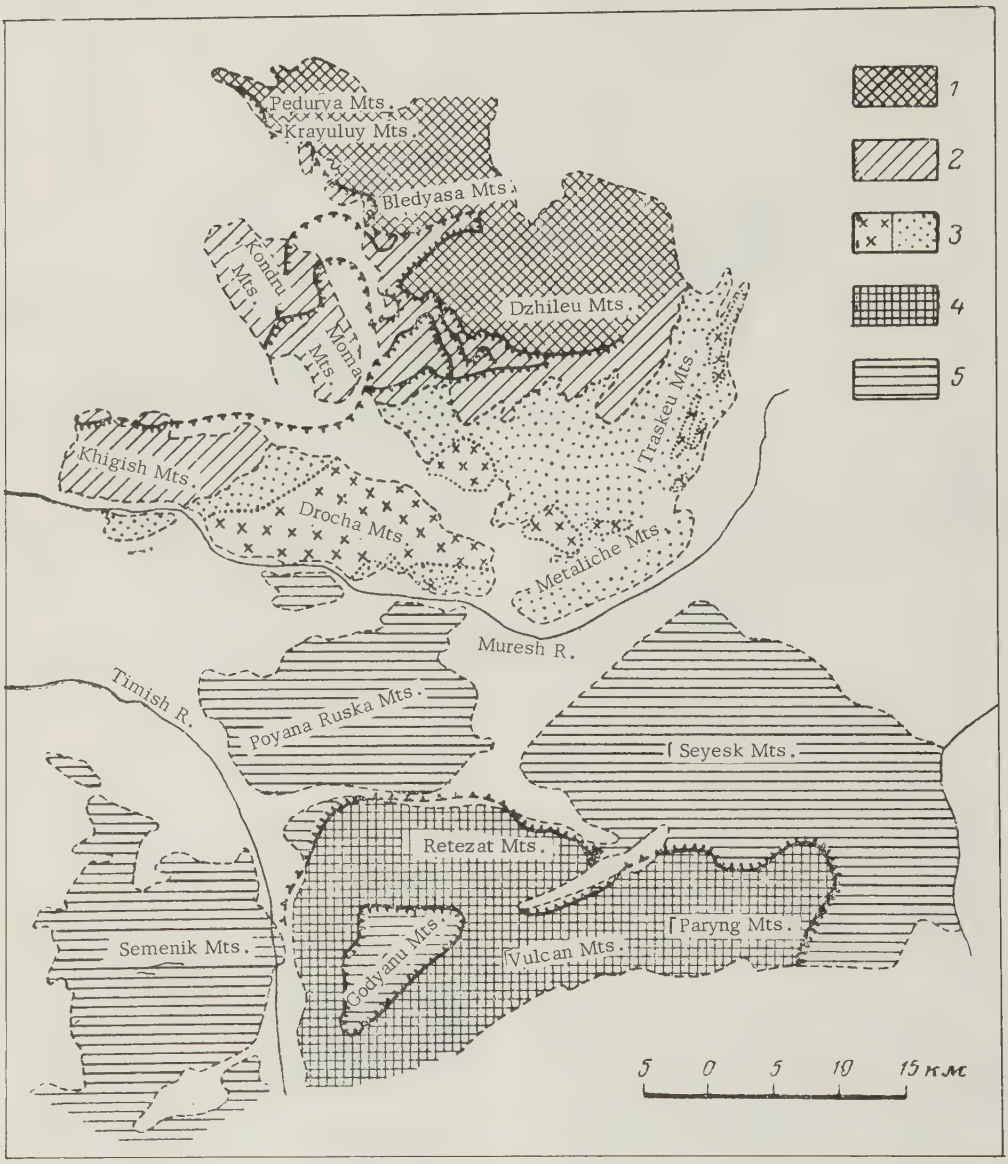

FIGURE 4. Scheme of the Cretaceous thrust systems in the western Romanian Carpathians

1) Dzhileu-Bikhor autochthon, 2) Kodru thrust sheets and others 3) ophiolites and Cretaceous flysch zone, 4) Dunay (Danube) autochthon, 5) Get thrust sheet.

is concealed here by dips which converge toward the depression; this is also reflected in the erosional fault scarps of the Triassic thrust sheets. The location of the thrusts has confused some of the earlier investigators who have thought that the Kodru-Moma massif thrust faults had a direction opposite from that of the Bikhor and Pedurya-Krayuluy thrusts.

The region of subsidence encroached upon a north-trending fault zone which extends into eastern Banata. Both Permian extrusives, as well as the much later banatite extrusives, have been found in this zone.

The structures of the Zapadnyye mountains can be explained if the presence of thrust sheets within it are postulated. However, the fantastic theories of the past, which allow the presence of colossal thrust movements stretching for hundreds of kilometers, as was proposed by I. Popesku-Voyteshti, should not be accepted. This theory postulated the presence of thrust sheets (imagined) from the Zapadnyye mountains to the eastern Carpathians and related them to the Alpine thrusts. Thrust sheets in the Zapadnyye mountains, according to contemporary data, are not more than several dozen kilometers along the line of thrust (in exceptional cases, they may be as much as 200 km). The amplitude of movement does not generally exceed 30 km; this amplitude can be determined only in unusual cases (from fensters or subfensters). However, as is usually the case, the upper tectonic elements have rather small amplitudes in relation to the length of the thrust sheets. From careful field observations, it was determined that individual thrust sheets, composed of older rocks (crystalline schists or Permi-Werfernian [Lower Triassic] formations), were thrust above younger sheets (Triassic, Jurassic, or Cretaceous). Moreover, it was noticed that varying facies zones were directly adjoining in certain instances. Tectonic contacts of the crystalline schists with the Permo-Carboniferous, or the superimposition of the latter on Mesozoic rocks, was determined from several bore holes.

Gravitational gliding is not an adequate explanation for the development of these thrust sheets. The hypothesis of gravitational gliding from an elevated basement does not explain the presence of the crystalline basement in tangential tectonic movements, as has been observed in the Zapadnyye mountains. Moreover, this hypothesis contradicts geophysical data, which indicate a relationship between orogeny and deep normal faulting in the earth's crust and with a general subsidence (not an uplift) of the basement in the axial zone. On the other hand, the development of the sheets by means of folding is difficult to imagine from a mechanical point of view. Therefore, stress as an explanation of the thrusting is favored. Nevertheless, although the fold formation in the upper stage and the tangential movements in the lower stage are equivalent from a hypsometric point of view, they are different from a mechanical one.

The movement of separate autochthonous blocks, resulting in a reorientation of these masses, is regarded by many as a bilateral phenomenon. Considering the Cretaceous thrust systems in the southern Carpathians and the Zapadnyye mountains (fig. 4), this idea is not improbable: the general direction of the main Kodru thrust sheet and its separate upper parts is from the south to the north, while the direction of the Getsky sheet is from the north. This suggests the existence of a bilateral orogeny

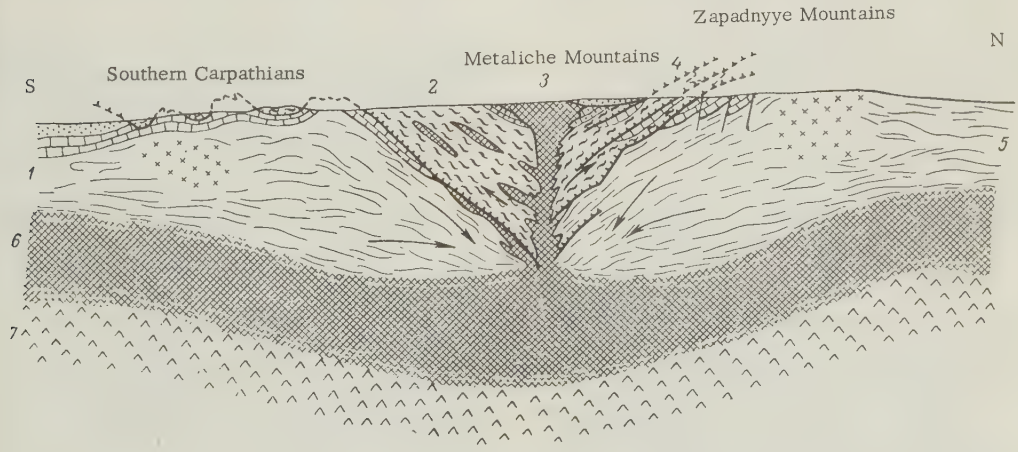

FIGURE 5. Composite (generalized) profile of the western part of the Romanian Carpathians (horizontal and vertical scale 1:1,500,000)

1) Dunay (Dąnube) autochthon, 2) Get thrust sheet, 3) ophiolites and Cretaceous flysch, 4) Kodru and upper thrust sheets, 5) Bikhor-Dzhileu autochthon, 6) basalt belt, 7) sima.

(according to the theories of L. Kober, Kh. Stille, and Ye. Kraus) during Cretaceous time in the Zapadnyye mountains and in the southern Carpathians (fig. 5). The axial zone of this orogeny coincided with the Cretaceous flysch depression (Meresh mountains), which is located along a deep-seated fault along which numerous ophiolitic melts have been extruded, developed between the Drocha and Turda mountains. This fault could be a northeastern continuation of the "radophite" zone (ophiolites, radiolarites) which, according to Kober, divides the Balkans from the Dinaric Alps in central Siberia.

However, the facies of the crystalline massif, and the Paleozoic and Mesozoic rocks of the Zapadnyye mountains tend to link them to the Hemarides. The Bikhor autochthon has its analogue in the sub-Tatra structures. On the other hand, the Zapadnyye mountains are closely linked with the southern Carpathians.

The bilateral transformation of the Dunay (Danube) autochthon and the Dzhileu autochthon can be explained either by Kober's contraction hypothesis (although without full adherence to his theory) or by Kraus's convection hypothesis. Geophysical investigations are nevertheless necessary for a final solution of this problem.

REFERENCES

1. Arabu, N., LA GEOLOGIE DES ENVIRONS DE BĂIŢA [GEOLOGY OF THE BĂIŢA REGION]: Inst. Geol. Roum., v. 25 (1936-37), 1941.

2. Bleahu, M., CERCETĂRI GEOLOGICE ÎN REGIUNEA PADIŞ-CETĂTILE PONORULUI [GEOLOGIC RESEARCH IN THE PADIS-CETĂTILE PONORULUI REGION]: D. S. Com. Geol., v. 41 (1953-1954), 1957.

3. Dimitrescu, R., STUDIUL GEOLOGICAL CRISTALINULUI DINTRE GÎRDA ŞI LUPŞA [GEOLOGIC STUDY OF CRYSTALLINE ROCKS BETWEEN GÎRDA AND LUPŞA]: An. Com. Geol., v. 31, 1958.

4. Gheorghiu, C., STUDIUL GEOLOGICAL VĂII MUREŞULUI ÎNTRE DEVA ŞI DOBRA [GEOLOGIC STUDY OF THE MERESH VALLEY BETWEEN DEVA AND DOBRA]: An. Com. Geol., v. 27, 1954.

5. Gherman, J., CERETĂRI GEOLOGICE ÎN COLŢUL DE S. V. AL DEPRESIUNII TRANSILVANIEI [GEOLOGIC RESEARCH IN THE SOUTHWEST CORNER OF THE TRANSYLVANIAN DEPRESSION]: Rev. Muz. Geol. Miner., v. 7, 1943.

6. Gherman, J., INCĂLECĂRI POST-SENONIENE ÎN BAZINUL AMPOIUIUI [POST-SENONIAN FOLDING IN THE AMPOIUL BASIN]: Rev. Muz. Geol. Miner., v. 6, nos. 1-2, 1937.

7. Giuşcă, D., LES PHÉNOMÈNES DE METAMORPHISME HYDROTHERMAL DES RÔCHES PALÉOZOIQUES DES MONTS DE BIHOR [HYDROTHERMAL METAMORPHISM OF ROCKS OF THE BIKHOR MOUNTAINS]: Univ. Bucaresti, Lab. Miner., Bull., v. 2, 1937.

8. _____, LE MASSIF ERUPTIF DE VLĂDEASA [THE VLĂDEASA EXTRUSIVE MASSIF]: Inst. Geol., An., v. 23, 1950.

9. _____, OBSERVAŢII ASUPRA MINERALIZAŢIILOR CUPRIFERE DIN MASIVUL HIGHIŞ [OBSERVATIONS ON COPPER MINERALIZATIONS IN THE HIGHIŞ MASSIF]: Univ. C. I. Parhon, An., Ser. St. Nat., no. 16, 1957.

10. Giuşcă, D., and G. Cioflică, PÎNZA INTRUZIVĂ DE LA CIUNGANI-CĂZĂNEŞTI [INTRUSIVE ROCKS IN CIUNGANI-CAZANESTI]: Univ. C. I. Parchon, An., Ser. St. Nat., no. 12, 1956.

11. _____, STRUCTURA PÎNZEI INTRUZIVE DE LA CĂZĂNESTI-CUINGANI [STRUCTURE OF INTRUSIVE ROCKS OF CAZANESTI-CUINANI]: Univ. C. I. Parhon, An., Ser., St. Nat., no. 13, 1957.

12. Givulescu, R., FAUNA CRETACICUIUI SUPERIOR DE LA BORODCORNIŢE [FAUNA OF UPPER CRETACEOUS STRATA OF BORODCORNIŢE]: Acad. R. P. R., Filial Cluj., Studii şi Cercetări, v. 2, nos. 1-2, 1951.

13. Iacob, D., CONTRIBUŢII LA CUNOAŞTEREA STRATIGRAFIEI ŞI TECTONICII REGIUNII ZAM-GODINEŞTI-CĂRMĂZĂNEŞTI [CONTRIBUTIONS TO THE STUDY OF STRATIGRAPHY AND TECTONICS OF THE ZAM-GODINEŞTI-CĂRMĂZĂNEŞTI REGION]: Acad. R. P. R., Bull., Sec. St. Biol. Geol., v. 5, no. 3, 1953.

14. _____, CONTRIBUŢIUNI LA STRATIGRAFIA ŞI TECTONICA REGIUNII VESTICE A MUNŢILOR METALICI [CONTRIBUTIONS TO THE STRATIGRAPHY AND TECTONICS OF THE WESTERN REGION OF THE METALLIFEROUS MOUNTAINS]: Acad. R. P. R., Filiala Cluj., Studii şi Cercetări, v. 4, nos. 3-4, 1953.

15. Ilie, M., RECHERCHES GÉOLOGIQUES DANS LES MONTS DE TRASCĂU ET DANS BE BASIN DE L'ARIES [GEOLOGIC STUDIES OF THE TRASCĂU

MOUNTAINS AND THE ARYESH BASIN]: Inst. Geol. Roum., An., v. 17, 1935.

16. Ilie, M., STRUCTURE GÉOLOGIQUE DE LA REGION DE ZLANTA [GEOLOGIC STRUCTURE OF THE ZLANTA REGION]: Inst. Geol. Roum., An., v. 20, 1940.

17. _____, RECHERCHES GÉOLOGIQUES ENTRA LA VALEA STREMŞULUI ET LA VALEA AMPOIULUI [GEOLOGIC STUDIES OF THE REGION BETWEEN THE STREMŞULUI AND AMPOIULUI RIVER VALLEYS]: Inst. Geol. Roum., An., v. 23, 1950.

18. _____, STRUCTURA GEOLOGICĂ A DEPRESIUNII ABRUD [GEOLOGIC STRUCTURE OF THE ABRUD DEPRESSION]: Com. Geol., An., v. 25, 1953.

19. Kräutner, Th., DIE GEOLOGISCHEN VERHÄLTNISSE DES ÖSTLICHEN TEILES DER PĂDUREA CRAIULUI [GEOLOGIC CONDITIONS IN THE EASTERN PART OF THE CRAIUL FOREST]: Soc. Roum. Geol., Bull., v. 4, 1933.

20. _____, ÉTUDES GÉOLOGIQUES DANS LA PĂDUREA CRAIULUI [GEOLOGIC STUDIES IN THE CRAIUL FOREST]: C. R. Inst. Geol. Roum., v. 25 (1936-1937), 1941.

21. _____ OBSERVATIONS GÉOLOGIQUES DANS LES MONTS DU BIHOR [GEOLOGIC OBSERVATIONS IN THE BIKHOR MOUNTAINS]: C. R. Inst. Geol. Roum., v. 26 (1937-1938), 1941.

22. LES DÉPÔTS MÉSOZOIQUES DANS LA REGION DES SOURCES DU SOMEŞUL CALD ET DE VLĂDEASA [MESOZOIC DEPOSITS IN THE UPPER REACHES OF THE SOMEŞUL CALD AND VLĂDEASA RIVERS]: C. R. Inst. Geol. Roum., v. 27 (1938-1939), 1944.

23. _____, OBSERVATIONS GÉOLOGIQUES SUR LE MÉSOZOIQUE À L'OUEST DU MASSIF CRISTALLIN DU GILĂU ET SES RAPPORTS TECTONIQUES AVEC LA SÉRIE DU CODRU ET LA SÉRIE DE BIHARIA [GEOLOGIC STUDIES ON THE MESOZOIC ROCKS OF THE EASTERN GILĂU CRYSTALLINE MASSIF AND ITS TECTONIC RELATIONSHIPS WITH THE KODRU AND BIKARIYA SERIES]: C. R. Inst. Geol. Roum., v. 28, (1939-1940), 1944.

24. Lupu, M. D., RAPORT ASUPRA CERCETĂRILOR GEOLOGICE ÎN REGIUNEA VIDRA-SOHODOL [REPORT ON GEOLOGIC STUDIES IN THE VIDRA-SOHODOL REGION]: Com. Geol., Comunicare, 1956.

25. Macovei, G., and I. Atanasiu, L'ÉVOLUTION GÉOLOGIQUE DE LA ROUMAINE, CRÉTACÉ [GEOLOGIC EVOLUTION OF ROUMANIA, CRETACEOUS]: Inst. Geol. Roum., An., v. 16, 1933.

26. Mataş, I., and Gr. Popescu, CERCETĂRI GEOLOGICE ÎN PARTEA DE E ŞI SE A MUNŢILOR MUREŞUIUI [GEOLOGIC STUDIES IN EASTERN AND SOUTH-EASTERN PART OF THE MERESH MOUNTAINS]: (In manuscript) 1954.

27. Nitulescu, O., CONTRIBUŢINI LA STUDIUL GEOLOGICAL REGIUNII SCHIOPI-PESTRESI, JUD TURDA [CONTRIBUTIONS TO THE GEOLOGIC STUDY OF THE SCHIOPI-PESTRESI REGION, TURDA DISTRICT]: Rev. Muz. Geol. Min., v. 6, no. 1-2, 1937.

28. Papiu Corvin, V., CERCETĂRI GEOLOGICE ÎN MASIVUL DROCEI [GEOLOGIC RESEARCH IN THE DROCHA MASSIF]: Acad. R. P. R., Bull., Sec. St. Biol. Geol., v. 5, no. 1, 1953.

29. Patrulius, D., CONTRIBUŢINI LA STUDIUL GEOLOGICAL PĂDURII CRAIULUI [CONTRIBUTIONS TO THE GEOLOGIC STUDY OF THE CRAIUL FOREST]: D. D. S. Com. Geol., v. 40 (1952-1953), 1956.

30. Paucă, M., LE BASSIN NÉOGÈNE DE BEIUS [THE BEIUS NEOGENE BASIN]: Inst. Geol. Roum., An., v. 17, 1935.

31. _____, RECHERCHES GÉOLOGIQUES DANS LES MONTS CODRU ET DE MOMA [GEOLOGIC STUDIES OF THE KODRU AND MOMA MOUNTAINS]: Inst. Geol., Roum., An., v. 21, 1941.

32. _____, RECHERCHES GÉOLOGIQUES DANS LA REGION DE SIRIA [GEOLOGIC STUDIES IN THE SIRIA REGION]: C. R. Inst. Geol. Roum., v. 25 (1936-1937), 1941.

33. Preda, I., CERCETĂRI GEOLOGICE ÎN REGIUNEA ROŞIA-MESIAP [GEOLOGIC RESEARCH IN THE ROŞIA-MESIAP REGION]: Univ. Bucuresti, Dizertatie, 1957.

34. Raileanu, Gr., CERCETĂRI GEOLOGICE ÎN REGIUNEA ROŞIA [GEOLOGIC RESEARCH IN THE ROŞIA REGION]: C. I. Parhon Univ., An., Ser. St. Nat., 1956, no. 12.

35. Rozlozsnik, R., and M. Palfy, GEOLOGIE

DES BIHOR- UND BELERGEBIRGES. I. KRISTALLIN UND PALÄOZOIKUM. GEOLOGIA HUNGARICA [GEOLOGY OF BIKHOR AND BELER MOUNTAINS. I. CRYSTALLINE AND PALEOZOIC ROCKS. GEOLOGY OF HUNGARY]: Ser. Geol., v. 7, 1938.

36. Socolescu, M., and T. P. Ghiţulescu, ÉTUDE GÉOLOGIQUE ET MINIERE DES MONTS METALLIFÈRES [GEOLOGIC AND MINING INVESTIGATIONS OF THE METAL-BEARING MOUNTAINS]: Inst. Geol. Roum., An., v. 21, 1941.

37. Socolescu, M., LES AFFLEUREMENTS DE MINERAI DE LA RÉGION DE VATA-SOIMUŞ-BUCEAVA-SĂVIRŞIN-ZAM [ORE OUTCROPS IN VATA-SOIMUS-BUCEAVA-SĂVÎRŞIN-ZAM REGION]: C. R. Inst. Geol. Roum., v. 28, (1939-1940), 1944.

38. Trig, A., SILIMANITUL DE PE VALEA IERII [SILLIMANITE IN THE IEREA VALLEY]: Acad. R. P. R., Fil. Cluj., St. St., v. 3, nos. 1-2, 1952.

NEW STUDIES ON THE GEOTECTONIC SUBDIVISIONS OF EASTERN CHINA AND THEIR CHARACTERISTICS[1]

by

T. K. Huang

• *translated by Royer and Roger, Inc.* •

ABSTRACT

The major characteristics and subdivisions of the Chinese platform are described and compared with standard Russian platforms. Because a typical Chinese platform subdivision is clearly different it is proposed to designate such a subdivision a paraplatform. Two paraplatforms and a massif comprise the Chinese platform. The South Chinese paraplatform is the most mobile, having undergone multiple folding and faulting with magmatic activity. By comparison, the Sino-Korean massif is less mobile and underwent only one cycle of deformation. The Northeast paraplatform is similar to the South-Chinese paraplatform in structural elements and history. Deep rupture zones are significant elements of the structure of the Chinese platform. --M. Russell.

GEOTECTONIC SUBDIVISIONS OF EASTERN CHINA

The Characteristics and Three-Fold Subdivision of the Chinese Platform

Eastern China and western China constitute two distinct geotectonic units: The western part is the more intensely deformed and folded; it was affected by Paleozoic tectonic activity, then with Mesozoic and Cenozoic tectonic movements folded belts were interspersed with troughs of different dimensions. The eastern part is less intensely deformed, and is underlain by pre-Sinian crystalline schist and weakly metamorphosed rocks overlain by Paleozoic shallow-water marine sediments and Mesozoic continental sediments. The dividing line between these two structural regions runs from north to south along the Great Khingan range in Manchuria to the northern edge of Inner Mongolia, thence to Liupan-shan and the northern Tsingling range; it then follows the southern boundary of the Tsingling geosyncline, the Lung-meng-shan and Tapa-shan folded belt to the north-south trending Kam-Yunnan axis. This Chinese platform not only covers the vast eastern part of China but also includes the Burea massif of the Soviet Far East, all of Korea and the northeastern part of Indochina.

The Chinese platform itself is a huge complicated structural system, the northern, central and southern parts of which form distinct structural units. The middle unit is called the Sino-Korean massif, the northern, the Northeast paraplatform, and the southern, the South-Chinese paraplatform.

The major geotectonic characteristics of the Chinese platform are as follows: (1) The pre-Sinian crystalline basement rocks crop out in many areas. (2) The sedimentary cover of the platform ranges from 4,000 to 7,000 meters in thickness, with only local exceptions. (3) Although the movement has not been as intense as in folded geosynclines, much of the deformation has resulted from oscillatory movement and faulting. Folding is present in some areas, but generally is of the transitional type.

The above characteristics of the Chinese platform are typical of true platforms as contrasted with geosynclines. The following points, however, indicate its affinity with geosynclines. (4) Although the intensity of its folding is not so great as in other geosynclines, it is much stronger than is characteristic of such typical platforms as the Russian and North American platforms. Its oscillatory movements, which commonly reached 10,000 m, and tectonic activity belong to different orogenic cycles. (5) Large-scale magma eruption accompanied the folding and faulting, giving rise to various kinds of extrusive and intrusive rocks. The granitic rocks are of special importance. (6) Contemporaneous with magmatic activity was the formation of metallic ore deposits: tungsten, tin, molybdenum and copper.

The three main subdivisions of the Chinese platform (fig. 1) are as follows:

I. The Characteristics and Subdivisions of the Sino-Korean Massif

Briefly, the Sino-Korean massif is a huge platform-type unit south of the Mongolian geosyncline and its eastern extension, the Kirin basin. It lies east of Nan-Shan and Tsingling geosyncline, and north of the Nanking sink. It includes all Korea and the subsided area of Po-hai and Hung-hai. The massif is subdivided into the following:

(1) Inner Mongolian Axis

This is an east-west trending linear structure

[1]Translated from Acta Geologica Sinica, v. 39, no. 2, p. 115-134, 1959.

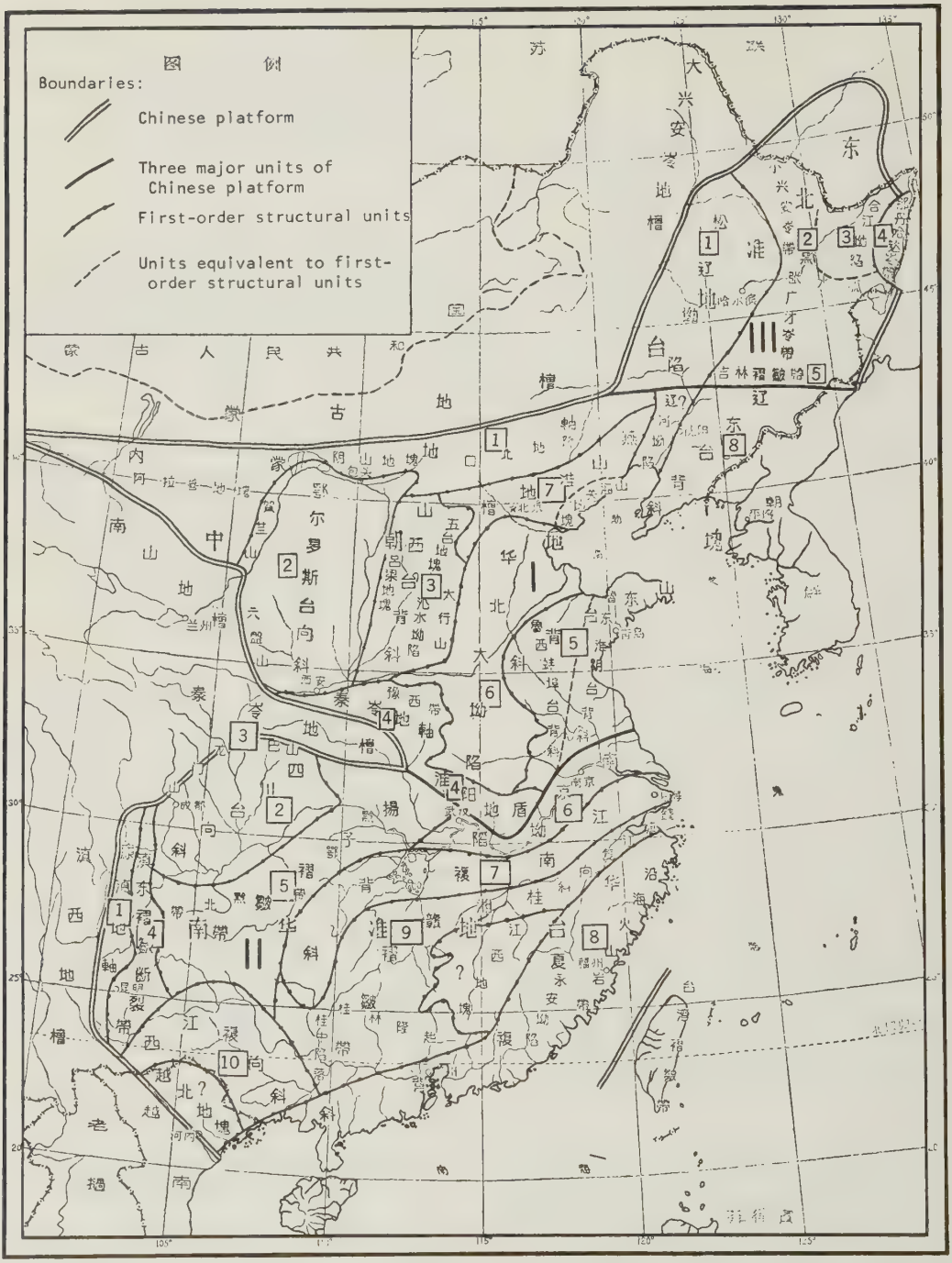

FIGURE 1. Geotectonic map of eastern China (scale: 1:12,000,000).

I. Sino-Korean massif: (1) Inner Mongolian axis; (2) Ordos syneclise; (3) Shansi anteclise; (4) Tsingling axis and Huai-yang shield; (5) Shan-tung anteclise; (6) Great North China sink; (7) Yenshan parageosyncline; (8) Liaotung anteclise.

II. South-Chinese paraplatform: (1) Kam-Yunnan axis; (2) Szechuan syneclise; (3) Lung-men-shan and Ta-pa-shan folds; (4) Fold-fault zone of eastern Yunnan; (5) Yangtze fold zone; (6) Nanking sink; (7) Chiangnan anticlinorium; (8) Cathaysian anticlinorium; (9) Kuei-hsiang-kan fold zone; (10) Hsi-chiang (West River) synclinorium.

III. Northeast paraplatform: (1) Sungliao sink; (2) Hei-shui arc and the granite zone of the Little Khingan; (3) Ho-chiang sink; (4) Na-tan-ha-ta-ling fold zone; (5) Kirin fold zone.

of pre-Sinian crystalline schists. Here, uplift and erosion since Sinian time is evident. The overlying beds are thin, scattered, and consist mostly of continental sediments. Much folding and faulting occurred during the Mesozoic and large quantities of extrusive and intrusive rocks (largely granites) were formed in the eastern part. The Inner Mongolian axis is the boundary between the Mongolian geosyncline and the platform deposits of North China. It can be divided into three parts:

The Western part comprises the Ala-shan massif, which is bounded on the north by the Mongolian geosyncline, on the south by the Nan-shan geosyncline (The Chi-lien-shan geosyncline) and on the east by the Ho-lan-shan folds and Ordos syneclise. The Ala-shan massif is composed of pre-Sinian crystalline schists and weakly metamorphosed rocks. Its sedimentary cover is very thin. Except for local upper Paleozoic marine sediments, the cover is mostly Mesozoic and Cenozoic continental basin deposits, which have neither undergone pronounced folding nor been affected by igneous intrusion. Because of its shape the Ala-shan massif has also been called the Ala-shan triangle.

The Inner Mongolian axis has a very narrow middle part because of the existence of a Mesozoic and Cenozoic depression -- the Wu-yuan depression. It is south of the northeast-southwest trending Lang-shan metamorphic belt which in turn is northeast of Ala-shan. Further east is the Yin-shan massif, which is separated from the Ala-shan massif on the west by a large rupture zone occupied by Yen shan granite and Cenozoic basalt. The Yin-shan massif is separated from the folded belt of the Mongolian geosyncline to the north by an east-west middle Cenozoic depression. On the south, it is separated from the Ordos syneclise by the Pao-t'ou and Hu-ho-hao-te' depressions. The Yin-shan massif consists of east-west trending Archaean and Proterozoic folds intruded by several igneous bodies. Paleozoic marine sediments occur locally; upper Paleozoic, Mesozoic, and Cenozoic continental deposits are widely scattered. The presence of Variscan and Yenshan granites indicates that structural movements occurred during these two periods.

The Wu-yuan and Hu-ho-hao-te' depressions were the result of a great rupture zone that possibly extended through Chi-ning to the Chang-pei area. This rupture zone is the boundary between the Yin-shan massif and the so-called "K'ou-pei Barrier" of the eastern part of the Inner Mongolian axis. The K'ou-pei Barrier borders the Lin-si sink, a depression containing Paleozoic marine deposits, and is bounded on the north by a possible deep rupture along the line from To-lun to Chih-feng. It is separated on the south from the Yen-shan parageosyncline by a deep rupture extending from Hsuan-hua through Ch'eng-teh to Pei-piao. The structural characteristics of the K'ou-pei Barrier are similar to those of the Yin-shan massif, but here the Yenshan movement is especially well manifested, chiefly by normal faulting accompanied by the intrusion of granite and extrusion of intermediate and acid volcanic rocks, the latter covering large areas of this structural unit. Cenozoic basalt occurs extensively along the northern margin of K'ou-pei Barrier.

The rocks west of Chang-chia-k'on (Kalgan) and north of Ta-t'ung also consist of crystalline schist. Whether it belongs to K'ou-pei Barrier or Shansi syneclise depends on whether a deep rupture occurs between Chang-chia-k'on and Ta-t'ung; the rupture is the western extension of Hsuan-hua - Ch'eng-teh - Pei-piao deep rupture zone, a natural boundary between two structural units.

(2) Ordos Syneclise (Ordos Platform)

This is the rectangular, stable, major structural unit of the Sino-Korean massif. It is separated from the Inner Mongolian axis to the north by the Wu-yuan and Hu-ho-hao-t'e depressions; on the south a similar middle Cenozoic depression (Wei-ho graben) becomes the boundary between the Ordos syneclise and the Tsingling axis. The eastern boundary is a north-south trending deep rupture belt (Li-shih fault). The western boundary is the complex Ho-lan-shan and Liu-p'an-shan fold and fracture systems.

The main characteristics of the Ordos syneclise are: (a) it is very stable. Except for the part adjacent to the Wei-ho graben on the south, it has not been markedly affected by folding and faulting. (b) Magmatic activity was completely absent. (c) Blanketing sediments are thicker here than in any other part of the Sino-Korean massif; Mesozoic continental deposits are several thousand meters thick here but are absent elsewhere. (d) The blanketing sediments maintain a constant gentle westward dip.

The western margin of Ordos syneclise is separated from the Ho-lan-shan and Liu-p'an-shan systems by a deep rupture zone probably formed during the Mesozoic, possibly Paleozoic. Although apparently it resembles a deep rupture, there were no accompanying magmatic injections.

The Ho-lan-shan system lies primarily in the sunken belt adjoining the Ala-shan massif. Subsidence took place in three periods; in early Paleozoic time with marine deposition, in late Paleozoic time with continental and onlap marine deposition, and during the Mesozoic with deposition of continental sediments. The major orogenic movement occurred during the late Mesozoic or Yenshan period; it gave rise to north-northeast trending folds and fractures and was accompanied locally by igneous activity. East of this (the Ho-lan-shan belt) is the subsided belt, down-faulted during

the Cenozoic period -- the Yin-chu'an graben.

The structure of the Liu-p'an-shan system is even more complex than the Ho-lan-shan system; it can be divided into three zones: in the middle is the north-south trending ridge of the Niu-shou-shan and Ta-t'ang-shan, composed essentially of Sinian, Cambrian, and Ordovician marine sediments; the ridge apparently was formed by the Variscan movement. East of the ridge, along the western margin of the Ordos syneclise, is a zone underlain by thousands of meters of Mesozoic sediments. West of the ridge is the narrow Liu-p'an-shan subsided belt containing thick Mesozoic beds, especially the Cretaceous sandstone and shale series. Folding and faulting of the three zones during the Yenshan period resulted in the Yuan-yang-hu folds of the east, the ridge zone in the middle, and the Liu-p'an-shan folded and faulted belt in the west. The latter was again folded and faulted during the Cenozoic.

(3) Shansi Anteclise

The Shansi anteclise is separated from the Ordos synclise on the west by the great Li-shih fault, separated from Inner Mongolian axis on the north by a hypothetical fault extending from the Chang-chia-k'on to Ta-t'ung. To the east and south are rupture zones bordering the great North China sink. The anteclise itself consists of individual uplifts and downfaulted troughs of various sizes and shapes: the major ones are the Wu-t'ai massif, the Lu-liang massif and the Chung-tiao-shan massif. The Wu-t'ai massif is an old area of uplift underlain by a pre-Sinian crystalline basement. It is the boundary between the Shansi anteclise and the Yen shan folded belt. The southern extension of the Wu-tai massif is the north-south trending T'ai-hang-shan, the northern part of which is the Tsan-huang well; the southern part consists of lower Paleozoic limestone which forms the "Great Wall" of Tai-hang; on the east, a rupture zone adjoins the great North China sink. The Lu-liang massif occurs in the western part of the anteclise; it is similar in character to the pre-Sinian crystalline massif of Wu-t'ai. Its southern part also consists of a long, uplifted ridge of lower Paleozoic limestone. Between the Lu-liang uplift and the T'ai-hang uplift mentioned above, is a large depression underlain chiefly by upper Paleozoic sediments -- the Hsin-shui sink. Its relationship with the Lu-liang uplifted belt is complicated by the existence of a narrow, north-south trending rupture zone known as the Fen-ho graben. The Chung-tiao-shan massif, composed of crystalline schists, forms the southwestern most part of the Shansi anteclise. It is bordered on the north by the Fen-ho graben and on the south by the Wei-ho graben.

(4) Tsingling Axis and Huai-yang Shield

The Tsingling axis is an east-west trending crystalline axis between the platform deposits of North China and the Tsingling geosyncline. The Lung-hsi massif is a western extension of this axis and separates the Tsingling geosyncline from the Nan-shan geosyncline. Its eastern extension passes the Nan-yang basin and is connected to the Huai-yang shield. The logical boundary between an axis and a geosyncline should be a deep rupture belt. The northern boundary of the Tsingling axis is the Wei-ho graben mentioned previously. The structure of the eastern part of the axis is quite complicated: here, Archaean and Proterozoic crystalline schists trend west-northwest and are separated by similarly trending faults south of Hua-shan, down-faulted lower Paleozoic beds appear on top of the crystalline basement, but north of Fu-niu-shan, large areas were covered by Proterozoic volcanic rocks of intermediate composition.

Fu-niu-shan is the eastern part of the Tsingling axis, north of which lies the Yu-hsi folded and faulted belt. Thrust faults trending nearly east-west and west-northwest sliced the Paleozoic blanketing sediments into several strips. The structure was further complicated by numerous transverse and oblique faults. Crystalline schists commonly form the backbone of strips such as Sung-shan. Geophysical data indicate that the strips extend eastward under the Cenozoic cover of the North China plain. Because of the west-southwest extent of the Cenozoic Lo-ho depression, the Yu-hsi folded and faulted belt was divided into two parts: the southeastern part is the Sung-shan area mentioned previously, and the northwestern part is the Huan-chu region. The latter is an area of gently folded and faulted Paleozoic deposits, and is separated from the Shansi-anteclise by a large fault.

The Huai-yang shield, composed of crystalline schist, is actually the eastern extension of the Tsingling axis. These two have been considered as one structural unit by Chang-wen-you; the unit is known as the Fu-niu - Ta-pieh anteclise. The southern boundary of the Huai-yang shield is a hypothetical deep rupture, which is the eastern extension of the Ta-pa-shan deep-rupture, which is the eastern extension of the Ta-pa-shan deep-rupture zone (see below); farther east it joins the Tan-cheng - Lu-chiang deep-rupture zone. The northern boundary is the Pei-huai-yang fractured zone, which separates the shield from the Great North China sink. In the past, the shield was thought to continue to the east of the Peiping -P'u-k'on railroad; however, since the discovery by aeromagnetic survey of the presence of the Ho-fei subsidence, the eastern boundary of the shield is put at Liu-an and Shu-ch'eng.

(5) Shan-tung Anteclise

This is a large swell, east of the Great North China sink and bounded by the ocean on the east.

A large rupture possibly separates the adjoining Great North China sink on its northwest margin. In the south it sinks gradually under the Su-pei (northern Chiangsu) plain. The Tan-cheng - Lu-chiang deep rupture divides the Shan-tung anteclise naturally into an eastern and a western part: the eastern part is the Lu-tung - Huai-ying anteclise, basically a crystalline massif with no sedimentary cover that to the south extends under the Su-pei plain. The only important subsided area within this anteclise is the Mesozoic Kao-mi depression. The western part is the Lu-hsi - Peng-fu anteclise. Here, the Paleozoic limestone cover is relatively extensive. Because of northwest-southeast-trending faults which sliced the basement and its overlying rocks into many strips, and because of the additional complication of transverse faults trending north-south and other directions, the Lu-hsi area appears as a jigsaw pattern on the map. The fracture pattern was believed to be a result of Mesozoic movement that recurred during Cenozoic time. The fractures were probably a result of the northward movement of the Lu-hsi massif along the Tan-cheng - Lu-chiang deep rupture. A small area of crystalline rocks forms a bulge south of Peng-fu. It forms the saddle of the Lu-hsi - Peng-fu anteclise with the Lu-hsi massif in the north and the gently folded and faulted region of Paleozoic sediments of Hsu-chou and Peng-fu in between.

(6) Great North China Sink

The great plain east of Shansi anteclise, west of the Shantung anteclise, south of the Yenshan folded belt (see below), and north of the Tsingling axis and Huai-yang shield is a large area subjected to post-Yenshan movement, a depression that subsided during the Cenozoic era. It is composed of gently folded and faulted Paleozoic basement rocks, unconformably overlain by essentially continental Cenozoic sediments. The swelling and sinking of the Paleozoic basement is notable. The major subsurface structure is the north-northeast-trending Ts'ang-hsien swell composed of Paleozoic limestone. This swell divides the northern part of the Great North China sink into two parts: the Po-yeh sink in the west and the Huang-hua - Lin-ching sink in the east. The southern part of the great North China sink is known as the Kai-feng sink. It extends southward to merge with the western part of the Ho-fei sink mentioned previously. The western part of the Kai-feng sink is in juxtaposition with the buried part of the Yu-hsi folded and faulted belt. In the deepest part of the Great North China sink, sediments probably range from 4,000 to 7,000 meters in thickness: Paleozoic sediments in the lower part (Sinian, Cambrian, Ordovician, and Permo-Carboniferous) and Tertiary and Quaternary sediments in the upper part; Mesozoic sediments are present only locally.

This is the most mobile belt of the Sino-Korean massif; folding and faulting clearly affected sediments of this parageosyncline. The north boundary is the Hsuan-hua - Cheng-teh-Pei-piao deep-rupture zone mentioned above, the south boundary is the Great North China sink. What we refer to as a parageosyncline is the structural feature of the Sinian period, when this Yenshan region rapidly subsided. The marine sediments attained a thickness of more than 10,000 meters with a facies similar to that of a geosyncline (flysch facies with intermediate volcanic rocks). Although marine sediments were deposited here in the Cambrian and Ordovician time, they are truly platform facies. The mass was uplifted and became land afterwards. The Permo-Carboniferous sediments are interbedded marine and continental deposits. The Mesozoic is represented by thick continental sediments and volcanic tuff. The first orogenic movement since Sinian time occurred at the end of the Jurassic and the beginning of the Cretaceous -- the Yenshan movement, which produced large-scale folding and faulting. East of Peking, these folds and faults trend east northeast to northeast; west of Peking they trend northeast. There were at least three periods of igneous activity during the Mesozoic era as represented by: (a) Triassic-Jurassic basic volcanic rocks; (b) Middle and Upper Jurassic intermediate volcanics, (c) Cretaceous silicic volcanics. Many granitic bodies, some of batholithic size, were intruded along the ruptured zones.

The Yenshan folded belt can be divided into one part east of Peking and another part west of Peking: East of Peking is the Yenshan parageosyncline proper, lying between Mi-yun and Fu-hsin. Here, the Sinian as well as Cambrian and Ordovician sediments thin out toward the east. In contrast are the Jurassic and Cretaceous sediments which are thick in the east and scarce and thin in the west. Numerous thrust faults exist, some several kilometers long. West of Peking is a folded and faulted zone between Chuntu-shan and the Wu-tai massif. Because of a bulge of crystalline rocks, the Chu-ma-ho swell, this folded belt was divided again into two parts, the southeast and the northwest part. Numerous faults occur here; the large strike faults, designated north to south, are: the Hsuan-hua - Cheng-teh - Pei-piao deep rupture (overthrust from north to south), the Chi-ming-shan thrust fault (from south to north), the Huai-lai thrust fault (from south to north), the Great Nan-kou fault (from north to south), and the Fang-shan - Pa-pao-shan thrust fault (from south to north).

East of the Yenshan parageosyncline is a small crystalline massif similar to that of Wu-tai - the Shan-hai-kuan massif. Sinian sediments thin out in the direction of this massif, indicating that uplift had already started in Sinian time.

The tubular-shaped western part of this massif extends into the folded and faulted Paleozoic rocks forming the Chi-tung (eastern Hopei) swell.

(8) Liaotung Anteclise

The Cambro-Ordovician sediments of the Yenshan parageosyncline thin out in the direction of the Fu-hsin - Ch'a-hsien line. East of it, Sinian basement rocks are exposed again at I-wu-lu-shan. Farther east lies a Cenozoic depression -- the Liao-ho sink. This and the Po-hai sink are a part of the Sino-Korean massif.

The Liaotung anteclise is east of the Liao-ho sink. It is a structure with characteristics similar to the Shantung anteclise (especially the Lu-tung part); possibly they once formed a continuous uplift. The Liaotung anteclise consists of three parts: the southern part is an uplifted area of pre-Sinian crystalline schist with the Chin-chou-wan sink, a subsided area of Sinian deposits, to the southwest. The central part is a downwarped area of Paleozoic sediments and includes the folded and faulted belts of Tai-tzu-ho and Tung-hua. The northern part is a crystalline uplift known as the Chin-yu swell, southeast of which lies an extensive Cenozoic volcanic area, the Ch'ang-pai-shan volcanic province. The Chin-yu swell consists of many fault slices trending northeast-southwest. The more important ones are the Fu-shun - Hai-lung rupture, the Liu-ho rupture, the Chiao-ho rupture and the Tung-hua rupture. These ruptures originated mainly during Mesozoic time and were rejuvenated in Cenozoic time.

To the north the Liaotung anteclise is bounded by the northeast paraplatform. The boundary is indistinct. The southeastern part of this anteclise extends into Korea.

II. Characteristics and Subdivisions of the South-Chinese Paraplatform

The Sino-Korean massif is comparatively a more mobile area; its mobility is manifested by faulting. Folding is more pronounced only in particular areas such as the Yenshan parageosyncline. In contrast to this, not only widespread faulting occurred on the South-Chinese Paraplatform, but distinct folding movement of various orogenic cycles also occurred, accompanied by large extrusions and intrusions of volcanic and other igneous rocks. The South-Chinese paraplatform constitutes a major structural unit. It is south of the Sino-Korean massif and the Tsingling geosyncline; it includes and extends eastward from the Kam-Yunnan axis. It also includes Hainan Island and the northeastern part of Indochina (north of the Red River).

The South-Chinese paraplatform consists of the following structural units:

(1) Kam-Yunnan Axis

This is an area of uplift composed of pre-Sinian crystalline schist and low-grade metamorphic rocks, extending north-south from Kang-ting to the valley of the Red River. In the past, this area was believed to have been uplifted during Sinian time. However, the discovery of extensive Cambrian and Ordovician beds within it proved that the Kam-Yunnan axis could not have been uplifted before Caledonian time. Permian basalt and Upper Triassic continental deposits cover extensive areas of the axis; the latter everywhere overlie older beds with angular unconformity. Therefore we believe that Variscan and Indochina movement were also present. The assessment of the importance of these movements must await future study. Both the east and the west side of the Kam-Yunnan axis are delineated by deep ruptures. Variscan basic and ultrabasic rocks and Permian basalts have been intruded along these ruptures. In Yunnan, west of the axis, a Variscan folded belt was covered by Upper Triassic red beds. East of the axis is an area covered by platform-type Paleozoic limestones. It is also evident that during the Yenshan and the Himalayan movements, strong faulting movements occurred in the axis where the old faults were rejuvenated.

(2) Szechuan Syneclise

This is a downwarped area east of the Kam-Yunnan axis, south of Lung-meng-shan and Ta-pa-shan, and north of the Hupeh and Kueichou folded belt; it is equivalent to von Richthoven's red Szechuan basin. The syneclise consists of three parts: the southeastern folded belt, where the Permian and Triassic limestone from elongated anticlines alternating with synclines underlain by Jurassic continental sediments; the central part, which consists of gently dipping Jurassic sediments showing disjunctive but not transitional type of folding; and the northwestern part, which is a large-scale frontal trough where Jurassic and Cretaceous sediments are 4,000 to 5,000 meters thick. Between the Szechuan synclise and the Kam-Yunnan axis is a block-faulted area of Paleozoic limestone and Permian basalt known as the O-mei-shan block.

(3) Lung-men-shan and Ta-pa-shan Folds

The Lung-men-shan folded-faulted zone originated as a result of Yenshan movement; it is a narrow, northeast-trending belt between the Szechuan syneclise and the Tsingling geosyncline. It is composed of Paleozoic, principally Devonian, sediments. After Caledonian folding, this trough subsided. It is separated from the Tsingling folded belt by a deep rupture. During the Yenshan period, movement was resumed along this rupture so that the Caledonian folds were thrust from northwest to southeast over the middle-upper Paleozoic limestone. As a result, the Paleozoic limestone was thrust a

great distance over the Jura-Cretaceous sediments on the southeast, forming the schuppen structure of Peng-hsien and Kuan-hsien.

The Lung-men-shan fold was connected northeastward to the Ta-pa-shan fold. The Ta-pa-shan consists of two parts: The western part, or the Ying-tsui-yen uplift, which is an east-west trending pre-Sinian crystalline zone, surrounded by Paleozoic marine sediments on all sides; and the eastern part, a northwest-trending folded arc, convex towards the Szechuan basin, where the Jurassic strata were infolded, faulted and overturned towards the southwest. The boundary between the Ta-pa-shan fold and the southern Tsingling axis is the Ta-pa-shan deep rupture.

(4) Fold-Fault Zone of Eastern Yunnan

This zone is east of the Kam-Yunnan axis and west of the Hsi-chiang (West River) synclinorium. It consists of two parts: the western part is the eastern Yunnan rupture zone, extending from Hui-tse to Kunming and southward to the Red River valley. Numerous north-south trending faults occur within the Paleozoic limestone and Permian basalt. The major one is the great Hsiao-chiang fault, an old fracture extending from Hsun-tien to I-liang and southward. Large quantities of lava poured out along the ruptured zone in Permian time. Such north-south trending faults were again active during Mesozoic and Cenozoic time. The eastern part of the zone, the Niu-shou-shan swell, formed by a nucleus of pre-Sinian and lower Paleozoic rocks, is flanked on both sides by middle and upper Paleozoic sediments. The west limb is adjacent to the eastern Yunnan rupture zone which is a complex graben between the Kam-Yunnan axis and the Niu-shou-shan swell. The east limb broadens towards the east, forming a northeast-southwest flexure which is the boundary between the fold-fault zone of eastern Yunnan and the Hsi-chiang (West River) synclinorium. The major folding of the eastern Yunnan belt is of Yenshan age. Except for Permian basalt, there is no igneous rock.

(5) Yangtze Fold Zone

This is a broad fold-fault zone north of Chiangnania (see below), south of the Szechuan synclise, and west of the Tung-ting sink. It is characterized by: (a) a cover mainly of Paleozoic platform-type limestone and of Triassic limestone; (b) strong folding of the thick sedimentary sequence, including Jurassic, as a result of the Yenshan movement, forming mutually parallel anticlines and synclines, the anticlines of which are commonly elongated and comb-shaped or box-shaped; (c) numerous faults; the major faults are thrust faults along the axial portion of the anticlines; (d) complete absence of igneous rocks. The Yangtze fold zone can be divided into three parts: the west-northwest trending Chin-shan belt in the north, which bends around the Huang-ling anticline and connects with the Ta-pa-shan folds; the central part, which consists of the northeast-southwest trending Hupei-Kueichou folded belt bounded on the west by the north-south Tsun-i rupture; the western and southern part, which consists of the Lou-shan arc and the stable central Kueichou plateau. The Lou-shan arc extends into northeast Yunnan and becomes a part of the fold-fault zone of eastern Yunnan and abuts against the Hsiao-chiang deep rupture. This third part is known as the northern Kueichou fold-fault belt. It is separated from the fold-fault zone of eastern Yunnan by the Wei-ning arc, an arcuate structure convex towards the north, consisting of a strongly subsided Carboniferous trough.

(6) Nanking Sink

This is a large linear depression occurring north of Chiangnania (Chiangnan old land mass), and south of the Huai-yang shield and Shantung anteclise. It is separated from the Huai-yang shield by a deep rupture. The sink proper is also a deeply-ruptured zone, known as the "Lower Yangtze fractured zone", which extends from T'ai-chou in northern Kiangsu to Nanking and Wu-hu and to the west of Au-ching. Lower Paleozoic beds are sparsely exposed in the Nanking sink. In the east, Silurian beds commonly form the core of anticlines and in the west, especially in eastern Hupeh, Cambrian-Ordovician beds commonly form the axial part of anticlines. Upper Paleozoic and Triassic limestones are widespread and, in places, form schuppen structure. All the Jurassic and Cretaceous continental sediments unconformably overlie older beds, suggesting that Indochina movement and Yenshan movement are important here. Mesozoic silicic volcanic and plutonic rocks are widely scattered within the Nanking sink. Plutonic dioritic rocks are closely related to the copper and iron deposits of this region.

(7) Chiangnan Anticlinorium

The Yangtze fold zone and the Nanking sink are both downwarped areas of the South-Chinese paraplatform. South of these, however, is the Chiangnan old landmass (Chiangnania) which has been an area of uplift throughout many geologic periods. This uplifted area has actually undergone many cycles of folding so that it cannot be called an anteclise, but rather an anticlinorium. This area is thus tentatively named the Chiangnan anticlinorium. The Chiangnan anticlinorium extends from Shanghai westward through the region of Po-yang-hu and Tung-ting-hu and the uplifted and folded belt of northern Kwangsi province. It separates the Yangtze trough on the north from the southern China trough on the south. With respect to folding movement, the pre-Sinian folds, occupying the central part of the anticlinorium, constitute the primitive Chiangnan anticlinorium. The primitive, or proto-Chiangnan anticlinorium has been expanded

to its present extent since the Caledonian movement. Our present knowledge shows that the Caledonian movement is well manifested on the south side of the Chiangnan anticlinorium, where Devonian sediments overlie the lower Paleozoic sediments unconformably. The intensity of the folding movement decreases from south to north so that such unconformities are rarely observed in the northern part of this anticlinorium. Yenshan movement has affected the entire Chiangnan anticlinorium where the sparsely distributed upper Paleozoic and Mesozoic were folded and faulted. Numerous granitic intrusions occur in the Chiangnan anticlinorium; a few are of Caledonian age, but most are of Yenshan age. In western Kiangsi and northeastern Kiangsi and western Chekiang, the Yenshan granites are contemporaneous and are associated with essentially rhyolitic volcanic rocks. Eastward, the Chiangnan anticlinorium was buried under a [coastal] plain. Recent drilling has revealed this structure 200 to 300 meters under the city of Shanghai.

(8) Cathaysian Anticlinorium

Located along the southeastern coast of China, including eastern Chekiang, most of Fukien, and the southern part of Kwangtung (including Hainan Island) is an uplifted area similar in size and character to the Chiangnan anticlinorium. Its original name is "Cathay old landmass" (Cathaysia) now renamed Cathaysian anticlinorium. It is composed of intensely folded and faulted pre-Devonian metamorphic and including some low-grade metamorphic rocks. The latter have been cut by widely scattered granite batholiths.

A part of the granite is of Yenshan age; the rest, the gneissic granite together with its surrounding schist, have, in the past, been referred to the Archaean. Recent studies indicated that the gneissic granites are possibly the products of Caledonian granitization. Upper Paleozoic marine sediments and continental Jurassic and Cretaceous sediments unconformably overly the Cathaysian anticlinorium. Such deposits appear in areas of subsidence of various sizes; the most important of which is the Yung-an sink in southern Fukien province. Late Mesozoic silicic volcanic rocks also occur within such basins. In eastern Chekiang and coastal parts of Fukien, rhyolites are extensive. They constitute the coastal volcanic province. Intruded within this volcanic belt are many granites and dikes and stocks of rhyolitic composition. We have reasons to believe that the igneous rocks came up along northeast-southwest fractures, the largest of which are the Shou-wu rupture, the Tui-ching rupture, and the Li-shui and You-c'hi rupture. Because of the great abundance of such ruptures, volcanic rocks which were extended along them form a continuous sheet, giving rise to the coastal volcanic province already mentioned.

As mentioned previously, the major orogenic movement of the Cathaysian anticlinorium is Caledonian; however, the Indochina movement is also important as shown by the pronounced unconformity between lower Jurassic and lower Triassic rocks. Yenshan movement accompanied by magmatic activities also greatly modified the features of the Cathaysian anticlinorium.

(9) Kuei-hsiang-kan Fold Zone

This zone occurs between the Chiangnan anticlinorium and the Cathaysian anticlinorium. It is distinguished from the Chiangnan anticlinorium by the presence of a pre-Devonian regional unconformity. It is separated from the Cathaysian anticlinorium by the great Shou-wu - Tui-ching rupture and the marginal rupture zone of Cathaysian anticlinorium in western Kwangtung. This fold zone unit consists of three parts: the easternmost is the Ch'ien-t'ang-chiang synclinorium. It is a narrow fold-fault belt, trending northeast-southwest along the river Ch'ien-t'ang-chiang from a point south of Shanghai through Hangchou to Lin-ch'uan of Kiangsi province in the southwest. It is restricted on both sides by great ruptures, some of which are deep and accompanied by numerous intrusions and volcanic rocks. The southeastern part of the fold zone is occupied by the Kiangsi massif which is basically composed of Caledonian folds. This massif can be divided from north to south into the Wu-kung-shan swell, the Chen-shan swell, the Ho-shui synclinorium, the Wan-yang-shan swell and the Chiu-feng-shan massif. Several post-Yenshan depressions occur east of Kiangsi massif, namely, the Chi-an depression, the Chang-shui depression and the Chen-shui depression. The origin of these depressions is possibly related to faulting. Numerous granitic intrusions occur in the Kiangsi massif, most are of Yenshan age, some are Caledonian. The so-called Wu-kung-shan gneiss could be Caledonian. Most [of China's] tungsten deposits are concentrated in the Kiangsi massif. The third part of this fold zone is the fold zone proper north and west of the Kiangsi massif. Devonian and marine Triassic sedimentary rocks, largely limestones, were folded by the Indochina movement and modified by the Yenshan movement. Granites of both periods are widespread. In a few cases, Caledonian folds in the form of swells or anticlines occur amid Mesozoic folds. The fold zone proper can further be divided into the Yuan-shui synclinorium, the Hsiang-si fold zone, the Hsiang-yu fold zone, the Kueilin swell (composed of Devonian sedimentary rocks), and Kuei-chung depression (mainly Permo-Carboniferous sediments).

(10) Hsi-chiang (West River) Synclinorium

This fold zone is east of the fold zone of eastern Yunnan and west of Chiangnan anticlinorium and the Kuei-chung depression. Here,

transitional folds of Permian and Triassic marine sediments are widespread. Triassic sediments of the Flysch-type (the Ping-erh-kuan series) are several thousand meters thick. Devonian and Carboniferous strata are exposed on the south limb of the synclinorium in association with numerous small granitic intrusions. This south limb of the synclinorium is the outer rim of the northern Indochina (Tonkin) massif. The West River synclinorium consists of an east and west part. The eastern part, which has been named You-chiang synclinorium, is separated by the You-chiang fault into a northern and a southern segment. The western part is the Nan-p'an-chiang synclinorium. It includes the southeastern part of Yunnan and is in direct contact with the Red River deep rupture and the Ai-lou-shan metamorphic belt. The famous Ko-chiu tin deposit is located at the western tip of this unit.

In summary, the structure of the South-Chinese paraplatform is very complicated. Folds of many types occur. The Yangtze fold zone, the Szechuan syneclise and its surrounding fold zones, and the fold zones of eastern Yunnan are all of Yenshan age and occurred with no magmatic activity. Nanking sink, Kuei-hsiang-kan fold zone, and West River synclinorium are all products of the Indochina movement; they were subsequently modified by the Yenshan movement which was accompanied by magmatic intrusions (the West River synclinorium excepted). The Chiangnan anticlinorium, the Cathaysian anticlinorium, and the Kam-Yunnan axis are large uplifts which have undergone several cycles of intense folding. The Cathaysian anticlinorium structural system was formed by the Caledonian movement but is further complicated by the Indochina and Yenshan movements. The Chiangnan anticlinorium has a similar history, but is not as intensely deformed as the Cathaysian anticlinorium; magmatic activity is scarce in the western part. The Kam-Yunnan axis differs in that it was uplifted in Caledonian time modified by Variscan, Indochina and Yenshan movements, and strongly affected by the Himalayan movement.

III. Characteristics and Subdivisions of the Northeastern Paraplatform

Regional geological surveys of recent years has fully confirmed the typically geosynclinal nature of the Great Khingan folded belt. Thick Paleozoic geosynclinal deposits, including a sandstone series and large quantities of volcanic rock, were deformed in a northeast-southwest folded zone by the Variscan movement, which was accompanied by batholithic intrusions of granite. The Great Khingan fold zone is abruptly truncated by a north-northeast rupture zone, the Great Khingan deep rupture. This deep rupture was not discovered by aeromagnetic surveys but rather by other recent geophysical studies. The great volume of Mesozoic silicic extrusive rock and Cenozoic basalt along the east slopes of the Great Khingan also indicated the presence of this rupture zone. East of the Great Khingan fold zone is the broad Sungliao sink, the northern end of which borders the Ai-huei fold zone. The Ai-huei fold zone consists of the same lithologic facies, and was formed in the same period, as the Great Khingan fold zone, and thus should be considered as part of it. East of the Ai-huei belt is a narrow area of subsidence, the Sun-wu graben. The Northeastern paraplatform is a large area east of the Sun-wu graben and north of the Liaotung massif. It consists of the following subdivisions:

(1) Sungliao Sink

This is a large plain drained by Sung-hua-chiang and Liao-ho. It extends north-northeast and east of the Great Khingan deep rupture. Recent drilling shows a pre-Sinian basement of metamorphic rocks overlain by Mesozoic continental sediments, mainly Cretaceous from 2,000 to 6,000 meters thick. These sediments were only slightly folded and have no igneous intrusions. The sink is deeper in the southern part where possibly a thick sequence of Paleozoic marine sediments may be present under the Mesozoic beds.

(2) Hei-shui Arc and Granite Zone of the Little Khingan Range

The Little Khinghan range, east of the Sun-wu graben, is the southern extension of the Burea massif of the U. S. S. R. An area of crystalline schist outcrops with a north-south strike, situated north of the Hao-kang coal fields, was considered to be of Proterozoic age. The same rock formation was shown on the Russian geological map as of Archaean age. This is the Hao-kang massif; because of its rather small extent it is known as the Hao-kang swell. A belt of crystalline schist extends southward across the Sung-hua-chiang, then turns northwestward towards Po-li, and then heads eastward to Mi-shan and continues on in an east-northeast direction, forming an arc which was named by Yu-teh-yuan as the Hei-shui arc. North of the Po-li - Mi-shan line and unconformably overlying a Proterozoic arcuate structure is a similar and significant arcuate fold of Mesozoic continental sediment.

West of the Hao-kang swell is a narrow north-south zone of granites. These are old, mostly Caledonian, but in part possibly Proterozoic. Farther west, granites cover all of Little Khingan. On the basis of age determination, these granites are Variscan. The granite zone of the Little Khingan range include both Variscan and Caledonian granites with some associated Paleozoic metasedimentary rocks. The Chang-kuang-ts'ai-ling granite zone is the southern extension of the Little Khinghan granite zone. It also consists of two types of granites, Cale-

donian on the east and Variscan in the west, and inclusions of Paleozoic rocks. The Chang-kuang-ts'ai-ling is separated from the Little Khingan range by the great I-tung rupture of Yenshan age. The A-ch'eng granite zone of Yenshan age occurs in a large area in the southwestern-most part of the Little Khingan granite zone and south of Harbin.

(3) Ho-chiang Sink

The Ho-chiang sink is a large depression, north of the Hei-shui arc, that extends into Russia. It probably has a basement of Proterozoic crystalline schist overlain by thin Paleozoic and Mesozoic continental sediments interbedded with some marine sediments. The latter are coal-bearing and may constitute a potential coal field.

(4) Na-tan-ha-ta-ling Fold Zone

A north-northeast fold-fault zone indicated by extensive outcrops of Mesozoic geosynclinal sediments is located at the Soviet border, in the lower reaches of Jao-li-ho and the areas south of it. Large blocks of granite were intruded in it. These Mesozoic sediments consist of the Upper Triassic Ch'ing-chiang series (3,500 meters thick and unconformably overlying the Proterozoic), Lower Jurassic San-yang series (3,300 meters thick) and the Middle Jurassic Jao-li-ho series (1,700 to 2,000 meters thick).

The Na-tan-ha-ta-ling fold zone extends northward nearly to Po-li (Khabarovsk) in the U. S. S. R. According to the Russians, the fold zone is a product of Yenshan, not Indochina, movement.

Hsing-k'ai-hu Arch and the Yen-pien Fold Zone
(Ed.: Not shown in Figure 1)

Located in the south of Na-tan-ha-ta-ling, in the lower reaches of Mu-lin-ho is a northeast-southwest rupture zone. It extends for 500 kilometers from Mi-shan, through Mu-lin to Tun-hua. Mesozoic silicic volcanic rocks and great volumes of Cenozoic basalts occur along this rupture zone. This is tentatively recognized as a deep-rupture zone, the Mi-shan - Tun-hua deep rupture. It separates the Hei-shui arc and the Hsing-k'ai-hu arch. The Hsing-k'ai-hu arch is an uplifted area of crystalline schist intruded by Variscan granites. Its eastern part extends into Russia and forms the western border of the great Sikhota-Alin fold zone.

The Hsing-k'ai-hu arch plunges southwestward under large areas of Paleozoic sedimentary rocks, forming a broad Variscan fold-fault zone intruded by large bodies of granite. This is known as the Yen-pien fold zone.

(5) Kirin Fold Zone

This is a Paleozoic fold zone, equivalent to the Yen-pien fold zone, but situated north to the Liaotung anteclise and west of Mi-shan - Tun-hua deep rupture. Large areas of Paleozoic marine sediments, known as the Kirin formation, are exposed and form several strips surrounded by Variscan granites. The Kirin fold zone is gradually replaced northward by granite, so that only isolated inclusions are left. This is the area of the Chang-kuang-ts'ai-ling granite zone mentioned above.

In summary, the Northeastern paraplatform has the following characteristics:

(1) The Sinian basement rocks crop out extensively. The Paleozoic cover is thin and was largely eroded after folding. The only part of the paraplatform where it is preserved is in the Kirin and the Yen-pien fold zone.

(2) Evidence of many cycles of orogenic movement, such as the Caledonian, Variscan, Yenshan, and Himalayan, is well displayed, with Variscan being the major movement. Variscan movement is characterized by folding, and Yenshan movement by faulting and gentle folding, whereas Himalayan movement is characterized by faulting.

(3) The orogenic movements were accompanied by magmatic activity. Caledonian granites and larger and more extensive Variscan granite are widespread. Yenshan granites and volcanic rock, however, occur in areas of faulting and fractures. Cenozoic basalts also rose along rupture zones.

(4) Paleozoic granites, especially Variscan, are the most extensive rock type of this region, and they comprise a rigid Variscan platform. During the Mesozoic era, swells and depressions were formed on the platform by faulting. Thick Jura-Cretaceous sediments were deposited in these depressions.

MAJOR CHARACTERISTICS OF THE CHINESE PLATFORM

Multicycle Orogenic Movement and Magmatic Activities

In the past, the author has emphasized that cyclic orogenic movements are characteristic of the geotectonic features of China. This is mainly in reference to such areas as Tien-shan and Chi-lien-shan. Recent research shows that multicycle orogenic movements (folding) are also well displayed in the eastern part of the platform. Using the South-Chinese paraplatform as an example, the Chiangnan anticlinorium, the Cathaysian anticlinorium, and the Kuei-hsiang-kan fold zone are all areas that have undergone many cycles of deformation

The arches and swells of the Kuei-hsing-ken swell, and the Fu-jung-shan swell are all composed of pre-Devonian slightly metamorphosed flysch sandstone and shale of the Lung-shan group. Recent detailed geological studies have proven without a doubt the existence of a regional unconformity between the Devonian rocks and the Lung-shan group. We can therefore be sure there was widespread pre-Devonian folding. In the past, many have considered the Lung-shan group to be of Sinian age, so that the pre-Devonian unconformity would represent the pre-Sinian Lu-liang movement. Recent discovery of Ordovician and Silurian graptolites and abundant Sinian and Cambrian algae in the Lung-shan group in Kwangtung and Kwangsi has proven that a portion of the Lung-shan group is lower Paleozoic. Because of the lack of an angular unconformity between the Proterozoic portion of the Lung-shan group (the Pan-chi series) and its lower Paleozoic portion, the pre-Devonian regional unconformity could only represent Caledonian folding and not the Lu-liang movement. Recent field work shows further that the so-called Archaean granite gneiss, such as those of Wu-kung-shan in the Lung-shan group, was the result of grantization, probably Caledonian. The determination as to whether any part of the grantization is later Yenshan age must await further research.

Swells of Caledonian age appeared as an island in the Kuei-hsiang-kan fold zone. Caledonian folds generally occur under cover of several thousand meters of Devonian to Triassic sediments. The last of these have undergone intense Late Triassic folding and faulting, namely the Indochina movement. There are three stages in the Indochina orogenic cycle: one is pre-upper Middle Triassic (the pre-Ping-erh-kuan series), the second is pre-Upper Triassic, and the last is pre-Rhaetic. It is not known which of these is most important. The Indochina movement is most important within the Kuei-hsieng-kan fold zone, where the marine sediments were folded into mountains then extensively eroded. Many continental basins occur on the Indochina fold surface where Rhaetic and Lias coal-bearing series were deposited. Subsequently, there was a movement between Lias and the old red-bed series (middle Upper Jurassic, including rhyolites), one between the old red-bed series and the Cretaceous red-bed series (Wen-ming-ssu red beds), and one between the latter and the new red-bed series (the lower Tertiary Heng-yang red beds). Here, at least three orogenic phases took place between Lias and early Tertiary time, corresponding to the Yenshan orogenic cycle. The Yenshan cycle, on the one hand, folded and faulted the continental sediments and, on the other hand, modified and rejuvenated the Indochina and the Caledonian folding. The structure, displayed by a vertical cross section in areas covered by Mesozoic continental deposits and showing the superimposed folding of Caledonian, Indochina, and Yenshan movements, is understandably very complex.

The multicycle foldings described above not only occur in the Kuei-hsiang-kan fold zone but also are well developed in the Cathaysian anticlinorium and the Chiangnan anticlinorium. Nevertheless, because of the extensive exposure of the Caledonian folds, the upper Paleozoic and Mesozoic cover occurs in a few scattered subsided areas. The structural appearance is therefore quite different from that of the Kuei-hsiang-kan fold zone.

Cyclic magmatic activity accompanied multicycle orogenic movements, as is well shown in the South-Chinese paraplatform. Caledonian granites occur in the Caledonian folds; the so-called Archaean granite gneiss of Kwangtung and Fukien may prove also to be Caledonian age. It is an undebatable fact that granite intrusion accompanied the Indochina movement. Some of these intrusions occur as large batholiths. Examples are the Meng-chu-ling granite and the Ta-tung-shen granite. Magmatic activity which accompanied the Yenshan movement was even more extensive. Most of the granitic bodies of the coastal areas are of Yenshan age. Of equal importance are the extrusive rocks of this age. The most extensive rocks are rhyolites, that cover Chekiang and the coastal areas of Fukien. Slightly older than the silicic volcanic extrusives are a group of intermediate volcanic and pyroclastic rocks in the eastern part of Chekiang. Although the view that most granitic rocks of South China are of Yenshan age has been criticized, the problem remains as to which belong to the Caledonian, to the Indochina, and to the Yenshan period. Furthermore, it is possible that the single granite body may be the product of two or three periods of activity. Classification and differentiation of the periods of activity would depend on detailed facies study supplemented by careful field work. The possibly of the existence of Tertiary granite, which is another problem for future research, cannot be excluded.

The Northeastern paraplatform is also characterized by cyclic magmatic activity accompanying multicycle orogenic movement. As mentioned above, Caledonian movement was shown by the occurrence of Caledonian granites in the Little Khingan and the Chang-kuang-ts'ai-ling granite zone. West of the Caledonian granite, the Variscan granites, which contain remnants of folded Paleozoic beds, are widespread. The Variscan granite zone extends southward into the Kirin fold zone. It could be seen that Variscan was the most important folding movement of the Northeastern paraplatform. It is responsible for the conversion of the large marine basin of northern Manchuria into a rigid platform. Nevertheless, the mobility of the Northeastern paraplatform is notable: intense rupturing during the Yenshan

period caused the Mesozoic cover to be folded and ruptured, and at the same time widespread magmatic activity was manifested by the outburst of multiple volcanic activity and granitic intrusions. The Northeastern paraplatform was ruptured again in Cenozoic time. Large quantities of basalt poured out along the ruptures. In general there are three orogenic cycles represented in the Northeastern paraplatform: Caledonian, Variscan, and Yenshan cycles, Variscan being the most important; each cycle was accompanied by extensive magmatic activity.

The Sino-Korean massif was largely the result of one cycle of deformation, the Yenshan orogenic cycle, although there are local exceptions. The Inner Mongolian axis has suffered intense Yenshan movement and magmatic activity. Furthermore, there is evidence of Variscan movement, indicated by the presence of Variscan granite intrusives. Such granites are especially abundant near the Mongolian geosyncline (the pre-Middle Jurassic Chang-chia-chuang granite is probably a Variscan granite). The Tsingling axis is similar to the Inner Mongolian axis where both Variscan and Yenshan cycles and granitic intrusions were present.

The Significance of Mesozoic Orogenic Movement, Particularly the Yenshan Movement

Mesozoic movement of the Chinese Platform consists, as described above, of two cycles of folding: the Indochina cycle and the Yenshan cycle. Indochina folding is most clearly displayed in the South-Chinese paraplatform (including the southern part of Indochina). In general, it consists of transitional type of folding with frequent faulting (reverse fault and low-angle thrust faults). The trend of the folds commonly coincides with the elongation of the sedimentation trough and the trend of the neighboring old structure (chiefly the Caledonian). The Indochina movement is not obvious in the Yangtze fold zone. In the Sino-Korean massif, especially in the Peking - Hsi-shan region, basalt (dolerite of the past) is exposed below the Lias coal series. Whether it is Lower Jurassic or Triassic has not been determined. The hypothesis that Indochina folding occurs in the Peking - Hsi-shan region was shown to be wrong because the upper Permian (or Permo-Triassic) Shuang-ch'uan formation at Pata-ch'u is disconformable below the plant-bearing Jurassic sandy shale. The contact is not an unconformity. Basalt overlies this sandy shale. With no new evidence indicating otherwise, we assume that the Indochina movement is absent in the Yenshan parageosyncline; at least it is not apparent. It is not known whether the Indochina is present in northeastern China, because except in a few areas, Triassic strata absent. It is doubtful whether the pre-Jurassic unconformity here represents the Variscan movement. In the Na-tan-ha-ta-ling fold zone, the pre-Upper Triassic unconformity could represent the Indochina movement, a problem of future study.

A similar problem exists in the Amur district of the U. S. S. R. where the unconformity between Lower Jurassic and older sediments was also considered to be Variscan. The importance of Chiu-tien movement in Japan (a pulse in the Indochina cycle) has been overemphasized and exaggerated. In general, the Indochina cycle in the Indochina and southern China is important but in other areas is weak or poorly understood. The Indochina movement is definitely a part of the Pacific movement. It is the early phase of the Pacific movement, whereas the Yenshan and the Cenozoic movements are middle and late phases respectively, of the Pacific movement.

Yenshan movement is more important and widespread than Indochina movement. The cycle began in Middle Jurassic and lasted until the end of Cretaceous. The best evidence of Yenshan movement is seen in areas with only one cycle of deformation, for example in the Yenshan parageosyncline, the Ho-lan-shan and Liu-pan-shan fold-fault zones, the Yangtze fold zone, the area around the Szechuan syneclise, the fold-fault zone of eastern Yunnan, and the Na-tan-ha-ta-ling fold zone of the Northeastern paraplatform. Most folds are of the transitional type; in a few places the folds are fully developed. Folding is everywhere accompanied by faulting. In some areas there is more folding than faulting, such as in the Yangtze fold zone and on the eastern part of the Szechuan syneclise. In other areas there is more faulting than folding, for example, in the eastern Yunnan zone and in parts of the Yenshan zone. In areas with several cycles of deformation, such as the southern part of the South-Chinese paraplatform and the Northeastern paraplatform, the Yenshan folds are commonly superimposed on Variscan or the Indochina folds; its main features are faulting or broad gentle folding. In a few large swells of the Sino-Korean massif, such as the Shansi anteclise, the Shantung anteclise, the Tsingling axis, and the Inner Mongolian axis, Yenshan movement is primarily represented by faulting.

Generally, in eastern China, including the fairly stable Sino-Korean massif, Yenshan movement prevails. The special importance of Yenshan is therefore self-evident. Another reason why the Yenshan movement is important is the occurrence of various metallic mineral deposits related to contemporaneous magmatic activities. As described above, granites (including granodiorite, monzonite, diorite, and syenite) are widespread along the southeastern coastal areas. Studies in the Hongkong area indicate granites of three periods: Upper Jurassic, Lower Cretaceous and early Tertiary. If the so-called early Tertiary granite intruded the Cretaceous red beds, then granite of all three ages should belong to the Yenshan cycle. In Fukien province, the Upper Jurassic granite is older than the Pan-tou series and intrudes the Chien-te series. In Hunan, at Shui-kou-shan, granite older than the Heng-yang red beds intrudes Cretaceous sand-

stones. In Kwangtung granite intrudes red beds. If the Heng-yang red beds and the red beds in Kwangtung are of the same age, then the granites of Hunan and Kwangtang can be correlated with those of Hongkong; this problem requires further study.

The volcanic rocks of Yenshan age are also quite complex. In the Peking - Hsi-shan region, there are three periods of Mesozoic volcanic rocks: Triassic-Jurassic basalt, late Jurassic intermediate extrusives (the Chao-chi-shan series), and Cretaceous silicic extrusives (the Tung-ling-tai rhyolites). Volcanic rocks of the two latter periods are also present in Liao-hsi and Kirin. In Shantung province, the Cretaceous Ching-shan silicic tuff-conglomerate is equivalent to the Tung-ling-tai series. In Chekiang and Fukein, rhyolites are widespread. Intermediate (andesitic) volcanic rocks of the Ju-hsiang series and its interbedded tuff-conglomerate underlie rhyolites in eastern Chekiang. If the Ju-hsiang series is equivalent to the Chao-chi-shan series, then the rhyolites may be correlated with the Tung-ling-tai rhyolites. However, the rhyolites of Chekiang and Fukien actually underlie the Cretaceous Pan-tou series, so that they should be Upper Jurassic or equivalent to the Chao-chi-shan series. The age correlation still contains unresolved conflicts. In general, there are at least two phases of extrusives in eastern China of Yenshan age: one Upper Jurassic and the other Cretaceous; the two phases are represented by various rock types in different regions. Whether there are three periods of extrusion to compare with three periods of granitic intrusion is another problem for future study.

Yenshan movement is not only a major orogenic movement in eastern China but also in the Soviet Far East and eastern Siberia. The great Verkhoyansk and the Sikhota-Alin ranges were formed by Yenshan folding. It can be firmly stated that Yenshan movement is the backbone of the Pacific movement. It is not only prevalent in eastern China along the Pacific coast, but it also affected western China. The Variscan folds of Tsingling, Chi-lien-shan, and Tien-shan have all undergone intense Yenshan movement. The great Karakurum and its eastern extension the Tang-ku-la-shan contain a "core" of Yenshan folds.

Deep Rupture and Great Rupture Zone and their Effect on the Uplift of Large Swells and Arches

In the past, study and knowledge of the rupture zone and faulting movement of eastern China were quite inadequate, which is why I scarcely discussed them in my paper, "The Major Geotectonic Units of China" [20]. Large-scale, general surveys of ore deposits and regional geology since liberation have amassed a wealth of data. Preliminary analysis of such data has established the important part played by various ruptures on the structure of the Chinese platform. The ruptures can be divided into two types: one, the so-called deep rupture type of Professor Billings, is of large scale and old age; the other type, the synorogenic type, is contemporaneous with folding and is closely associated. In addition, there are large ruptures of younger or unknown age, which we tentatively designate as great ruptures. They also can be divided into the above two types. Geophysical exploration, regional geological surveys, and the author's own research indicate the deep ruptures are as follows:

(1) Tan-cheng - Lu-chiang Deep Rupture

This deep rupture extends from southern Shantung to Lu-chiang of Kiangsu province. It divides the Shantung anteclise into two parts. This deep rupture was first discovered by aeromagnetic surveys. It is a normal fault begun in Sinian time, and with recurrent movement during the Mesozoic and Cenozoic.

(2) Hsuan-hua - Cheng-teh - Pei-piao Deep Rupture

This is the boundary between the Yenshan parageosyncline and the Inner Mongolian axis. It began in Sinian time and was strongly reactivated in the Mesozoic. This deep rupture was discovered by the Geological Survey of Hopei. It is a north-to-south overthrust.

(3) The Deep Rupture Along the Eastern Great Khingan Range

This deep rupture occurs between the Great Khingan geosyncline and the Sungliao sink. Recent geophysical work has proven its existence.

(4) Deep Rupture of the Nanking Sink

This is the lower Yangtze fractured zone mentioned above. It was discovered by aeromagnetic surveys.

(5) Deep Rupture Along the Southern Tsingling Range

The eastern part is the Ta-pa-shan deep rupture. It extends from Chen-pa of Shensi province along the northern slope of Ta-pa-shan eastward to Hsiang-yang. It is a north-south overthrust. The western part is the Lung-meng-shan deep rupture. It extends from Pao-ching of western Szechuan along the northern slope of Lung-men-shan northeastward to Nan-chen of southern Shensi province. It is also a north-south overthrust. Its movement was intense in Yenshan time, giving rise to the complex structure of the Peng-hsien-Kuan-hsien region.

(6) Deep Rupture of Eastern Yunnan

The basic structure of this rupture zone is an old north-south trending deep rupture. The major one is the Hsiao-chiang rupture which extends from south of Hsiao-chiang to east of Fu-hsien-hu. The extrusion of Permian basalts is related to this deep rupture zone.

(7) Red River Deep Rupture

It occurs in southern Yunnan and extends southeastward along the Red River valley to Hanoi. Its northwestward extension may go through Erh-hai.

(8) Deep Rupture Along the Southern Margin of Chiangnan Anticlinorium

This deep rupture is located in northern Kwangsi, at the southern tip of the Chiangnan anticlinorium. It is the great Nan-tan - I-shan rupture which extends northeastward to the hills of Hsueh-feng-shan in western Kiangsi.

(9) Chien-tang-chiang Deep Rupture

It is located in the Chien-tang-chiang synclinorium and is separated by fault contact from the Chiangnan anticlinorium to the northwest and the Cathaysian anticlinorium on the southeast. Northeastward this deep rupture extends to south of Shanghai. It probably has existed since early Paleozoic time.

(10) The Marginal Deep Ruptures of the Cathaysian Anticlinorium

The most important one is the great Shou-wu - Jui-ching rupture which trends northeast-southwest along the border of Kiangsi and Fukien. The deep ruptures of northern Kwangtung consist of the rupture south of Yin-teh, the Lien-chiang rupture, the Hsin-hsien rupture, and the Nan-ning rupture.

Ruptures probably of the deep-seated type but poorly known are described as follows: (1) Chih-feng-To-lun rupture. It is located at the northern margin of the Inner Mongolian axis. Large quantities of Mesozoic and Cenozoic volcanic rocks occur along this rupture. (2) Rupture along the western margin of Ordos syneclise. It separates the syneclise from Liu-pan-shan. It is an overthrust from west to east. (3) Ruptures on both sides of the Tsingling axis. On the north is the Wei-ho rupture, a normal fault which has existed probably since Mesozoic time. The large rupture in the south in contact with the Tsingling geosyncline is probably of the deep rupture type. (4) Ruptures on both sides of the Huai-yang shield. A large fractured zone occurs along the northern margin of the shield. It has been present at least since Mesozoic time. A deep rupture was postulated to be present from Hsiang-yang, north of Hankow along the Yantze river to Au-ching, on the south side of the shield. This has not been substantiated by aeromagnetic survey. If this rupture does exist, then it would have connected the rupture of the Nanking sink in the east to the Ta-pa-shan rupture in the west to a gigantic rupture belt, the largest in China, extending from Tai-chou of Kiangsu province to Pao-hsin in Szechuan.

Not belonging to or unlike the deep rupture type, as of our present knowledge, are the following ruptures or rupture zones. Because of limited space, we mention a few important examples by name only:

(1) Northeastern paraplatform (including Liaotung Anteclise):

(a) I-lan - I-tung rupture.
(b) Mi-shan - Tun-hua rupture.
(c) Fu-shun - Hai-lung rupture.
(d) Tung-hua rupture zone.
(e) Liu-ho rupture.

(2) Sino-Korean massif:

(a) Pei-piao - Chou-yang rupture zone (induced by the Hsuan-hau-Cheng-teh - Pei-piao deep rupture).
(b) Rupture along the northern margin of the Shan-hai-kuan massif.
(c) Chi-tung (eastern Hopei) rupture zone (including the parallel ruptures between the Hsuan-hua - Cheng-teh - Pei-piao deep rupture and the Chi-tung arch).
(d) Rupture between Peking and Hsuan-hua (see above).
(e) Tai-hang-shan rupture zone (mainly of Mesozoic and Cenozoic age; see above).
(f) Chiao-tso rupture zone.
(g) Parallel ruptures of the Tsingling axis (located within and parallel to the axis, they sliced the axis into several strips, forming elongated troughs with middle Cenozoic deposits).
(h) Ruptures around the Ordos syneclise (including the Wei-ho graben; see above).
(i) Fen-ho rupture zone.
(j) Liu-pan-shan rupture zone.
(k) Parallel ruptures of the Inner Mongolian axis (which sliced the axis into oblique strips).
(l) Lu-hsi rupture zone.

(3) South-Chinese paraplatform:

(a) Lung-men-shan overthrust and isoclinal fold structure (controlled by the Lung-men-shan deep rupture).
(b) O-mei-shan fault block.
(c) Rupture zone of northeastern Yunnan (contemporaneous with folding).

(d) Rupture zone of eastern Yunnan (controlled by the deep rupture of eastern Yunnan).
(e) Chien-chiang graben (located in eastern Szechuan and western Hopei).
(f) Tsun-i rupture zone.
(g) Chien-tung rupture zone.
(h) Kuei-chung rupture zone.
(i) Other rupture zones such as those of the Cathaysian anticlinorium, the Chien-tang-chiang syneclise, and the Nanking sink, which were either induced by deep ruptures or were rejuvenated deep ruptures.

The deep ruptures and the large rupture zones gave rise to, as well as controlled, the large uplifted and subsided areas on the Chinese platform. A clear example of the large subsided area is the Ordos syneclise. Its shape and limit of subsidence were determined by the Li-shih fault, the Liu-pan-shan fault, and the rupture north of Tsingling and south of Yin-shan. Because these faults were largely formed during or after the Yenshan period (the western part may be an exception), the birth of the Ordos syneclise can only have been during Mesozoic or later time. There is no syneclise prior to Mesozoic where the Ordos is connected with the Shansi anteclise to form a single plate. From this point of view, naming the Ordos and Shansi as syneclise and anteclise is not logical.

The control of large-scale uplifts by ruptures is even more obvious. Using the Inner Mongolian axis as an example, it is bordered on both sides by ruptures: by the Hsuan-hua - Cheng-teh - Pei-piao deep rupture on the south and the Chih-feng - To-lun deep rupture on the north. The characteristics of the development of the Inner Mongolian axis are: (1) After Sinian time, it underwent a long period of uplift, accompanied by erosion, (2) Areas of subsidence, either scattered or overlapping, of various sizes developed on the axis during different eras -- upper Paleozoic, Mesozoic and Cenozoic. (3) Because it adjoins the Mongolian geosyncline with Variscan folding, the Inner Mongolian axis was partly active during Variscan time as shown by faulting and weak magmatic activity. (4) The most important movement was in Yenshan time. Not only did strong movement occur along the rupture zones on both sides, but it was accompanied by magmatic activity -- volcanic extrusions and granite intrusions. Deep ruptures induced the further breakup of the axis proper which was sliced into diagonal strips by parallel ruptures, accompanied by magmatic activities -- extrusion of volcanic rocks and intrusion of granite. (5) The rupture movement also caused folding and fracturing of the upper Paleozoic and Mesozoic continental deposits which cover the axis; this is well apparent in the in the eastern part of the axis. (6) Similar rupture movement accompanied by magmatic activity (the outpouring of large quantities of basalt in the eastern part of the axis) occurred in Tertiary time.

The history of development of the Tsingling axis is similar to that of the Inner Mongolian axis. This axis began to rise after Sinian or even Proterozoic time along the deep ruptures north and south of it. Uplift was represented by Variscan and particularly by the Yenshan movement when large amounts of granite were intruded into the axis, accompanied by some of the metallic mineral deposits. The thin Paleozoic and Mesozoic basin deposits were folded and faulted. The extensive Proterozoic andesites which occur in the northern part of Tsingling axis are absent in Inner Mongolia. The Huai-yang shield is similar to the Tsingling axis except that sedimentary cover there is very sparse.

Like the Inner Mongolian axis and the Tsingling axis, the Cathaysian anticlinorium and the Chiangnan anticlinorium (especially the eastern part) are controlled by deep ruptures. The anticlinoria however, differ from the axes in that: (1) the axes consist of Proterozoic and lower Paleozoic sandstone and shale; (2) because of this lithologic difference, the less competent rocks of the Cathaysian and the Chiangnan anticlinoria were more mobile, as shown by their fracture and folding; (3) they suffered folding and faulting of several cycles, Sinian, Caledonian, Indochina and Yenshan movements, accompanied by various types of volcanic and granitic activity. Various types of metallic deposits are associated with the granitic rocks.

The character of the Kam-Yunnan axis seems to be between that of the Inner Mongolian axis and the Cathaysian anticlinorium. Its history requires further study.

This brief discussion shows that the Inner Mongolian axis is not the same as the anteclise described in Russian literature. The Cathaysian anticlinorium structure is quite different from it. It would not therefore be suitable to label as anteclises such large uplifted areas of China.

CONCLUSIONS

In section one of part one we briefly discussed the Chinese platform and its contrast with standard platforms. In the second and the third sections of part one, the major characteristics and subdivisions of the Chinese platform were described. Using these major characteristics and comparing the subdivisions of the Chinese platform with some of the well known Russian platforms, we can see that they are clearly different from the Russian ones. To avoid confusion, I propose to call the typical Chinese platform a paraplatform, and the standard platform, such as those of Russia, an orthoplatform.

The characteristics of each of the three

major units of the Chinese platform differ from those of the other units: the South-Chinese paraplatform is the most mobile, as shown by the multiple folding and faulting, with accompanying magmatic activities. This is known as the South-Chinese type paraplatform. In contrast, the Sino-Korean massif is less mobile, except in some areas, and generally underwent only one cycle of deformation. This is the Sino-Korean massif type of paraplatform. The characteristics of the Northeastern paraplatform resemble those of the South-Chinese paraplatform and it is tentatively classified as such. Professor Chen-kuo-ta has designated the South-Chinese paraplatform as a "mobilized platform". The word "mobilized" implies that the platform was stable or inactive before. Since the South-Chinese paraplatform was definitely active during the Lu-liang movement and particularly during Caledonian time, the facts would seem to contradict Professor Chen's idea. Except in the marginal areas, the Sino-Korean massif was actually a very stable area in Paleozoic time. It became really active in Yenshan time. The Sino-Korean massif would therefore be a better example of a mobilized platform.

REFERENCES

[Ed.: The following references are listed, with only minor editorial revision, as they appear, in straight translation, from the original journal. Even if adequate bibliographic details were readily available, it is believed that very few of the items cited are available in the United States]

1. Geologic map of China (1:3,000,000, 1st edition, 1951.
2. Geologic map of China (1:3,000,000), 2nd edition (first draft).
3. Geologic map of China (1:1,000,000), eastern part, 14 sheets, 1st edition, 1948-1951.
4. Geologic map of China (1:1,000,000), eastern part, 18 sheets, 14 of these were revised. The Shen-yang, Yen-pien, Cheng-teh and Huhohoute (4) sheets are first drafts.
5. Geologic and geotectonic maps of Hopei province (1:500,000), Geological Survey of Hopei, 1958, manuscript map.
6. Geologic maps of Kwangtung, Fukien, Yunnan etc., (1:500,000), first drafts.
7. Geologic and geotectonic maps of Heilungkiang (1:500,000), Geological Survey of Heilungkiang, 1958, first draft.
8. Unpublished geologic map of Nanling Geological Survey party, Tsingling Geological Survey party, Northern and Eastern Hopei Geological Survey party and other regional survey parties. (1:1,000,000 to 1:500,000).
9. Unpublished geologic maps and reports of the petroleum survey parties of Kwangsi, Szechuan, Hopei and Honan (1:300,000).
10. Survey maps of petroleum geology, the Ordos region, Bureau of Petroleum Industry, vol 5, 1957.
11. Results of aeromagnetic surveys of geotectonic and metallogenic belts of recent years. Bureau of Geological Exploration, 1958.
12. Geotectonic map of the Great North China Plain (1:1,000,000) North China petroleum survey party, (no date).
13. Geotectonic maps of China and adjacent areas, (1:4,000, 000). Geological Institute, Academia Sinica (in print).
14. Geotectonic map of China (1:3,000,000), being compiled by the Geotectonic system of the Geological Institute of the Ministry of Geology. The eastern part is completed. (This is the principal reference).
15. Geologic map of the Mongolian Peoples Republic (1:2,500,000); source: U. S. S. R Geology and Ore Preservation Bureau.
16. Geotectonic map of the Mongolian Peoples Republic (1:2,500,000), Academy of Sciences, U. S. S. R. compiled by Ivanov, 1957.
17. Geologic map of U. S. S. R. (1:2,500,000), Geological Institute U. S. S. R., 1956.
18. Geotectonic map of U. S. S. R. (1:4,000,000). Academy of Sciences U. S. S. R., 1956.
19. Stratigraphic charts of China, Science Publishing House, 1956.
20. Huang, T. K., The major tectonic units of China, 1954.
21. _____, Contributions to regional geology of China, Acta Geologica Sinica, v. 34, no. 3, 1954.
22. _____, New studies on the geotectonic subdivisions of eastern China and their characteristics, Geology Monthly, January 1959.
23. Chen, Kuo-ta, Actual examples of mobilized belts of the Chinese Platform with emphasis on the problem of Cathaysia. Acta Geologica Sinica, v. 36, no. 3, 1956.
24. Tsao, Kuo-chuan, Prospecting guide for ore deposits, based on the study of the Hopei geotectonic unit and its related magmatic activity (unpublished manuscript), 1958.

PHYSICAL AND CHEMICAL PROPERTIES OF BITUMINOUS COAL CONSTITUENTS (MACERALS)[1]

by

Carl Kröger[2]

• *translated by Gilbert H. Cady* •

Investigation of bituminous-coal macerals, accomplished through the Institut für Brennstoff Chemie (Fuel Chemistry Institute) of Aachen, is summarized here. Coal from five Ruhr coal beds was processed to obtain pure macerals in quantities sufficient to study their individual structure and chemical composition. Vitrinite, micrinite and exinite were recovered accordingly, and their chemical and physical properties studied; detailed, graphical interpretation of these data has been included. Chemical composition is derived for vitrinite, exinite, micrinite, and fusinite individually. Chemical structure of the macerals is discussed in relation to aromatically bound carbon content. It has been possible thus far, to determine maceral properties with respect to coalification rank as well as to indicate differentiation of these properties in macerals from the same coal bed. --D. D. Fisher.

Bituminous coal consists of a microscopically heterogeneous mixture of different macerals (structural components). Petrographically differentiated are vitrinite, fusinite, and exinite; and substances presently regarded as inert; micrinite, semifusinite, and sclerotinite. Mixtures of these constitutents in varying amounts, form the banded coals: vitrite (vitrain) clarite (clarain), durite (durain) and fusite (fusain); from these glance coal, dull coal, and mineral charcoal develop.

The physical and chemical properties of standard coal varieties are therefore, derived from average values determined by petrographic composition which, as yet, could not be established in terms of maceral properties. However, it is possible to extract pure vitrinite (vitrain) and fusinite (fusain) without much difficulty in amounts sufficient to study their chemical and physical properties; for dull coal this had not yet been done. Accordingly, in designation of coal properties, vitrain is taken as the standard. This, however, does not explain adequately the apparent anomalies in coal properties. We have in previous years, undertaken refinement of the pure constituents vitrinite (vitrain), exinite (sporinite) and micrinite from the bright and dull coals of 5 Ruhr coal beds (R. Zollverein, Anna and Wilhelm, Auguste Viktoria Shaft I$_1$, and Consolidation Shaft). Thus it has been possible not only to determine their properties in relation to rank, but concurrently, to show differentiation of these properties in macerals from the same bed.

Concentration of material

The glance and dull coals extracted from underground beds, were crushed to hazelnut size and ground in a disc-mill (Scheibenmühle) from 1 to 2 mm size; they were dried to a nitrogen atmosphere ranging in temperature from 60 to 65°C. Grading of macerals by heavy liquid separation required the most thorough breaking up possible of the often closely associated initial substances. Further reduction in their size was accomplished in a rod-mill (Stiftmühle) by elastic impact, at approximately 18,000 revolutions per minute in an inert atmosphere. The grain fineness attained for vitrinite (vitrain) and micrinite ranged from 1 to 20 microns (μ) for exinite up to 100μ. After preliminary treatment in a spinning box (Spitzkasten) there followed further gravity separation in a continuous centrifuge (at 12,000 to 25,000 revolutions per minute) whereby, if necessary one could obtain material of less or greater density, and where repeated operation was possible. The resulting suspensions were then run over the pressure filter (Druckfilter); residual material on the filter was freed of any remaining heavy liquid (carbon tetrachloride - toluol) in a vacuum of about 85 Tor [Ed. pressure of 1 mm mercury; 1/760 atm] (nitrogen), from 60 to 65°C. Upon suitable examination we found that the supposed effect of heavy liquids on the macerals did not exist. For example, Figure 1 illustrates schematically the gravity separation of the dull coal from bed R.

In this way, macerals (af) could be separated into the following grades of purity: Vitrinite (vitrain), about 90 percent; exinite, 94 to 97 percent; and micrinite, 91 to 95 percent. The ash content of exinite was similar to the amount of organic mineral matter (about 0.5 percent); in vitrinite about 1.3 percent; and in micrinite 3 to 6 percent.

---

[1] Translated from Die physikalischen und chemischen Eigenschaften der Steinkohlengefügebestandteile (Macerale): Brennstoff-Chemie v. 37, nos. 11-12, pp. 182-186, 1956.

[2] Institut für Brennstoff-Chemie (Kohle-Chemie) der Rhein.-Westf. Technischen Hochschule, Aachen, Germany.

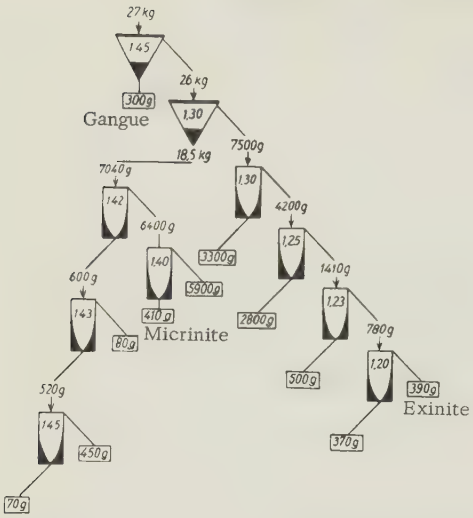

FIGURE 1. Ore preparation process for dull (matte) coal of bed R.

Chemical Analysis

The chemical-analytic investigations consisted, in addition to immediate and proximate analyses, of determinations of the heat value and of hydroxyl- and carbonyl- oxygen. The differentiation of these values for individual macerals is represented in figures 2 to 5 inclusive.

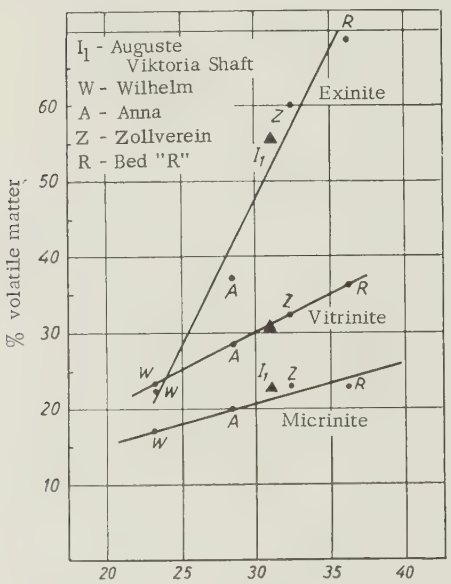

FIGURE 2. Volatile components of exinite and micrinite as compared to vitrinite.

In figure 2 the progression in volatile-matter content of the exinite and micrinite compared to that of equivalent vitrinite from the same coal is apparent. The coalification of all maceral thus proceeds uniformly (not erratically even in the case of exinite). In exinite the changes are greatest, and the least in micrinite. The volatile-matter content of exinite and vitrinite coincides at about 24 percent; and, for vitrinite and micrinite, at about 10 percent.

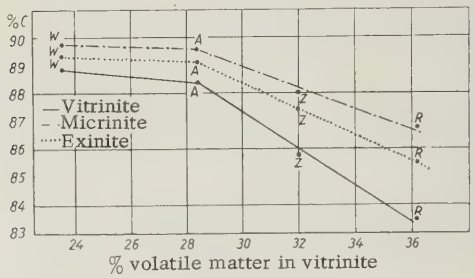

FIGURE 3. Variation in C-content of macerals with coalification

W - Wilhelm; A - Anna; Z - Zollverein; R - "R"

Figure 3 shows the progression in carbon content in relation to the percentage content of volatile matter assumed as standard for rank. In this case, where volatile-matter content is below 29 percent, there is generally a slight increase in C content because the (H plus O)/C relationship for volatile matter is reduced to its lowest value. The nitrogen content of micrinite and exinite is about two-thirds that of vitrinite; the same relationship applies to sulfur content.

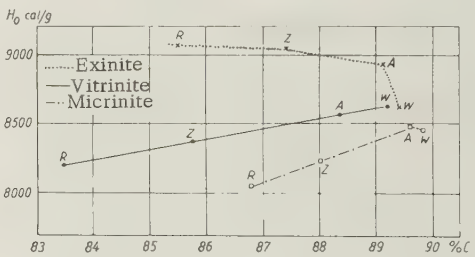

FIGURE 4. Heat of combustion (H_o) of macerals

W - Wilhelm; A - Anna; Z - Zollverein; R - "R"

The values derived for heat of combustion (H_o) provide the data for figure 4. The differences following have slight relationship to the elementary composition; compared to H_u values [Ed. : H_u values, as in original paper] calculated from the Dulong formula, they are as follows: for micrinite, from 15 to 40 calories (cal) (the Wilhelm bed, 100 cal); for vitrinite, from the R and Wilhelm beds, 20 and 50 cal respectively; and for Zollverein and Anna beds, 250 and 120 cal, respectively; and for exinite, from 130 to 170 cal.

Consequently, establishment of calorific values is unsuited to determination of differences in the chemical structure of macerals.

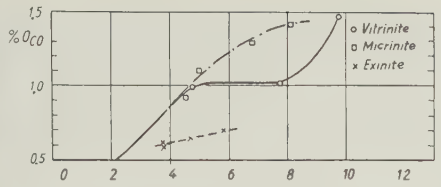

% total oxygen content

FIGURE 5. Carbonyl-oxygen in relation to total-oxygen content of macerals

TABLE 1. Hydroxyl values of macerals*

Coal beds and macerals	Without carbazol		With carbazol	
	mMol/g	% O_{OH}	mMol/g	% O_{OH}
Vitrinite	2.94	4.7	2.96	4.7
R Micrinite	1.69	2.7	2.02	3.2
Exinite	1.01	1.6	0.97	1.6
Vitrinite	2.17	3.5	2.17	3.5
Z Micrinite	1.76	2.8	1.74	2.8
Exinite	0.96	1.5	0.95	1.5
Vitrinite	1.29	2.1	1.80	2.9
A Micrinite	0.92	1.5	1.00	1.6
Exinite	0.92	1.5	1.06	1.7
Vitrinite	0.24	0.4	0.40	0.6
W Micrinite	0.96	1.5	1.24	2.0
Exinite	1.12	1.8	1.22	2.0

*For these values, the author is grateful for the kind cooperation of Dr. G. Davis, Carbide and Carbon Chemicals Co.

The hydroxyl- and carbonyl-numbers, as shown in figure 5, have an almost constant relationship to the total oxygen content of coal; this relationship, in addition, is dependent on the total content of the macerals. The OH-relationship of exinite is an exception, for 3.7 to 5.8 percent zone the total oxygen content (0.06 percent) is practically constant. Structual differences of the individual macerals agree well with this value. Differences for micrinite and vitrinite are less; when total oxygen content is under 5 percent, they disappear. From figure 5 [Ed.: In original text fig. 5a and 5b. The author has stated 5a to be obsolete; in its place he has given the table "Hydroxyl values of macerals" (table 2 from Brennstoff-Chemie, v. 40, p. 79, 1959).] it is quite evident that hydroxyl and carbonyl content of coal practically disappears below 4 percent and 1.5 percent to 2 percent total oxygen content, respectively.

The previously given differentiation of chemical analysis values for macerals, moreover, may make possible analysis from these values of petrographic composition of the normal coal of a bed; suitable equations were developed to that end.

Physical Properties

Specific gravity (methanol), heat of wetting (methanol), and compressibility values were determined: for the first two measurements, the coal was extinguished at about 120°C. Compressibility was measured after the powdered coal had been compressed into cubes under 3 t/cm^2. The results are presented in figures 6 to 10, inclusive.

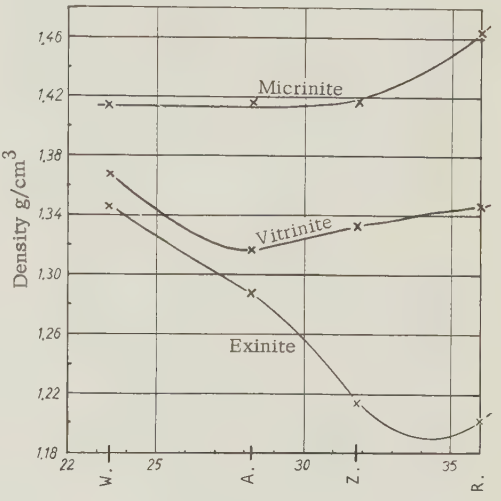

% Volatile matter in vitrinite

FIGURE 6. Density in relation to coalification
W - Wilhelm; A - Anna; Z - Zollverein; R - "R"

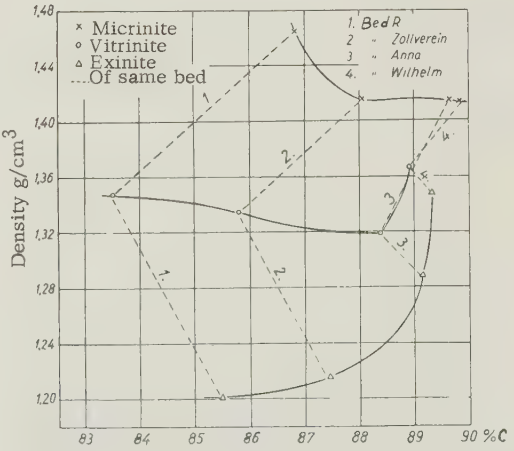

FIGURE 7. Density - carbon content (waf)

Density variations of separate macerals from individual beds are presented in figure 6, whereas figure 7 shows their relationship to the true carbon content of the coal. Along with increase in rank (fig. 6); the density of exinite like that of vitrinite first diminishes, then increases; only the minima occur at different values, about 34.3 percent as compared to 27.7 percent volatile matter. Micrinite density values are nearly constant below approximately 30 percent volatile matter content. The approach of density values with increasing

rank is well shown in figure 7.

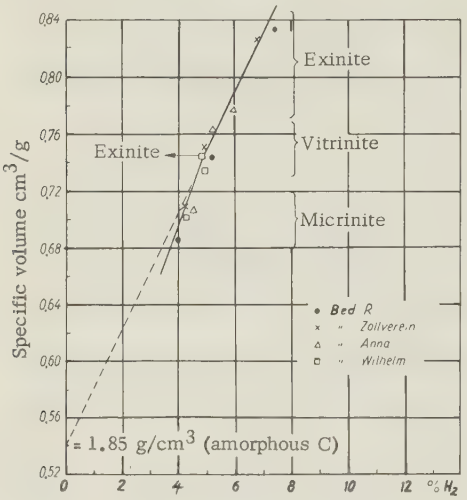

FIGURE 8. Specific volume - hydrogen content

Figure 8 shows that the known linear relationship in normal coal of its specific volume to hydrogen content also exists for macerals. As usually the slope has a definite bend at approximately 5 percent hydrogen content.

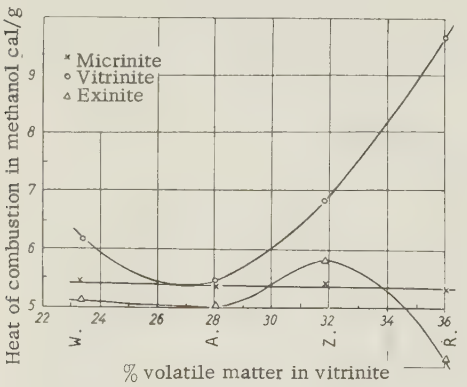

FIGURE 9. Heat of wetting of macerals
W - Wilhelm; A - Anna; Z - Zollverein; R - "R"

Figure 9 illustrates the derived heat of wetting values. The vitrinite curve shows the known minimum for normal coal was displaced in this case from, approximately, 22 percent to 27 percent volatile matter content. The values are quite constant for micrinite, whereas for exinite, a maximum occurred near 22 percent. If one assumes the relation, formulated by Franklin for normal coal, between the methanol contraction ($V_{He}-V_{Me}$), (V_{He} and V_{Me} represent the specified volumes of helium and methanol, respectively) and the heat of wetting (Q_B):

$$(V_{He}-V_{Me}) = 0.0026\ Q_B$$

to be correct, then helium densities are determinable from the measured values.

Compressibilities of macerals measured ranged from 0.01 to 3 t/cm^2, and, were found to be related to the pressure.

However, if one were to plot average compressibility (κ), as determined experimentally of the macerals, in relation to the true content of volatile matter (fig. 10), a direct proportionality would result. Accordingly, it is concluded that compressibility, particularly that statically measured, is essentially a function of the non-aromatic portion of coal structure in the investigated range of rank.

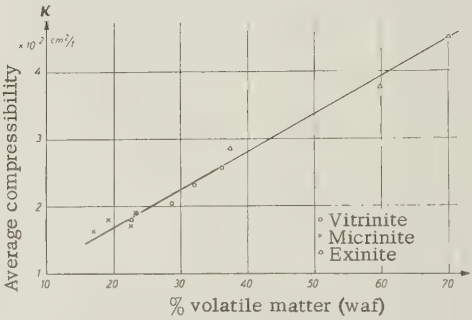

FIGURE 10. Average compressibility (κ) of macerals as compared to volatile-matter content

Coalification and Coal Structure

At this time the results previously given, lack only conclusions concerning the coalification process and structure of macerals.

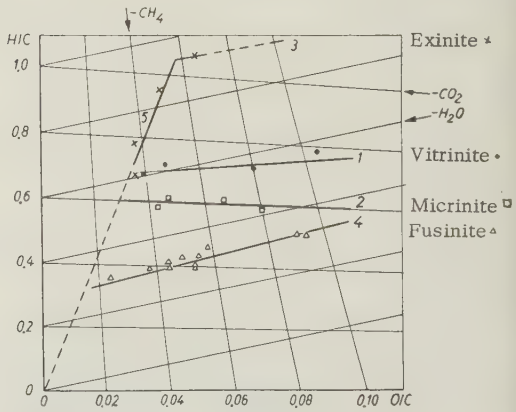

FIGURE 11. Coalification trend of macerals in the H/C - O/C diagram

Figure 11 shows the elementary analyses, ascertained by us, for individual macerals. This method of representation, after van Krevelen, was selected because it was more easily interpreted than other methods involving the changes in original composition by coalification through liberation of methane, carbon dioxide, and water. It is evident that designated analytical values lie irregularly along straight lines, each representing a maceral, 1 through 4.

These straight lines for determined H/C and O/C values terminate at line 5, now valid for all macerals and whose slope corresponds to a determined constant H/O relationship lying between 20 and 25 percent. From this follows for the individual macerals, the summarized rank equation below (related to the smallest integral ratios):

Line 1: Vitrinite A = Vitrinite B + H_2O + CO_2;
Line 2: Micrinite A = Micrinite B + CO_2;
Line 3: Exinite A = Exinite B + $5H_2O$ + CO_2;
Line 4: Fusinite A = Fusinite B + H_2O

The macerals attain the following composition:

		g/Mol/wt
Vitrinite	$C_{96}H_{66}O_3$	1, 266
Micrinite	$C_{114}H_{66}O_3$	1, 482
Exinite	$C_{88}H_{88}O_4$	1, 208
Fusinite	$C_{138}H_{40}O_2$	1, 712

thus, further coalification proceeds for all macerals according to the following equation:

Line 5: Coal A = Coal B + $5CH_4$ + H_2O

Coalification reactions 1 and 5 are endothermic; coalification reaction 2, exothermic.

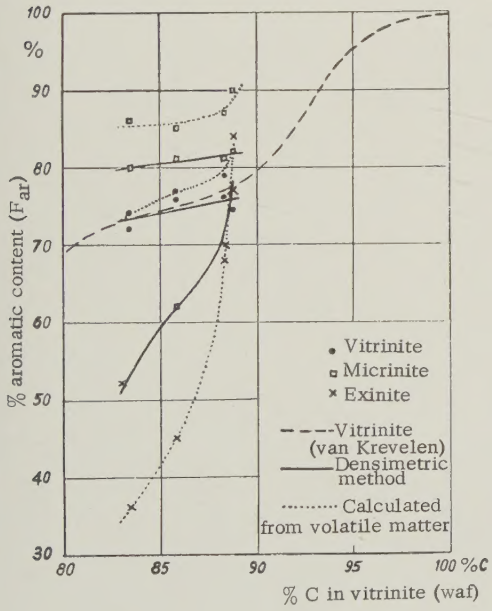

FIGURE 12. Aromatic content

In reference to the distinct chemical structure of banded ingredients it is equally possible to draw conclusions from the elementary-analysis values, combined with values for density or, volatile matter, respectively.

Figure 12 indicates in the portion calculated by van Krevelen, aromatically bound carbon (f_{ar}) in relation to rank for the individual macerals, from density and molecular weight; and, in the other portion, from volatile-matter content. The differences are particularly important in the case of exinite; possibly to indicate that the f_{ar} portion, as determined by the first method, is related to the aromatic framework and side chains, while, by the second calculation method the latter are not entirely understood.

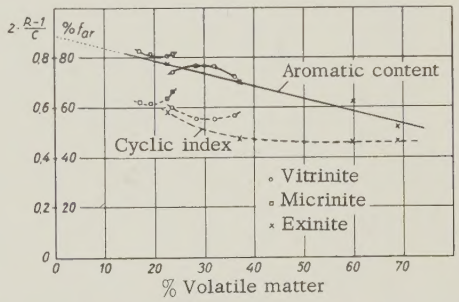

FIGURE 13. Cyclic index and f_{ar} with respect to true volatile-matter content

Figure 13 shows, moreover, that by plotting the former value against percentage of volatile matter, an approximately straight line results. No real significance should be attached to variation of this line produced by changes in the method of calculation. The degree of its validity for minima of the cyclic index curves, remains to be determined.

This preliminary report represents summarization of work accomplished, through the Institut für Brennstoff-Chemie der Technischen Hochschule Aachen, since the initiation of investigation of macerals from bedded coal (see my contribution at the bituminous-coal meeting at Aachen 1954); and, in which Messrs. A. Pohl, Fr. Kuthe, J. Bakenecker, W. Ruland and H. Hovestadt have participated. Will the Steinkohlebergbauverein of Essen and the operation Auguste-Viktoria, Marl-Hüls accept our thanks for making the investigation possible.